

Multicomponent Aerosol Formation Model

MAFOR Model version 1.9.9

User's Guide

2021

Author:
Dr. Matthias Karl

Table of Contents

1	Intro to MAFOR.....	3
1.1	Why was a new aerosol model developed?.....	4
1.2	History.....	4
1.3	Model documentation.....	4
1.4	Changes in version 1.9.9.....	5
1.5	Computer information.....	7
1.6	Graphical display.....	7
1.7	Download.....	7
1.8	Problems.....	7
2	Input Files.....	8
2.1	Configuration.....	8
2.2	General.....	12
2.3	Aerosol.....	14
2.4	Gas phase.....	19
2.5	Aqueous phase.....	20
2.6	Organics.....	21
2.7	Dispersion and deposition data.....	24
2.8	Chamber Data.....	27
3	Output Files.....	29
3.1	Concentration output.....	29
3.2	Aerosol output.....	29
3.3	Plume dispersion output.....	32
3.4	SOA distribution output.....	32
4	Running MAFOR.....	33
4.1	Trajectory simulation in boundary layer.....	33
4.2	Chamber experiment.....	33
4.3	Multiphase chemistry of fog/cloud.....	34
4.4	Plume dispersion.....	35
4.5	Nucleation.....	38
4.6	Secondary organic aerosol.....	40
4.7	Condensation of sulfuric acid and organosulfur compounds.....	43
4.8	Coagulation.....	44
4.9	Emission of particles.....	45
5	Test examples.....	46
5.1	Nucleation event.....	47
5.2	Chamber experiment.....	49
5.3	Diesel exhaust dilution and aging.....	51
5.4	Fog cycle chemistry.....	53
5.5	Traffic plume.....	55
5.6	Ammonium nitrate aerosol.....	58
6	References.....	60
7	Appendix A: List of species indices.....	64
8	Appendix B: The Chemical Mechanism of MAFOR v1.9.9.....	74
9	Appendix C: List of Error Messages.....	75

MAFOR v1.9.9 – User’s Guide

1 Intro to MAFOR

The MAFOR (**M**ulticomponent **A**erosol **F**ORmation) model is a zero-dimensional Lagrangian type sectional aerosol box model which includes gas phase and aqueous phase chemistry in addition to aerosol dynamics. MAFOR consistently solves the time evolution of the particle number and mass concentration distribution of a multicomponent aerosol using the fixed sectional method and simultaneously the time-dependent concentrations of chemical compounds in the gas phase and also in the aqueous phase of supermicron droplets. Until MAFOR v1.9, the basic gas phase chemistry and aqueous phase chemistry was based “Module Efficient Calculating the Chemistry of the Atmosphere (MECCA)” from CAABA/MECCA v3.0 (Sander et al., 2011). With MAFOR v2.0, the multiphase chemistry is based on CAABA/MECCA v4.0 (Sander et al., 2019).

The kinetic pre-processor KPP version 2.2.3 (Sandu and Sander, 2006) is used to generate Fortran 90 code for the chemistry module. The Rosenbrock ROS3 solver with automatic time step control is used to integrate the differential equation system of gas phase and aqueous phase reactions. In short, MAFOR is the coupling of the (dynamically generated) chemistry module from MECCA and a new aerosol dynamics module. The treatment of aerosol dynamics is based on the concepts by M. Z. Jacobson described in his book “Fundamentals of Atmospheric Modeling” (Jacobson, 2005a). The MAFOR model offers great flexibility to the user who may decide about the included aerosol processes, the included chemistry, the size resolution of the model aerosol and many other parameters of the simulation.

MAFOR version 1.4 was the first version of the model that was distributed as binary executable on <http://mafor.nilu.no> in June 2012. Version 1.5 fixed a bug for reading tab-delimited input files and improves the calculation of aerosol water content. Version 1.9.5 is the last version of the model that was distributed under a commercial license.

With version 2.0, the source code of the model is released as open source under the GNU General Public License (GPL) as the new community aerosol dynamics box model MAFOR.

The use of MAFOR on a personnel computer (Linux) is quite simple if the instructions and test examples in this User’s Guide are followed. The user should have some experience with running computer models because there are many options in the input files and there is little built-in error checking on the input.

The main intention of distributing the executable of the MAFOR model is the usage for educational purposes. If you should plan to use the model in a research project it is strongly recommended to contact the author (matkar ‘at’ gmail.com) to clarify for example if all necessary processes are implemented in the model.

1.1 Why was a new aerosol model developed?

Novel aspects of the coupled gas phase / aerosol model MAFOR are 1) the full flexibility of gas phase chemistry and the degree of detail specifically in the chemistry of dimethyl sulphide (DMS), isoprene, and amines, 2) the detailed treatment of liquid phase chemistry (gas/liquid equilibrium partitioning, dissociation equilibrium reactions, aqueous phase chemical reactions) in the droplet mode, which can be extended according to needs, 3) simultaneous solution of the time evolution of the particle number and mass distribution of a multicomponent aerosol using a sectional approach. The high flexibility of the chemistry part of MAFOR makes it an ideal tool for future studies on multiphase chemistry of DMS, amines, and other water-soluble organics relevant to the marine atmosphere. The MAFOR model is increasingly used for simplified plume simulations to study the temporal evolution of traffic-generated aerosols, such as vehicle exhaust particles and ship emissions.

The aerosol model MAFOR is very versatile and meanwhile has been adapted to address various research questions: 1) new particle formation over the Arctic Ocean, 2) gas phase chemistry and particle formation in environmental chambers, 3) aqueous phase chemistry of amines in fog/cloud, and 4) ultrafine exhaust particles emitted by road traffic and ship traffic in cities.

1.2 History

The code development for MAFOR started in autumn 2008 using the first released version of MECCA, version 0.9.1 (Sander et al., 2005), KPP version 1.1-f90-alpha12 (Sandu et al., 1997), the code of MONO32 by L. Pirjola, and an aerosol model code freely distributed by K. E. J. Lehtinen at the CESAR Summer School (Research Centre Jülich, Germany, Aug. 21st – Sept. 1st, 2006). The aerosol code was then completely transformed to be in accordance with the treatment by M. Z. Jacobson using the fixed sectional method. The first stable version of the MAFOR model was used in a Lagrangian type scenario simulation for the Arctic Ocean. The model code of MAFOR version 1.0 was finally revised to be in full accordance with theory of aerosol dynamics as published by Karl et al. (2011). In the model versions 1.1, 1.2, and 1.3 mainly the gas phase chemistry of the model was extended and the aerosol dynamic processes were made modular. In version 1.3 the photolysis calculation routine was revised and now data on absorption coefficients and quantum yields recommended by the Jet Propulsion Laboratory (JPL) Evaluation no. 15 is used. In MAFOR version 1.4 the aqueous phase chemistry was comprehensively tested and extended. In version 1.5 the calculation of aerosol water content was improved. In version 1.6 the condensation of ammonium as ammonium bisulphate, ammonium sulphate or ammonium nitrate was included. In version 1.7 the gas phase chemistry was extended and the aqueous phase chemistry was restricted to the droplet mode. In version 1.8 three alternative options for plume dispersion and three alternative options for dry deposition of particles became available. In version 1.9 the Multicomponent Equilibrium Solver for Aerosols (MESA) was coupled to MAFOR to solve the growth of particles by dissolution of nitric acid. MESA is part of the MOSAIC code (Zaveri et al., 2008) distributed with the community developed model WRF-Chem. In version 2.0, the 2-D volatility basis set (VBS) developed by Donahue et al. (2011) was introduced together with nine lumped organic vapor species.

1.3 Model documentation

A detailed model description of MAFOR (version 1.0) is provided in the following article:

Karl, M., Gross, A., Pirjola, L., and C. Leck, A new flexible multicomponent model for the study of aerosol dynamics in the marine boundary layer, *Tellus B*, 63(5), 1001-1025, doi: 10.1111/j.1600-0889.2011.00562.x, 2011.

Applications of the model using later versions of MAFOR are presented in the following articles:

Karl, M., Leck, C., Gross, A. and L. Pirjola, A study of new particle formation in the marine boundary layer over the central Arctic Ocean using a flexible multicomponent aerosol dynamic model, *Tellus B*, 64, 17158, doi: 10.3402/tellusb.v64i0.17158, 2012a.

Karl, M., Dye, C., Schmidbauer, N., Wisthaler, A., Mikoviny, T., D'Anna, B., Müller, M., Clemente, E., Muñoz, A., Porras, R., Ródenas, M., Vázquez, M. and T. Brauers, Study of OH-initiated degradation of 2-aminoethanol, *Atmos. Chem. Phys.*, 12, 1881-1901, 2012b.

Keuken, M., Henzing, J. S., Zandveld, P., van den Elshout, S., and M. Karl, Dispersion of particle numbers and elemental carbon from road traffic, a harbor and an airstrip in the Netherlands, *Atmos. Environ.*, 54, 320-327, 2012.

Karl, M., Leck, C., Coz, E., and J. Heintzenberg, Marine nanogels as a source of atmospheric nanoparticles in the high Arctic, *Geophysical Research Letters*, 40 (14), 3738-3743, doi: 10.1002/grl.50661, 2013.

Pirjola, L., Karl, M., Rönkkö, T., and F. Arnold, Model studies of volatile diesel exhaust particle formation: Organic vapours involved in nucleation and growth?, *Atmos. Chem. Phys.*, 16, 4817-4835, doi:10.5194/acp-16-4817-2016, 2016.

Karl, M., Kukkonen, J., Keuken, M. P., Lützenkirchen, S., Pirjola, L., and Hussein, T., Modeling and measurements of urban aerosol processes on the neighborhood scale in Rotterdam, Oslo and Helsinki, *Atmos. Chem. Phys.*, 16, 4817-4835, doi:10.5194/acp-16-4817-2016, 2016.

Karl, M., Pirjola, L., Karppinen, A., Jalkanen, J.-P., and Ramacher, M. O. P., Kukkonen, J. Modeling of the concentrations of ultrafine particles in the plumes of ships in the vicinity of major harbors, *J. Environ. Res. Public Health*, 17, 777, 1-24, doi:10.3390/ijerph17030777, 2020.

Zhang, X., Karl, M., Zhang, L., and Wang, J., Influence of aviation emission on the particle number concentration near Zurich Airport, *Environ. Sci. Technol.*, 54(22), 14161-14171, doi:10.1021/acs.est.0c02249, 2020.

1.4 Changes in version 1.9.9

Compared to MAFOR version 1.9 the following items were changed:

New utility (preprocessor) FITAERO for fitting of measured multicomponent particle size distributions. FITAERO produces the 'inaero.dat' input file for MAFOR.

Sea-salt particle emission flux, depending on wind speed (hourly changing) sea surface temperature (constant value) and salinity (constant value) using the parameterization of Spada et al. (2013) for the size range of 0.2 μm to 10.0 μm .

Coagulation:

New coagulation option 4: exact correction of the Brownian coagulation kernel for van der Waals and viscous forces is done as in Jacobson and Seinfeld (2004).

New coagulation option 5, allowing both fractal geometry and van der Waals forces (exact correction).

Nucleation:

Extended binary homogeneous nucleation of $\text{H}_2\text{SO}_4\text{-H}_2\text{O}$ to temperatures above $305\text{ }^\circ\text{C}$ according to Vehkamäki et al. (2003).

Implementation of the lookup-table parameterization of ternary nucleation (TIMN) by Yu et al. (2020). TIMN includes both ion-mediated and homogeneous ternary nucleation of $\text{H}_2\text{SO}_4\text{-NH}_3\text{-H}_2\text{O}$ and binary homogeneous nucleation.

Implementation of the new parameterization of neutral and ion-induced sulfuric acid-water nucleation by Määttä et al. (2018).

Implementation of a look-up table based on ACDC calculations for the homogeneous ternary $\text{H}_2\text{SO}_4\text{-NH}_3\text{-H}_2\text{O}$ system (Henschel et al., 2016) published by Baranizadeh et al. (2016).

Condensation of organic vapors:

The number of condensable organic vapors was increased from five to nine, where saturation concentration C_0 and other properties of the organic vapors can be provided in the user input file `organic.dat`. Biogenic secondary oxidized vapors are represented by BSOV (semi-volatile), BLOV (low-volatile) and BELV (extremely low-volatile). Aromatic secondary oxidized vapors are represented by ASOV (semi-volatile), ALOV (low-volatile) and AELV (extremely low-volatile). Primary emitted organic vapors, such as long-chained n-alkanes are represented by PIOV (intermediate volatility), PSOV (semi-volatile) and PELV (extremely low-volatile). All SOA compounds are represented by a gas phase component and a particle phase component. When using the SOA partitioning option, the effective saturation concentrations are calculated according to the 2-D volatility basis set (VBS) developed by Donahue et al. (2011). The new output file `soadis.res` gives saturation concentration, gas-phase concentration of organic vapors and particulate SOA concentrations for the nine lumped organics as function of time.

Dynamic partitioning of secondary inorganic aerosols:

The Multicomponent Equilibrium Solver for Aerosols (MESA), which is part of the MOSAIC code (Zaveri et al., 2008), can be optionally used to calculate the dynamic partitioning of secondary inorganic aerosol. The numerical solution for growth of particles by dissolution in MAFOR now follows the PNG solver presented by Jacobson (2005b). The growth by dissolution of hydrochloric acid is now considered.

Chamber experiment simulation:

For chamber experiments, the wall loss of organic vapors is treated as in Zhang et al. (2014) by using a first-order wall loss rate and the organic aerosol equivalent wall to account for evaporation of organics from the chamber walls. The chamber geometry and the properties of soot particles can be defined in the user input file `incham.dat`.

Plume dispersion simulation:

A new output for the plume dispersion simulations is `plume.res` which contains plume height and temperature. In total, seven different types of plume dispersion parameterizations are now available for use in dispersion for road traffic (type 1,2,4), flow tube chambers (type 3), and ship traffic (type 5-7).

Changed input files:

`dispers.dat` (two extra lines)

`sensitiv.dat` (new options)

`organic.dat` (one extra line for soot particles, several lines for the nine organics)

incham.dat (one extra line for chamber geometry)
inbgair.dat (additional background gas-phase species)

1.5 Computer information

The Linux executable was compiled with **gfortran-9** on Linux Ubuntu with 64bit. Testing was only done with the Linux 64bit executable. For Windows 10, two versions of Ubuntu are available to download from the Microsoft Store: adding to the existing Ubuntu 18.04, Ubuntu 20.04 has also now arrived. Ubuntu 20.04 requires the Windows Subsystem for Linux, WSL 2. The Ubuntu emulation on Windows 10 provides access to the Ubuntu Terminal, as well as the latest version of command line utilities such as bash, ssh, git, apt and so on. In order to install the software, you'll need to enable Windows' Subsystem for Linux. Windows 10 users are encouraged to test the Linux executable on Ubuntu 20.04 and report any issues to the author.

1.6 Graphical display

Several MATLAB scripts for plotting of the model's output are available together with the test examples (see chapter 5) for download. The scripts can be used with MathWorks® MATLAB and with the free open source software GNU Octave (<https://www.gnu.org/software/octave/>). The scripts can be easily modified to plot additional chemical species (see Appendix A) or components of the aerosol (section 3.2).

1.7 Download

Link to the github repository:

<https://github.com/mafor2/mafor.git>

Documentation:

[Users_Guide_MAFOR-v1.9.9.pdf](#)
[meccanism_mafor_v1.9.9.pdf](#)
[gas+aqueous_species-v1.9.9.pdf](#)
[chemprop-v1.9.9.pdf](#)
[README_caaba_mafor](#)

[README_caaba_mafor](#) explains how to add new chemical species and reactions to the chemistry mechanism of MAFOR.

1.8 Problems

First you should try to run the provided Test examples on your computer. If a problem occurs while running the Test examples, please post a description of the problem including information about your computer system and the error message to the Forum of mafor.nilu.no. If you experience problems with running MAFOR on a self created set of input files, contact the author (mattkar ' at' gmail.com) by email with a description of the problem and the error message, including the input files as attachment. A list of MAFOR error messages and instructions how to avoid the error can be found in the new Appendix C.

2 Input Files

This chapter provides an overview of the necessary input files to run the MAFOR model. Complete sets of input files are provided together with the test examples (see chapter 5). All input files are in ASCII format.

A minimum set of input files consists of:

Gas phase:	inchem.dat
Aerosol:	inaero.dat
Organic:	organic.dat
Dispersion	dispers.dat
General:	ingeod.dat
Configuration:	sensitiv.dat

Until now the program does little checking of the input. The program will stop if a required input file does not reside in the same folder. There is however no detailed check on the format and validity of the input data.

2.1 Configuration

The configuration of the MAFOR model run is controlled with the input file sensitiv.dat. With 0|1 switches it is possible to disable/enable certain processes during the model simulation.

Documentation for input file sensitiv.dat is given by the following list.

Entries in first line:

1. dry particle deposition	0 1 2 3	(1=water surface; Schack et al. (1985); 2= forest canopy; Kouznetsov and Sofiev (2012) 3= any rough surface; Hussein et al. (2012))
2. wet particle deposition	0 1	
3. coagulation of particles	0 1 2 3 4 5	(1 Brownian, 2 Brownian with fractal geometry of soot, 3 Brownian corrected for van der Waals forces, 4 Brownian with explicit kernel for van der Waals forces, 5 Brownian with fractal geometry and van der Waals forces)
4. condensation of vapors	0 1	
5. nucleation	0 1	
6. nucleation mechanism	1 2 3 4 5 6 7 8 9 10 11 12	(explanation of the different nucleation options see section 2.7).
7. chamber experiment	0 1 2	(2=wall loss aging chamber)

Entries in second line:

1. condensation of H2SO4 and MSA accommodation)	1 2	(1=accomm. coeff. see Table 4.2, 2= unity)
2. condensation of Organics	0 1	(1=condensation of organic vapors)
3. condensation of Amines	0 1	(if set to 1, AMMO in inaero.dat is treated as aminium)
4. condensation of Ammonium	0 1	(if set to 1, condensation of amines is disabled)
5. emission of particles	0 1 2	(1=continuous particle emission, 2=sea-air particle flux)
6. chemistry integration	0 1	
7. Kelvin effect considered	0 1	

Entries in third line:

1. read DMS and NH3 from input	0 1	(read from ingeod.dat)
2. read O3 from input	0 1	(read from ingeod.dat)
3. read SOA-1 from input	0 1	(read from ingeod.dat)
4. debugging information	0 1	(write to debug.res)
5. dilution with bg particles	0 1 2 3 4 5 6 7	(for plume simulation: 1=type 1, 2=type 2, 3=type 3, 4=type 4, 5=type 5, 6=type 6, 7=type 7)
6. SOA partitioning 2-D VBS	0 1 2	(1=absorptive partitioning, 2=absorptive partitioning + physical adsorption)
7. use nano-koehler	0 1	

Entries in the fourth line:

1. condensation of water	0 1 2	(1= condensation of H2O, 2 = condensation of H2O and MESA thermodynamic module activated)
2. partitioning to aqueous phase	0 1	
3. aqueous phase chemistry	0 1	

Deposition of particles:

In the first line of sensitiv.dat any of the aerosol dynamic processes can be switched off, by setting the flag to 0. For dry deposition to water surface (ocean) it is recommended to use the option 1 (Schack et al. (1985)). For dry deposition to a (vegetation) canopy of height ZCAP with rough surface (e.g. forest) it is recommended to use the option 2 (Kouznetsov and Sovief (2012)). For any rough surface it is recommended to use the option 3 (Hussein et al. (2012)). The control parameters of the two dry deposition schemes are entered in in dispers.dat (section 2.7).

Coagulation of particles:

Brownian coagulation is activated if the coagulation option is set to **1**. By setting the coagulation option to **2**, the effect of fractal geometry on coagulation is taken into account by considering the effect on radius, diffusion coefficient and the Knudsen number in the Brownian collision kernel. The radius of primary spherules is assumed to be 13.5 nm and the fractal dimension is assumed to be 1.7. These parameters can be changed in organic.dat. By setting the coagulation option to **3**, an empirical correction factor accounting for van der Waals and viscous forces is applied to the Brownian collision kernel (Karl et al., 2016). With the coagulation option **4**, an exact correction for van der Waals and viscous forces is done. With coagulation option **5**, both fractal geometry and van der Waals forces (exact correction) are used. Details in section **4.8**.

Nucleation:

It can be chosen among 12 different nucleation mechanisms. Details on the nucleation option are given in section 2.7.

Condensation:

The condensation of organic vapors is explained in section 2.7. The condensation of sulphuric acid and MSA is explained in section 4.7. Condensation of ammonium occurs either as ammonium bisulphate, ammonium sulphate or ammonium nitrate. By setting “Kelvin effect considered” to 1 the condensation of H₂SO₄, MSA; organics, amines, and ammonium will be corrected by the Kelvin effect. By setting “SOA partitioning” to 1 the condensation of organics is corrected by allowing partitioning to the organic liquid mixture following the description in Kerminen et al. (2000). This option makes of the two-dimensional volatility basis set (2-D VBS) developed by Donahue et al. (2011) that employs saturation mass concentration C_0 and the oxygen content (O:C ratio) to describe volatility and mixing thermodynamics of organic aerosol. By setting “SOA partitioning” to 2 in addition considers physical adsorption (Pankow, 1994) to ECBC and DUST primary particles. By setting “use nano-koehler” to 1 the Nano-Köhler theory as outlined by Kulmala et al. (2004) is used. The implementation of Nano-Köhler theory is experimental and its use is not recommended.

Uptake of water and dissolutional growth:

By setting “condensation of water” to 1 the aerosol water content is calculated according to the Zdanovskii-Stokes-Robinson (ZSR) relationship. This option provides the wet diameter of the aerosol based on water content of each size bin. If the option is set to 0, aerosol water will not be considered and only dry diameter is used. Debugging information (debug flag = 1), e.g. on mass and number conservation during condensation and coagulation is written to debug.res.

Setting “condensation of water” to 2 activates the coupling between MAFOR and the MESA model (Zaveri et al., 2005b). MESA solver for solid, liquid and mixed phase aerosols enables the calculation of aerosol water content and activity coefficients of electrolytes in droplets within all size sections using the MTEM (Multicomponent Taylor Expansion Method; Zaveri et al., 2005a). MESA considers the aqueous solution system SO₄²⁻, NH₃/NH₄⁺, HNO₃/NO₃⁻, and typical crustal elements such as K⁺, Mg²⁺, Ca²⁺ of sea-salt and dust aerosols. Every two minutes, MAFOR aerosol components are mapped onto MESA species and the electrolyte composition in each size bin is re-

calculated. Finally, the MESA model calculates the parameters required for using the Analytical Predictor of Nonequilibrium Growth (PNG; Jacobson, 2002, 2005b) to solve growth by dissolution. PNG was implemented and coupled with MESA to solve the growth of particles by dissolution of HNO_3 and HCl . It is recommended to use this option if formation of ammonium nitrate is expected. An example demonstrating the effect of using the MESA/PNG solver is given in section 5.6.

Prescribed concentrations:

Controlled read of concentrations of DMS, NH_3 , O_3 , and SOA-1 from the input column in `ingeod.dat` (every hour) if the the read flag in `sensitiv.dat` is set to 1. If not, time dependent concentrations of these compounds will be calculated by the chemistry solver. In this case, the initial gas-phase concentration, emission strength (if needed) and dry deposition velocity of the chemical species has to be provided in the gas-phase input file `inchem.dat`.

Dilution with background particles:

Plume dispersion simulation are performed when the flag for dilution with background particles is set >0 . Different plume dispersion types, applicable for vehicle exhaust and/or ship exhaust plumes are available. More details are given in section 4.4.

2.2 General

The parameters of the trajectory along which the model is run are set in the input file `ingeod.dat`. Each line of `ingeod.dat` provides hourly values of a range of meteorological and other parameters. The input is read each hour of the model run. An Excel work sheet (`ingeod_prep.xls`) is available in the zip file `helper_tools.zip`. The Excel sheet can be used to prepare the input. Use copy-paste to transfer the content into a text editor (e.g. `notepad++`, <http://notepad-plus-plus.org>) and save as `ingeod.dat`. The input is table-style with 25 columns. The entry in column 11 (`incloud`) is a (0|1) switch; if `incloud=1` a droplet distribution will be prescribed in the fourth (CS) mode (see `inaero.dat`, section 2.3). The droplet number will be calculated using the liquid water content (column 22) assuming spherical droplets. The pH of the droplets is defined in column 23. The first column is runtime, which is the total simulation time period in hours (same value in all lines).

Documentation for input file `ingeod.dat` is given by the following list.

Column	Variable	Description
01	<code>runtime</code>	simulation time [hours]
02	<code>iday</code>	day [dd]
03	<code>imonth</code>	month [mm]
04	<code>starttime</code>	hour [hh]
05	<code>lat_deg</code>	latitude [decimal deg]
06	<code>lon_deg</code>	longitude [decimal deg]
07	<code>temp</code>	temperature [K]
08	<code>press</code>	air pressure [Pa]
09	<code>RH</code>	rel. humidity [-] Note: at $RH > 0.99$ a warning is given that the program may stop. At $RH > 1.1$ the program will stop.
10	<code>zmb1</code>	mixing height [m]
11	<code>incloud</code>	in-cloud flag [-] Note: (1 0) <code>incloud=1</code> prescribes droplet distribution in fourth (CS) mode
12	<code>u10</code>	wind speed 10m [m/s]
13	<code>rain</code>	precip. [mm/h]
14	<code>edms</code>	emission DMS [molec/cm ² /s]
15	<code>eso2</code>	emission SO ₂ [molec/cm ² /s]
16	<code>eh2o2</code>	emission H ₂ O ₂ [molec/cm ² /s]
17	<code>cnh3</code>	conc. NH ₃ [molec/cm ³]
18	<code>camidoh</code>	conc. SOA-1 [molec/cm ³]

19	cdms	conc. DMS [molec/cm3]	
20	co3	conc. O3 [molec/cm3]	
21	fnuc	nucleation scaling factor [-]	
22	lwcm	liquid water [m3/m3]	Note: only used if incloud=1
23	pH	pH of CS mode [-]	Note: only used if incloud=1
24	dila	dispersion parameter [-]	(for plume simulation type 1)
25	dilcoef	dilution coefficient [-]	(for plume simulation type 1)

2.3 Aerosol

2.3.1 Size distribution and aerosol components

The initial aerosol size distribution is provided in the input file `inaero.dat`. The initial aerosol distribution in the four modes (NU: nucleation mode, AI: Aitken mode, AS: accumulation mode, CS: coarse mode) is based on mass. The geometric mean diameter (GMD) of each mode has to be given based on mass. It is convenient to fill `inaero.dat` with mass concentrations (in ng/m^3) of aerosol components measured by a Berner Impactor or an Aerosol Mass Spectrometer (AMS). If measurements of the chemical composition of PM1.0, PM2.5, or PM10 are available, the total mass concentration (e.g. PM2.5) should be distributed between different aerosol components using estimated mass fractions of components in each mode. Finally, the total mass concentration MM (in ng/m^3) of each mode is determined by summing up the component mass concentrations in the mode. Table 2.1 lists the aerosol components and their basic properties included in the model.

Table 2.1 Aerosol components and properties in the MAFOR model.

Component	Name	Density (kg m^{-3})	Volatility
Sulfuric acid /sulfate	SULF	1770	Volatile
Organic Carbon (OC)	ORGC	Calculated according to OC fractions (see section 2.7)	Volatile (see section 2.7)
Ammonium	AMMO	1300	Volatile
Nitrate	NITR	1300	Volatile
Methane sulfonate (MSAp)	MSAP	1770	Volatile
Sea Salt	SALT	2240	Non-volatile
Primary biological material (PBA)	XXXX	1150	Non-volatile
Soot (EC or BC)	ECBC	1200 [Virtanen et al., 2002]	Non-volatile
Mineral Dust	DUST	1400	Non-volatile

The following example demonstrates how mass concentrations are initialized by estimated the mass fraction of each component and the mass concentration in each mode if only PM10 was measured. It is noted that input mass refers to the dry aerosol, and that water mass concentration per mode is calculated and added by the model.

1. Estimated mass fraction of aerosol components per mode

Mode	H2SO4 (frac.)	OC (frac.)	NH4 (frac.)	NO3 (frac.)	MSAp (frac.)	SALT (frac.)	PBA (frac.)	EC (frac.)	ASH (fraction)	Total
NU	0.00	0.00	0.00	0.00	0.00	0.00	0.00	0.00	0.00	0.00
AI	0.70	0.10	0.15	0.05	0.00	0.00	0.00	0.00	0.00	1.00
AS	0.50	0.00	0.20	0.05	0.00	0.25	0.00	0.00	0.00	1.00
CS	0.10	0.00	0.00	0.05	0.00	0.85	0.00	0.00	0.00	1.00

2. Measured total mass (=PM10) and estimated total mass concentration per mode

	Total mass	NU	AI	AS	CS
Mass fraction	1.00	0.00	0.01	0.09	0.90
Mass conc. MM (ng/m^3)	12000	0	120	1080	10800

3. Calculated mass concentration of components per mode

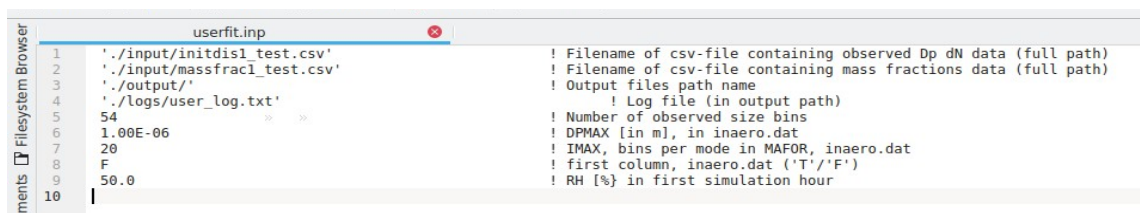
Mode	H2SO4 (ng/m ³)	OC (ng/m ³)	NH4 (ng/m ³)	NO3 (ng/m ³)	MSAp (ng/m ³)	SALT (ng/ m ³)	PBA (ng/m ³)	EC (ng/m ³)	ASH (ng/m ³)	MM (ng/m ³)
NU	0	0	0	0	0	0	0	0	0	0
AI	84	12	18	6	0	0	0	0	0	120
AS	0.50	540	216	54	0	270	0	0	0	1080
CS	0.10	1080	0	0	540	0	9180	0	0	10800

Next, if the initial number concentration distribution was also monitored, the mass distribution should be adjusted to match the number distribution. This can be done by fitting the mass distribution by variation of the (mass-based) geometric mean diameter (GMD) and/or bandwidth (SIGMA) of each mode in inaero.dat such that the calculated number distribution curve matches the measured number distribution curve.

2.3.2 FITAERO

The Fortran program FITAERO performs an automated fitting, creating the inaero.dat input file. The program uses the SIMPLEX algorithm for optimization of a non-linear least squares data fitting problem, by finding the minimum of a function (here the initial number size distribution) of more than one independent variable. The downhill simplex method is originally from Nelder and Mead (1965). The method requires only function evaluations, not derivatives. The actual implementation in FITAERO is based on the SIMPLEX code given in an online lesson from Oregon State University (<http://oregonstate.edu/instruct/ch490/lessons/lesson10.htm>). For multidimensional minimization, the best we can do is to give our algorithm a starting guess for the three parameters (GMD, sigma and mass) as the first point to try. The algorithm then makes its own way downhill through the unimaginable complexity of the 3-dimensional topography, until it encounters a local or global minimum. Three input files are required to run FITAERO: userfit.inp with the basic configuration, a table-style file of the initial particle concentration dN per size bin, and a table-style file of the mass fractions of the aerosol components in each mode.

userfit.inp:



```

userfit.inp
1  './input/initdis1_test.csv'      ! Filename of csv-file containing observed Dp dN data (full path)
2  './input/massfrac1_test.csv'    ! Filename of csv-file containing mass fractions data (full path)
3  './output/'                    ! Output files path name
4  './logs/user_log.txt'          ! Log file (in output path)
5  54                              ! Number of observed size bins
6  1.00E-06                       ! DPMAX [in m], in inaero.dat
7  20                              ! IMAX, bins per mode in MAFOR, inaero.dat
8  F                               ! first column, inaero.dat ('T'/'F')
9  50.0                           ! RH [%] in first simulation hour
10 |

```

The first two lines in userfit.inp give the filename (including relative or full path) of the user-provided file of the monitored number size distribution and of the estimated mass fractions. 3rd line is the path of output directory; 4th line is the location and name of the log file that is written by FITAERO; 5th line is the number of size bins of the monitor data; 6th line is DPMAX (diameter of maximum size in m, same value as in inaero.dat); 7th line is IMAX (number of bins per mode in MAFOR, same value as in inaero.dat); 8th line is the T/F flag in inaero.dat; 9th line is the relative humidity (in %) in the first simulation hour.

initial number size distribution:

Comma-separated file (csv format) containing three lines of data. First line: number of size bin in ascending order, diameter (nm) in each bin, number concentration dN (particles per cubic centimeter) in each bin. The file can be created in an Excel sheet and then saved as csv file. Make sure that values are separated by comma (.). An example of the initial number size distribution file can be found in the FITAERO input directory (initdis1_test.csv).

	A	B	C	D	E	F	G	H	I	J	K	L
1	1	2	3	4	5	6	7	8	9	10	11	12
2	10.4	11.1	12	12.9	13.8	14.9	16	17.2	18.4	19.8	21.3	22.9
3	526	653	716	709	665	635	608	627	796	793	710	661
4												
5												
6												
7												

mass fractions of the aerosol components:

As shown in the example file below (massfrac1_test.csv included in the FITAERO input directory), the mass fraction for each MAFOR aerosol component (H₂SO₄, ORGC, NH₄, NO₃, MSAP, SALT, BPA, EC, and ASH) is given in lines 2-5 for the modes NU, AI, AS, and CS. The sum in each line is controlled in the last column, and should give 1.00.

	A	B	C	D	E	F	G	H	I	J	K	L
1	H ₂ SO ₄	ORGC	NH ₄	NO ₃	MSAP	SALT	BPAB	BC	DUST	Total		
2	0.070	0.680	0.030	0.030	0.000	0.000	0.000	0.190	0.000	1.00		
3	0.196	0.147	0.114	0.297	0.000	0.044	0.000	0.136	0.067	1.00		
4	0.196	0.147	0.114	0.297	0.000	0.044	0.000	0.136	0.067	1.00		
5	0.060	0.147	0.114	0.297	0.000	0.240	0.000	0.062	0.080	1.00		
6												
7												

The output of the program is inaero.dat, that can be directly used for a MAFOR simulation, and out_sizedis.dat, that contains the comparison between fitted dN and (user-provided) observed dN for the user-provided diameters. Both files are created in the output directory specified in userfit.inp.

FITAERO has been tested for a limited number of cases. It is therefore possible that it does not give a suitable solution for the number concentration and mass fraction data provided by the user. It is hoped that over time, enough experience will be collected for various atmospheric particle distributions in order to adjust the program to better match new cases.

2.3.3 Aerosol input files for plume simulation

For a plume simulation, the mass distribution of the background aerosol has to be entered in inbgair.dat. The values in inbgair.dat should be taken from a monitored background aerosol mass distribution, e.g. speciated PM_{2.5} together with estimated mass fractions in the different modes. It is not necessary to provide inbgair.dat for a standard run of the model.

An Excel work sheet (inaero_prep.xls) is available in the zip file helper_tools.zip. The Excel sheet can be used to prepare the input of inbgair.dat and inaero.dat. Use copy-paste to transfer the content into a text editor. FITAERO can also be used to create the input files (inbgair.dat requires some modification). After a first version of inbgair.dat and inaero.dat are created, the model should be run for a short time with the input (abrupt the run by control-C). The computed initial distribution should be compared to the monitored number size distribution and the input should be adjusted to better match the monitored distribution (if the aim is to simulate real world observations). This procedure may have to be repeated until agreement is achieved.

2.3.4 Aerosol input files

The initial aerosol size distribution is provided in the input file `inaero.dat`. This file is always required. The input file `inbgair.dat` with the background aerosol distribution is required if the switch for dilution is set to 1 in `sensitiv.dat`. The input file `emitpar.dat` with constant emission rate for each aerosol component in each mode is required if the switch for particle emission is set to 1 in `sensitiv.dat`.

Documentation for input file `inaero.dat` is given by the following list.

Entries of first line:

01	DPMAX	diameter of max. bin [m] Note: DPMAX can be 1e-5 (10 µm) or 1e-6 (1 µm)
02	IMAX	number of bins per mode

Following lines: one line for each mode NU, AI, AS, CS. in one line, the order is:

01	Number-Option: F/T	If T (true), the initial mass and number concentration will be corrected to maintain the mass of the input (exactly as provided in <code>inaero.dat</code>). The option choice has to be the same in all lines.
02	GMD	geometric mean diameter [m]
03	SIGMA	band width [-]
04	NUMBER	number concentration [#m³]. Value is not used.
05	MSULF	sulfate mass concentration [ng/m³]
06	MORGC	total organic mass (OC) concentration [ng/m³]
07	MAMMO	ammonium mass concentration [ng/m³]
08	MNITR	nitrate mass concentration [ng/m³]
09	MMSAP	methane sulfonate (MSAp) mass concentration [ng/m³]
10	MSALT	sea-salt concentration [ng/m³]
11	MXXXX	primary biological aerosol (PBA) mass concentration] [ng/m³]
12	MECBC	EC or BC mass concentration] [ng/m³]
13	MDUST	mineral dust mass concentration] [ng/m³]

Documentation for input file `inbgair.dat` is given by the following list. Following lines: one line for each mode NU, AI, AS, CS. in one line, the order is:

01	GMD	geometric mean diameter [m]
02	SIGMA	band width [-]
03	MSULF	sulfate mass concentration [ng/m³]
04	MORGC	total organic mass (OC) concentration [ng/m³]
05	MAMMO	ammonium mass concentration [ng/m³]
06	MNITR	nitrate mass concentration [ng/m³]

07	MMSAP	methane sulfonate mass concentration [ng/m ³]
08	MSALT	sea-salt concentration [ng/m ³]
09	MXXXX	primary biological aerosol mass concentration [ng/m ³]
10	MECBC	EC or BC mass concentration [ng/m ³]
11	MDUST	mineral dust mass concentration [ng/m ³]

In the fifth line of inbgair.dat follow the background gas phase concentrations:

01	BGNO	background concentration of NO [molecules/cm ³]
02	BGNO ₂	background concentration of NO ₂ [molecules/cm ³]
03	BGSO ₂	background concentration of SO ₂ [molecules/cm ³]
04	BGO ₃	background concentration of O ₃ [molecules/cm ³]
05	BGNH ₃	background concentration of NH ₃ [molecules/cm ³]
06	BGSULF	background concentration of H ₂ SO ₄ [molecules/cm ³]
07	BGPIOV	background concentration of PIOV [molecules/cm ³]
08	BGPSOV	background concentration of PSOV [molecules/cm ³]

Documentation for input file emitpar.dat is given by the following list. Following lines: one line for each mode NU, AI, AS, CS. in one line, the order is:

01	GMD	geometric mean diameter of emission [m]
02	SIGMA	band width [-]
03	ESULF	sulfate emission rate [ng/m ² /s]
04	EORGC	total organic mass (OC) emission [ng/m ² /s]
05	EAMMO	ammonium emission [ng/m ² /s]
06	ENITR	nitrate emission [ng/m ² /s]
07	EMSAP	methane sulfonate emission [ng/m ² /s]
08	ESALT	sea-salt emission [ng/m ² /s]
09	EXXXX	primary biological aerosol emission [ng/m ² /s]
10	EECBC	EC or BC emission [ng/m ² /s]
11	EDUST	mineral dust emission [ng/m ² /s]

2.4 Gas phase

The initial gas phase concentration, the dry deposition velocity and emission rate for a range of compounds are set in the input file inchem.dat. A list of 81 gas-phase compounds is included in inchem.dat. An Excel work sheet (inchem_prep.xls) is available in the zip file helper_tools.zip. The Excel sheet can be used to prepare the input of inchem.dat. Use copy-paste to transfer the content into a text editor and save as inchem.dat.

Documentation for input file inchem.dat is given by the following list.

One line per chemical compound.

The entry in each line is:

01	compound name	
02	compound index	
03	gas phase concentration	[molecules/cm³]
04	emission rate	[molecules/cm²/s]
05	dry deposition velocity	[cm/s]

Note that compounds between no. 20 and no. 40 are only dummy entries and will be ignored by the program. Also entries for compound no. 43 (CO₂) are ignored. SOA compounds are given in the last nine lines (they can all have emissions).

Emissions of DMS, SO₂ and H₂O₂ given in inchem.dat are not used instead the emissions are taken from ingeod.dat and can vary every hour.

Concentrations of DMS, NH₃, O₃ and SOA-1 can be prescribed in ingeod.dat and can vary every hour. For this the read flags in sensitiv.dat have to be set to 1. If not, time dependent concentrations of the compounds will be calculated by the chemistry solver using the initial concentrations in inchem.dat. NH₃ has been added to inchem.dat as compound no. 72.

2.5 Aqueous phase

The concentration of 14 compounds in the aqueous solution of the droplet mode (see section 2.2) can be initialized in the input file inaqchem.dat. The input file inaqchem.dat is only required if the switch for aqueous phase chemistry is 1 in sensitiv.dat. Compound no. 14 (in_DOC_a) is the dissolved organic carbon.

An Excel work sheet (inaqchem_prep.xls) is available in the zip file helper_tools.zip. The Excel sheet can be used to prepare the input of inchem.dat. Use copy-paste to transfer the content into a text editor and save as inchem.dat.

Documentation for input file inaqchem.dat is given by the following list.

One line per chemical compound.

The entry in each line is:

01	aq. compound name	
02	compound index	
03	concentration in CS mode	[molecules/cm3(air)]

2.6 Organics

The parameters for the organic vapor and the organic aerosol are given in the input file organic.dat. The parameters for defining the fractal geometry and density of soot particles have to be specified in organic.dat as well. The standard values for soot are DENECS = 1200 kg/m³ [Lemmetty et al., 2008], rs = 13.5 nm and Dfrac = 1.7 [Jacobson and Seinfeld (2004)].

Documentation for input file organic.dat is given by the following list.

1st Line:

DENOC	particle density organics [kg/m ³]
surfin	surface tension from input or function [0 1]
surf_org	surface tension organics [kg/s ²]

2nd Line:

DENECS	particle density of soot [kg/m ³]
rs	radius of primary spherules in soot [nm]
Dfrac	fractal dimension of soot [-]

Next lines contain the properties of nine organic vapor classes of the 2D VBS (i.e. BSOV, BLOV, BELV, ASOV, ALOV, AELV, PIOV, PSOV, PELV):

3rd Line:

nc_bsov	number of carbon atoms for BSOV
no_bsov	number of oxygen atoms for BSOV
hvap_bsov	enthalpy of vaporization for BSOV [kJ/mol]
csat0_bsov	saturation concentration C0 for BSOV [ug/m ³]

4th Line:

nc_blov	number of carbon atoms for BLOV
no_blov	number of oxygen atoms for BLOV
hvap_blov	enthalpy of vaporization for BLOV [kJ/mol]
csat0_blov	saturation concentration C0 for BLOV [ug/m ³]

5th Line:

nc_belv	number of carbon atoms for BELV
no_belv	number of oxygen atoms for BELV
hvap_belv	enthalpy of vaporization for BELV [kJ/mol]
csat0_blov	saturation concentration C0 for BELV [ug/m ³]

6th Line:

nc_asov	number of carbon atoms for ASOV
no_asov	number of oxygen atoms for ASOV
hvap_asov	enthalpy of vaporization for ASOV [kJ/mol]
csat0_asov	saturation concentration C0 for ASOV [ug/m ³]

7th Line:

nc_alov	number of carbon atoms for ALOV
no_alov	number of oxygen atoms for ALOV
hvap_alov	enthalpy of vaporization for ALOV [kJ/mol]
csat0_alov	saturation concentration C0 for ALOV [ug/m ³]

8th Line:

nc_aelv	number of carbon atoms for AELV
no_aelv	number of oxygen atoms for AELV
hvap_aelv	enthalpy of vaporization for AELV [kJ/mol]
csat0_aelv	saturation concentration C0 for AELV [ug/m ³]

9th Line:

nc_piov	number of carbon atoms for PIOV
no_piov	number of oxygen atoms for PIOV
hvap_piov	enthalpy of vaporization for PIOV [kJ/mol]
csat0_piov	saturation concentration C0 for PIOV [ug/m ³]

10th Line:

nc_psov	number of carbon atoms for PSOV
no_psov	number of oxygen atoms for PSOV
hvap_psov	enthalpy of vaporization for PSOV [kJ/mol]
csat0_psov	saturation concentration C0 for PSOV [ug/m ³]

11th Line:

nc_pelv	number of carbon atoms for PELV
no_pelv	number of oxygen atoms for PELV
hvap_pelv	enthalpy of vaporization for PELV [kJ/mol]
csat0_pelv	saturation concentration C0 for PELV [ug/m ³]

Next lines contain the mole fraction of SOA components in mode NU to CS:

12th to 20th Line:

gamma-oc1(NU)	mole fraction of SOA-1 in mode NU (0,..,1)
gamma-oc1(AI)	mole fraction of SOA-1 in mode AI (0,..,1)
gamma-oc1(AS)	mole fraction of SOA-1 in mode AS (0,..,1)
gamma-oc1(CS)	mole fraction of SOA-1 in mode CS (0,..,1)

gamma-oc2(NU)	mole fraction of SOA-2 in mode NU (0,..,1)
gamma-oc2(AI)	mole fraction of SOA-2 in mode AI (0,..,1)
gamma-oc2(AS)	mole fraction of SOA-2 in mode AS (0,..,1)
gamma-oc2(CS)	mole fraction of SOA-2 in mode CS (0,..,1)

gamma-oc3(NU)	mole fraction of SOA-3 in mode NU (0,..,1)
gamma-oc3(AI)	mole fraction of SOA-3 in mode AI (0,..,1)
gamma-oc3(AS)	mole fraction of SOA-3 in mode AS (0,..,1)
gamma-oc3(CS)	mole fraction of SOA-3 in mode CS (0,..,1)

gamma-oc4(NU)	mole fraction of SOA-4 in mode NU (0,..,1)
gamma-oc4(AI)	mole fraction of SOA-4 in mode AI (0,..,1)
gamma-oc4(AS)	mole fraction of SOA-4 in mode AS (0,..,1)
gamma-oc4(CS)	mole fraction of SOA-4 in mode CS (0,..,1)

gamma-oc5(NU)	mole fraction of SOA-5 in mode NU (0,..,1)
gamma-oc5(AI)	mole fraction of SOA-5 in mode AI (0,..,1)
gamma-oc5(AS)	mole fraction of SOA-5 in mode AS (0,..,1)
gamma-oc5(CS)	mole fraction of SOA-5 in mode CS (0,..,1)

gamma-oc6(NU)	mole fraction of SOA-6 in mode NU (0,..,1)
gamma-oc6(AI)	mole fraction of SOA-6 in mode AI (0,..,1)
gamma-oc6(AS)	mole fraction of SOA-6 in mode AS (0,..,1)
gamma-oc6(CS)	mole fraction of SOA-6 in mode CS (0,..,1)

gamma-oc7(NU)	mole fraction of SOA-7 in mode NU (0,..,1)
gamma-oc7(AI)	mole fraction of SOA-7 in mode AI (0,..,1)
gamma-oc7(AS)	mole fraction of SOA-7 in mode AS (0,..,1)
gamma-oc7(CS)	mole fraction of SOA-7 in mode CS (0,..,1)
gamma-oc8(NU)	mole fraction of SOA-8 in mode NU (0,..,1)
gamma-oc8(AI)	mole fraction of SOA-8 in mode AI (0,..,1)
gamma-oc8(AS)	mole fraction of SOA-8 in mode AS (0,..,1)
gamma-oc8(CS)	mole fraction of SOA-8 in mode CS (0,..,1)
gamma-oc9(NU)	mole fraction of SOA-9 in mode NU (0,..,1)
gamma-oc9(AI)	mole fraction of SOA-9 in mode AI (0,..,1)
gamma-oc9(AS)	mole fraction of SOA-9 in mode AS (0,..,1)
gamma-oc9(CS)	mole fraction of SOA-9 in mode CS (0,..,1)

Next lines contain reaction rate factors:

21th Line:

feh3so2_dec **scal. Factor activation energy of CH₂SO₂ decomposition**

See section 2.7 for more details on the properties of the organic vapors and regarding the formation of SOA. In the nine lines for the organic mole fraction, one is for each SOA-type. By this, it is possible to prescribe the organic composition in each mode of the existing particles. For each mode (4 columns, NU, AI, AS, CS) the values distributed over the 9 SOA-types have to add up to 1 (in each column). If there is organic mass in the existing aerosol, the values in organic.dat must be non-zero. For example, if the nucleation mode should consist 25 % of each SOA-1 to SOA-4 and the other modes of SOA-2, then the lines in organic.dat would be:

```
0.25 0.00 0.00 0.00
0.25 1.00 1.00 1.00
0.25 0.00 0.00 0.00
0.25 0.00 0.00 0.00
0.00 0.00 0.00 0.00
0.00 0.00 0.00 0.00
0.00 0.00 0.00 0.00
0.00 0.00 0.00 0.00
0.00 0.00 0.00 0.00
```

Parameters for controlling the gas phase chemistry of DMS are in line 20. Currently, the only parameter to vary is a scaling factor for the activation energy of the thermal decomposition of the CH₃SO₂ radical. A standard value of feh3so2_dec is 0.90.

2.7 Dispersion and deposition data

The parameters for plume dispersion (dilution) and dry deposition of particles are given in the input file dispers.dat.

Documentation for input file dispers.dat is given by the following list.

1st Line:

hmix_st	mixing height @ station	[m]
dst_st	distance @ station	[m]
hsta_st	stack height above ground	[m]
ta_st	temperature @ station	[K]

2nd Line:

dil2_b	Type 2 dilution parameter for concentration	[-]
dil2_c	Type 2 dilution parameter for concentration	[s]
dil2_d	Type 2 dilution parameter for temperature	[-]
dil2_e	Type 2 dilution parameter for temperature	[s]
dil2_f	Type 2 dilution parameter for temperature	[-]

3rd Line:

DR_fin	Type 3 dilution: final dilution ratio after PD	[-]
tau_c	Type 3 dilution: dilution lifetime concentration	[s]
T_fin	Type 3 dilution: final temperature after PD	[-]
tau_d	Type 3 dilution: dilution lifetime temperature	[s]
BGH2O	Type 3 dilution: background H2O concentration	[molecules cm ⁻³]

4th Line:

u0	Type 4 dilution: initial exhaust gas velocity	[m/s]
sigw	Type 4 dilution: entrainment velocity	[m/s]
tend1	Type 4 dilution: width of line source 1	[m]
tbeg2	Type 4 dilution: downwind distance of line source 2	[m]
tend2	Type 4 dilution: width of street	[m]

5th Line:

ustar	friction velocity	[m/s]
znot	surface roughness	[m]
ADEP	dry deposition parameter A	
BDEP	dry deposition parameter B	

6th Line:

zcap	height of canopy	[m]
dcol	collector size	[m]
Fplus	roughness parameter (Hussein et al (2012))	[-]

7th Line:

vupdra	updraft velocity (value range 0 ... 0.5)	[m/s]
sst	sea surface temperature	[K]
sal	salinity of seawater	[g/kg]

For all types of plume simulations (see section 4.4) `hmix_st`, `dst_st`, `hsta_st`, and `ta_st` have to be provided in line 1. These are also the parameters required for plume simulation of Type 1.

For the plume simulation Type 2 (see section 4.4), in addition values for parameters `dil2_b`, `dil2_c`, `dil2_d`, `dil2_e`, and `dil2_f` have to be provided.

The plume simulation of Type 3 (diesel exhaust after treatment and ageing chamber) is described in more detail in section 4.4. For Type 3, the parameters `DR_fin`, `tau_c`, `T_fin`, `tau_d` and `BGH2O` have to be provided in line 3.

The plume simulation of Type 4 considers particle emissions from two road traffic line sources (two-stage dilution from road to ambient). The setup of Type 4 is described in more detail in section 4.4. For Type 4, the parameters `u0`, `sigw`, `tend1`, `tbeg2`, `tend2` have to be provided in line 4.

Dry deposition of particles is parameterized by `ustar` (friction velocity) and `znot` (surface roughness length). For dry deposition to water surface (ocean) it is recommended to use the parameterization by Schack et al. (1985). For this the dry deposition flag in `sensitiv.dat` has to be set to 1. The default set of parameters for water surfaces is: `ustar`=1.17, `znot`=0.001, `ADEP`=1.7, and `BDEP`=51.8. Table 2.2 shows the parameter values for other surfaces. For dry deposition to a canopy with rough surface (e.g. forest) it is recommended to use the option 2 (Kouznetsov and Sovief (2012)). The control parameters `zcap` (canopy height z) and `dcol` (collector size d_c) can be changed in `dispers.dat`. Typical values for `dcol` are 0.002 m for bare soil, 0.002 m for conifer forest and 0.02 m for broad-leaf forest. A logarithmic wind profile is assumed in the canopy. For dry deposition to rough surfaces it is recommended to use option 3 (Hussein et al. (2012)). The control parameter for the roughness of a surface, `Fplus`, can be changed in `dispers.dat`.

Table 2.2 Dry depositon of particles: parameter sets for option 1. Adopted from Schack et al. (1985). Values for `F+` adapted from Hussein et al. (2012).

Surface	<code>ustar</code> Friction velocity (m/s)	<code>znot</code> Surface Roughness (m)	<code>ADEP</code>	<code>BDEP</code>	<code>Fplus</code> F^+
Rye grass		0.008	8.99	186	
Crushed Gravel (road)	1.33	0.0013	4.0	121	0.55
Sticky Artificial Grass	0.50	0.01	2.39	885	0.4
Artificial Grass	0.19	0.0012	27.3	400	1.6
Grass	0.36	0.01			0.5
Water	1.17	0.001	1.7	51.8	0.2
Water	0.44	0.0002	0.19	18.8	0.5
Moss		0.0037	9.41	422	

Figure 2.1 shows a comparison of dry deposition velocity option 1 (black line), option 2 (red line), and option 3 (blue line) for water with $u_* = 1.17$, $z_0 = 1$ mm and average particle density of 1400 kg/m^3 .

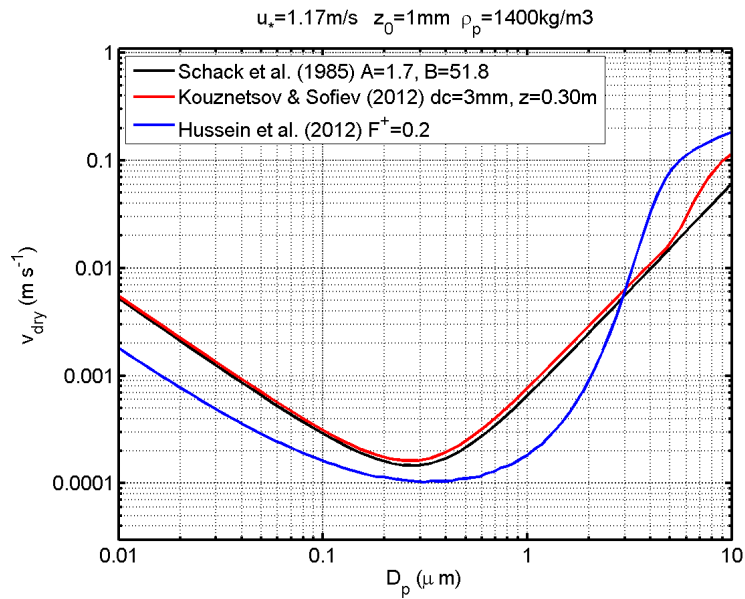


Figure 2.1 Dry deposition of particles with option 1 (black line), option 2 (red line), and option 3 (blue line).

2.8 Chamber Data

Two input files are required for the simulation of chamber experiments: `incham.dat` and `monitor.dat`. The two input files are only required if the chamber experiment switch in `sensitiv.dat` is set to 1. The input file `incham.dat` is used to control the chamber experiment simulation. The input file `monitor.dat` provides input of parameters monitored during a chamber experiment for every minute. Currently only chamber experiments on the photo-oxidation of amines have been simulated with the model and therefore the input file `incham.dat` is very specific for amines, but it is possible to simulate chamber experiments for various VOC. The wall loss of organic vapors is treated as in Zhang et al. (2014) by using a first-order wall loss rate and the organic aerosol equivalent wall to account for evaporation of organics from the chamber walls. The wall loss of VOC and major gaseous oxidation products is approximated by the wall loss rate of O_3 , given by the model user. The wall loss of particles (diffusion to surfaces and sedimentation) is controlled in `sensitiv.dat`, by setting the deposition flag to 0 (no wall loss) or 1 (wall loss activated).

Documentation for input file `incham.dat` is given by the following list.

Entries in first line:

IAM	selected amine (1-6; 1: MEA, 2: methylamine, 3: dimethylamine, 4: trimethylamine, 5: methylnmethanimine, 6: AMP) [ignore if not an amine experiment]
IOZ	read O3 conc from monitor.dat
KP_NIT	dissociation constant Amine-NO3 (molec/cm3)²
F_HONO	scaling factor HONO source
ya_soan1	SOA-1 yield (0-1)
ya_soan2	SOA-2 yield (0-1)
fco	scaling factor Amine-NO3 condensation rate

Entries in second line:

fkoh_mea	scaling factor k(MEA+OH)	(Note: only for IAM=1)
caml	nucleation constant (m³/molec/s)	
K_DIL	dilution rate constant for gases (s⁻¹)	
L_MEA	MEA wall loss rate constant (s⁻¹)	(Note: only for IAM=1)
L_NO2	NO2 wall loss rate constant (s⁻¹)	
L_HNO3	HNO3 wall loss rate constant (s⁻¹)	
L_O3	O3 wall loss rate constant (s⁻¹)	

Entries in third line:

DILPAR	dilution rate constant for particles (s⁻¹)
V_CHAM	Volume of the chamber (m³)
S_CHAM	Total surface area of the chamber (m²)

S_SED	Sedimentation surface area of the chamber (m2)
S_DIF	Diffusion surface area of the chamber (m2)
CWIN	Equivalent wall organic aerosol (mg/m3)

For the EUPHORE chamber, the following values apply: $DILPAR = 7 \times 10^{-6} \text{ s}^{-1}$, $V_CHAM = 177 \text{ m}^3$, $S_CHAM = 177 \text{ m}^2$ (giving a surface on volume ratio $S/V = 1$), $S_SED = 65 \text{ m}^2$, $S_DIF = 130 \text{ m}^2$, and $CWIN = 10 \text{ mg/m}^3$. The typical range of the equivalent wall organic aerosol is 2-20 mg/m^3 .

Documentation for input file monitor.dat is given by the following list.
One line for every minute of the simulation. In one line, the order is:

c(O3)	concentration of O3 in ppbv
c(NO)	concentration of NO in ppbv
c(NO2)	concentration of NO2 in ppbv
jno2m	measured j(NO2) in s-1
temp	measured temperature in K
c(IPN)	concentration of isopropyl nitrite (IPN) in ppbv (0.0 if not present)

3 Output Files

All output files generated by the MAFOR model are in table-style ASCII format. Every 60 second of the simulation a new line is added to the output files (note exception for plume dispersion simulations, section 4.4). The first column of the output file is the time of day in seconds.

For every simulation the following output files are generated:

Concentrations (gas phase and aq. phase)	concout.res
Mass concentration (aerosol components)	aerconc.res
Number size distribution	size_dis.res
Mass size distribution	size_dism.res
Total number concentration	total_n.res
Wet aerosol diameter	wetdp.res
Dispersion parameters	plume.res
SOA distribution	soadis.res
Debugging information	debug.res

3.1 Concentration output

The output file concout.res contains the concentrations of all compounds of the chemical mechanism in the gas phase and aqueous phase (unit: molecules/cm³(air)).

The last four columns of concout.res are: liquid water content (units m³/m³) of NU, AI, AS, and CS mode.

Appendix A provides a list of indices of the compounds in concout.res for use with MATLAB plotting scripts.

3.2 Aerosol output

The format of the number size distribution output file size_dis.res is (table R x C, R rows and C columns):

Line (1:R,1)	time of day	[s]	
Line (1,2:C)	dry diameter per bin	[m]	
Line (2,2:C)	dlogDp per bin	[-]	Note: natural log
Line (3:R,2:C)	dN/dlogDp per bin	[#/m ³]	Note: natural log

The format of the output file of the mass size distribution of dry particles, size_dism.res is (table M x N, M rows and N columns):

Line (1:R,1)	time of day	[s]	
Line (1:R,2:C)	dM/dlogDp per bin	[kg/m ³]	Note: natural log

For plume dilution type 3 and type 4 the output format of size_dism.res is

Line (1:R,1)	time of day	[s]	
Line (1,2:C)	dM/dlogDp per bin	[kg/m ³]	
Line (2,2:C)	dSulfate/dlogDp per bin	[ng/m ³]	
Line (3,2:C)	dMSAp/dlogDp per bin	[ng/m ³]	

Line (4,2:C)	dNitrate/dlogDp per bin	[ng/m3]
Line (5,2:C)	dAmine/dlogDp per bin	[ng/m3]
Line (6,2:C)	dAmmonium/dlogDp per bin	[ng/m3]
Line (7,2:C)	dSOA-1/dlogDp per bin	[ng/m3]
Line (8,2:C)	dSOA-2/dlogDp per bin	[ng/m3]
Line (9,2:C)	dSOA-3/dlogDp per bin	[ng/m3]
Line (10,2:C)	dSOA-4/dlogDp per bin	[ng/m3]
Line (11,2:C)	dSOA-5/dlogDp per bin	[ng/m3]
Line (12,2:C)	dSOA-6/dlogDp per bin	[ng/m3]
Line (13,2:C)	dSOA-7/dlogDp per bin	[ng/m3]
Line (14,2:C)	dSOA-8/dlogDp per bin	[ng/m3]
Line (15,2:C)	dSOA-9/dlogDp per bin	[ng/m3]
Line (16,2:C)	dSalt/dlogDp per bin	[ng/m3]
Line (17,2:C)	dSoot/dlogDp per bin	[ng/m3]
Line (18,2:C)	dDust/dlogDp per bin	[ng/m3]
Line (19,2:C)	dPBA/dlogDp per bin	[ng/m3]
Line (20,2:C)	dWater/dlogDp per bin	[ng/m3]

On line 21 again dM/dlogDp and so on.

The format of the wet diameter output file wetdp.res is (table R x C, R rows and C columns):

Line (1:R,1)	time of day	[s]
Line (1:R,2:C)	wet diameter per bin	[m]

The wet diameter will only be calculated if the switch for condensation of water is 1 in sensitiv.dat. Otherwise the output will be constant dry diameter. Calculation of the wet diameter depends on relative humidity and the aerosol composition.

Documentation for aerosol mass concentration output file aerconc.res is given by the following list (table R x C, R rows and C columns):

Line (1:R,1)	time of day	[s]
Line (1:R,2)	sulfate mass concentration NU mode	[ng/m3]
Line (1:R,3)	sulfate mass concentration AI mode	[ng/m3]
Line (1:R,4)	sulfate mass concentration AS mode	[ng/m3]
Line (1:R,5)	sulfate mass concentration CS mode	[ng/m3]
Line (1:R,6)	MSAp mass concentration NU mode	[ng/m3]
Line (1:R,7)	MSAp mass concentration AI mode	[ng/m3]
Line (1:R,8)	MSAp mass concentration AS mode	[ng/m3]
Line (1:R,9)	MSAp mass concentration CS mode	[ng/m3]
Line (1:R,10)	PBA mass concentration NU mode	[ng/m3]
Line (1:R,11)	PBA mass concentration AI mode	[ng/m3]
Line (1:R,12)	PBA mass concentration AS mode	[ng/m3]
Line (1:R,13)	PBA mass concentration CS mode	[ng/m3]
Line (1:R,14)	OC mass concentration NU mode	[ng/m3]
Line (1:R,15)	OC mass concentration AI mode	[ng/m3]
Line (1:R,16)	OC mass concentration AS mode	[ng/m3]
Line (1:R,17)	OC mass concentration CS mode	[ng/m3]
Line (1:R,18)	ammonium mass concentration NU mode	[ng/m3]
Line (1:R,19)	ammonium mass concentration AI mode	[ng/m3]
Line (1:R,20)	ammonium mass concentration AS mode	[ng/m3]

Line (1:R,21)	ammonium mass concentration CS mode	[ng/m ³]
Line (1:R,22)	nitrate mass concentration NU mode	[ng/m ³]
Line (1:R,23)	nitrate mass concentration AI mode	[ng/m ³]
Line (1:R,24)	nitrate mass concentration AS mode	[ng/m ³]
Line (1:R,25)	nitrate mass concentration CS mode	[ng/m ³]
Line (1:R,26)	EC mass concentration NU mode	[ng/m ³]
Line (1:R,27)	EC mass concentration AI mode	[ng/m ³]
Line (1:R,28)	EC mass concentration AS mode	[ng/m ³]
Line (1:R,29)	EC mass concentration CS mode	[ng/m ³]
Line (1:R,30)	dust mass concentration NU mode	[ng/m ³]
Line (1:R,31)	dust mass concentration AI mode	[ng/m ³]
Line (1:R,32)	dust mass concentration AS mode	[ng/m ³]
Line (1:R,33)	dust mass concentration CS mode	[ng/m ³]
Line (1:R,34)	seasalt mass concentration NU mode	[ng/m ³]
Line (1:R,35)	seasalt mass concentration AI mode	[ng/m ³]
Line (1:R,36)	seasalt mass concentration AS mode	[ng/m ³]
Line (1:R,37)	seasalt mass concentration CS mode	[ng/m ³]
Line (1:R,38)	water mass concentration NU mode	[ng/m ³]
Line (1:R,39)	water mass concentration AI mode	[ng/m ³]
Line (1:R,40)	water mass concentration AS mode	[ng/m ³]
Line (1:R,41)	water mass concentration CS mode	[ng/m ³]

The last aerosol output file is total_n.res. It contains total number concentration and a series of other aerosol parameters. Documentation for output file total_n.res is given by the following list (table R x C, R rows and C columns):

Line (1:R,1)	time of day	[s]
Line (1:R,2)	number concentration of nucleation mode particles with diameter>3nm	[#/m ³]
Line (1:R,3)	number concentration of nucleation mode NU	[#/m ³]
Line (1:R,4)	number concentration of Aitken mode AI	[#/m ³]
Line (1:R,5)	number concentration of accumulation mode AS	[#/m ³]
Line (1:R,6)	number concentration of coarse mode CS	[#/m ³]
Line (1:R,7)	number concentration of particles with 10-25 nm diameter	[#/m ³]
Line (1:R,8)	number concentration of particles with 25-100 nm diameter	[#/m ³]
Line (1:R,9)	loss rate of amine to particles	[1/s]
Line (1:R,10)	coagulation sink	[1/s]
Line (1:R,11)	condensation sink organic vapour	[1/s]
Line (1:R,12)	total growth rate	[m/s]
Line (1:R,13)	nucleation rate	[m ³ /s]
Line (1:R,14)	number concentration of particles with 25-50 nm diameter	[#/m ³]
Line (1:R,15)	number concentration of particles with 50-75 nm diameter	[#/m ³]
Line (1:R,16)	number concentration of particles with 75-1000 nm diameter	[#/m ³]
Line (1:R,17)	number concentration of particles with 1-2 μ m diameter	[#/m ³]
Line (1:R,18)	number concentration of particles with >2 μ m diameter	[#/m ³]
Line (1:R,19)	PNC1, particles with <25 nm diameter	[#/m ³]
Line (1:R,20)	PNC2, particles with 25-50 nm diameter	[#/m ³]
Line (1:R,21)	PNC3, particles with 50-75 nm diameter	[#/m ³]
Line (1:R,22)	PNC4, particles with 75-1000 nm diameter	[#/m ³]
Line (1:R,23)	PNC5, particles with 1-2 μ m diameter	[#/m ³]

Line (1:R,24)	PNC6, particles with >2 μm diameter	[#/m ³]
Line (1:R,25)	Ambient supersaturation ratio	[-]
Line (1:R,26)	Fraction of activated particle number	[-]
Line (1:R,27)	Fraction of activated mass	[-]
Line (1:R,28)	Critical particle diameter for activation	[m]
Line (1:R,29)	Air temperature	[K]

3.3 Plume dispersion output

The output file plume.res contains plume height, temperature, dilution rate and other parameters for plume dispersion.

Line (1:R,1)	time of day	[s]
Line (1:R,2)	time of plume travel	[s]
Line (1:R,3)	plume temperature	[K]
Line (1:R,4)	plume height	[m]
Line (1:R,5)	plume width	[m]
Line (1:R,6)	plume area	[m ²]
Line (1:R,7)	dilution rate	[1/s]
Line (1:R,8)	vapour concentration of H ₂ SO ₄	[$\mu\text{g}/\text{m}^3$]
Line (1:R,9)	vapour concentration of PIOV	[$\mu\text{g}/\text{m}^3$]
Line (1:R,10)	vapour concentration of PSOV	[$\mu\text{g}/\text{m}^3$]
Line (1:R,11)	vapour concentration of PELV	[$\mu\text{g}/\text{m}^3$]
Line (1:R,12)	total particle number emission rate	[1/(m ² s)]

3.4 SOA distribution output

The output file soadis.res is given by the following list (table R x C, R rows and C columns):

Line (1:R,1)	time of day	[s]
Line (1:R,2:10)	effective saturation concentration C*	[$\mu\text{g}/\text{m}^3$]
Line (1:R,11:19)	SOA gas-phase concentration	[$\mu\text{g}/\text{m}^3$]
Line(1:R,20:28)	SOA particle phase concentration	[$\mu\text{g}/\text{m}^3$]

4 Running MAFOR

4.1 Trajectory simulation in boundary layer

The most common application of an atmospheric aerosol/chemistry box model is probably the multi-day run of a clear sky situation along a trajectory or at a fixed observation location, assuming a well-mixed (homogeneous) boundary layer. The set of input files for a boundary layer simulation is:

Gas phase:	inchem.dat
Aerosol:	inaero.dat
Organic:	organic.dat
General:	ingeod.dat
Dry deposition	dispers.dat
Configuration:	sensitiv.dat

In sensitiv.dat the switches for aerosol processes should probably be 1 (“switched on”), the chemistry integration switch and the water condensation switch should also be 1. To prescribe the concentrations of DMS, NH₃, O₃ or SOA-1 the corresponding switches should be 1. All other switches can be 0. In ingeod.dat, lat_deg, lon_deg, temp, press, RH, u10 and zmb1 can be taken from an observed or calculated (pseudo-)trajectory. The switch incloud should be 0. A rainfall (drizzle) rate can be entered in the column rain. This rate will be used for wet scavenging of particles (wet deposition switch of 1 in sensitiv.dat). If all lines have the same values for lat_deg and lon_deg, the simulation is at a fixed location. The columns edms, eso2 and eh2o2 can be used to prescribe emissions of DMS, SO₂ and H₂O₂ if the corresponding switches in sensitiv.dat are set to 1. The corresponding entries in the emission column of inchem.dat will not be used. Gas phase concentrations of NH₃ can either be prescribed (every simulation hour) by using column cnh3 in ingeod.dat (set NH₃ flag in sensitiv.dat to 1) or computed freely as time-dependent concentrations (set NH₃ flag in sensitiv.dat to 0) using the supplied initial concentration and emission rate in inchem.dat.

A test example for a boundary layer simulation of a nucleation event is given in section 5.1.

4.2 Chamber experiment

The simulation of a chamber photo-oxidation experiments is the most adequate application of an aerosol/chemistry box model because the chamber volume is well-mixed.

The set of input files for a chamber experiment simulation is:

Gas phase:	inchem.dat
Aerosol:	inaero.dat
Organic:	organic.dat
General:	ingeod.dat
Configuration:	sensitiv.dat
Chamber control	incham.dat
Chamber monitors	monitor.dat

The chamber experiment switch in sensitiv.dat has to be 1, to read the information from incham.dat and moinitor.dat. Simulation of SOA formation in a chamber experiment is currently possible for amine experiments with different amines (incham.dat: switch IAM; 1: MEA, 2: methylamine, 3: dimethylamine, 4: trimethylamine, 5: methylmethanimine), for experiments with alpha-pinene

(APIN) and other terpenes, for isoprene and for aromatic VOC (toluene, xylene, trimethylbenzene). The molar yields of gaseous SOA precursors in the oxidation of these VOC is given in Table 4.2; see Section 4.6.

Simulation of experiments on gas phase oxidation of all the compounds that can be initialized in `inchem.dat` are possible. Monitored mixing ratios of NO and NO₂ in ppb, temperature in K and monitored photolysis rate of NO₂ in s⁻¹ are read every minute from `monitor.dat`. In addition, mixing ratio of O₃ in ppb will be read from `monitor.dat` if the switch IOZ is set 1 in `inchem.dat`.

Deposition of particles to the chamber walls is calculated by the model according to wall loss in the EUPHORE photoreactor; the wall loss rate of particles cannot be influenced by the user. The wall loss rate of organic vapors (SOA_{gas}) is determined by their saturation concentration and the equivalent wall organic aerosol. A test example for a chamber experiment simulation is given in section 5.2.

4.3 Multiphase chemistry of fog/cloud

Multiphase chemistry can also be simulated with the MAFOR model. This simulation considers chemistry in the gas phase and in the aqueous phase of droplets with diameter >1 μm. Fog or cloud events can be prescribed during the simulation in order to simulate a cycle of subsequent dry air and fog/cloud periods. The aerosol processes can also be considered in a multiphase chemistry simulation but this has not been tested thoroughly until now. The set of input files for a multiphase chemistry simulation is:

Gas phase:	<code>inchem.dat</code>
Aerosol:	<code>inaero.dat</code>
Organic:	<code>organic.dat</code>
General:	<code>ingeod.dat</code>
Dry deposition	<code>dispers.dat</code>
Configuration:	<code>sensitiv.dat</code>
Aqueous phase	<code>inaqchem.dat</code>

In `sensitiv.dat` all switches in the first and third line should be set to 0. In the second line only the chemistry integration should be 1. In the fourth line all the switches for partitioning to aqueous phase and for aqueous phase chemistry should be 1. The input file `inaqchem.dat` is read by the program if the aqueous chemistry switch is set to 1. The entries in `inaqchem.dat` will be used to initialize the aqueous phase composition in the droplets of the coarse (CS) mode if the simulation starts with fog/cloud (switch `incloud=1` in `ingeod.dat`). The following switches in `ingeod.dat` are relevant for the multiphase chemistry simulation: `incloud`, `lwcm` and `pH`. For the hours of the simulation with fog/cloud (line with `incloud=1`) a droplet distribution in the CS mode will be calculated based on the liquid water content provided in the column `lwcm` (and the geometric mean diameter of the CS mode) and the `pH` of the droplets in the CS mode will be set to the value provided in the column `pH`. Time dependent concentrations of aqueous phase compounds in the CS droplet mode will be calculated and written to the output in `concout.res`. The liquid water content of the CS mode is written to the last column of `concout.res`. If `incloud=0` follows the lines with `incloud=1` in `ingeod.dat` the fog evaporates and all droplets disappear, all dissolved gases will evaporate and the ionic compounds will remain stored in a “virtual” aqueous phase.

A test example for multiphase chemistry of a fog cycle is given in section 5.4.

4.4 Plume dispersion

The processes during the dilution of a plume from a industrial or traffic source are of great interest and therefore the possibility to perform a simulation of plume dispersion (along a x-axis) was implemented in MAFOR. The set of input files for a boundary layer simulation is:

Gas phase:	inchem.dat
Aerosol:	inaero.dat
Background aerosol	inbgair.dat
Organic:	organic.dat
General:	ingeod.dat
Dilution	dispers.dat
Configuration:	sensitiv.dat

The presumed situation is the dilution of an aerosol or gas mixture present close to an emission source (emission and the early stage of the plume is not implemented in MAFOR) with increasing time (distance along the x-axis), by entrainment of background air.

MAFOR offers four types of dilution parameterizations which assume a circular cross-section of the plume, in the following termed “Plume dispersion Type 1”, “Plume dispersion Type 2”, “Plume dispersion Type 3”, and “Plume dispersion Type 4”. When choosing the dilution options 1 or 2, a model time step of $t = 0.1$ s will be automatically applied. When choosing the dilution options 3 or 4, a model time step of $t = 0.01$ s will be automatically applied. The latter will increase the run time of the simulation. Calculations with option 3 and 4 are limited to 60 s and 120 s simulation time, respectively. Option 1 and 2 gives output every second while option 3 and 4 gives output every 0.1 s.

Further, MAFOR offers three types of dilution parameterizations which assume a semi-elliptic cross-section of the plume, in the following termed “Plume dispersion Type 5”, “Plume dispersion Type 6”, and “Plume dispersion Type 7”. For options 5-7, a model time step of $t = 0.1$ s will be applied and output is given every second. These three types are intended specifically for the dispersion of ship exhaust plumes. In the ship plume study by Karl et al. (2020), the “Plume dispersion Type 1” has been used.

Plume dispersion Type 1

The dilution of the traffic-influenced aerosol by background air was approximated by fitting a power-law function $y = a \cdot x^{-b}$ (where $x = u \cdot t$ with “u” the wind speed and “t” the time); where a is “dila” and b is “dilcoef” in the input file `ingeod.dat`. Temperature of the plume decreases correspondingly. The change of plume height with time is calculated according to the plume dispersion equations presented by Pohjola et al. (2003). The dilution switch in `sensitiv.dat` has to be set to 1 for dispersion Type 1.

Plume dispersion Type 2

The dilution of the traffic-influenced aerosol concentrations by background air was approximated by fitting a power-law function of the form: $y = (t+b)^c$ (with “t” being the time), where b is “dil2_b” and c is “dil2_c” in the input file `organic.dat`. Parameter “dil2_c” can take values between 0 and -2. The temperature in the plume is approximated with a separate function of the form: $T_{pl} = d \cdot (t+e)^f + T_{air}$, where d is “dil2_d”, e is “dil2_e”, and f is “dil2_f” in the input file `dispers.dat`. Values of the Type 2 parameters have to be provided in line 2 of the input file `dispers.dat`. The change of plume height with time is calculated according to the plume dispersion equations presented by Pohjola et al. (2003). The dilution switch in `sensitiv.dat` has to be set to 2 for dispersion Type 2.

Plume dispersion Type 3

The dilution of diesel exhaust in a laboratory dilution system with zero air is modelled by the exponential equation $DR(t) = DR_{fin}^{1/\tau_c}$, (with “t” being the time) where “DR_fin” is the final dilution rate after the primary diluter (PD) and “tau_c” is the dilution time constant for concentrations, i.e. the time in which the system has achieved the final dilution ratio. The temperature during dilution is assumed to follow Newtonian cooling, with $T_{pl}(t) = T_{fin} + (T_1 - T_{fin}) \cdot \exp(-t/\tau_d)$, where “T_fin” is the final exhaust temperature after PD and “tau_d” is the dilution time constant for temperature, i.e. the time when the remaining excess temperature is ~37% (=1/e %) of the raw exhaust temperature T1. The value of the raw exhaust temperature is “ta_st” in dispers.dat. Further, “BGH2O” is the background H2O concentration in the diluting air. Values of the Type 3 parameters have to be provided in line 3 of the input file dispers.dat. The dilution switch in sensitiv.dat has to be set to 3 for dispersion Type 3. Type 3 produces output every 0.1 s. Wall loss of H₂SO₄ in the ageing chamber (when time is > tau_d) can be taken into account by setting ICHAM to 2 in sensitiv.dat. The wall of sulphuric acid is treated according to Vouitsis et al. (2005).

Plume dispersion Type 4

Two-component dilution scheme for the dilution of vehicular traffic exhaust between the road edge and ambient air for a street with two line emission sources (air parcel moving over the street and picking up emissions). In the first dilution stage (along the width of the street until kerbside) the dilution function is derived from the jet plume model of Vignati et al. (1999), which considers the entrainment of fresh air due to the jet effect of the exhaust gas. For this model, the initial exhaust gas velocity “u0” and entrainment velocity “sigw” have to be provided in line 4 of the input file dispers.dat. In the second dilution stage, from kerbside to ambient the power-law function (as in Type 1) is used, for which parameter values of “dila” and “dilcoef” have to be provided in ingeod.dat. The remaining parameters describe the geometry of the traffic line sources in the street. One line source represents the vehicular traffic into one direction and can in principle consist of several lanes. The configuration of Type 4 considers two line sources. The geometry parameters are given in line 4 of dispers.dat: the width of line source no. 1 “tend1”, the downwind distance of line source no. 2 “tbeg2”, and the total width of the street “tend2”. The dilution switch in sensitiv.dat has to be set to 4 for dispersion Type 4.

Plume dispersion Type 5

Type 5 represents Gaussian dispersion with a semi-elliptic plume cross section. The dilution rate is given by $\lambda_{dil}(t) = 1/A_{pl} * dA_{pl}/dt$, where A_{pl} is the cross-section area of the plume. The time-dependent plume width and height are described by two power-laws. Type 5 can be used for dispersion scenarios of ship exhaust plumes. The plume dispersion parameters for Type 5 cannot be changed by the user. The dilution switch in sensitiv.dat has to be set to 5 for dispersion Type 5.

Plume dispersion Type 6

Modification of the Gaussian dispersion based on the formulation of Konopka (1995) that consider a horizontal and linear shear flow. Type 5 is recommended for dispersion scenarios of ship exhaust plumes in ports or close to shoreline. The plume dispersion parameters for Type 6 cannot be changed by the user. The dilution switch in sensitiv.dat has to be set to 6 for dispersion Type 6.

Plume dispersion Type 7

Valid for dispersion of ship plumes under convective conditions in the marine boundary layer (open sea) based on the parameterization of dispersion rates by Chosson et al. (2008). The plume dispersion parameters for Type 7 cannot be changed by the user. The dilution switch in sensitiv.dat has to be set to 7 for dispersion Type 7.

General notes:

Currently only dispersion of an (emitted) aerosol, NO, NO₂, SO₂, SO₃, H₂SO₄, NH₃ and the organic vapor compounds in a plume can be simulated. The dilution of other gases is not yet implemented. In the input file sensitiv.dat, the switch for dilution with background particles needs to be set to 1 in order to read the input file inbgair.dat which contains the background aerosol distribution and composition. The gas-phase concentrations in inchem.dat will be used as the initial concentrations inside the plume when the dispersion run is performed.

The gas-phase concentrations of the background air (NO, NO₂, SO₂, O₃, NH₃, H₂SO₄, PIOV, PSO_V) have to be given in inbgair.dat. Therefore O₃ concentration in inchem.dat should be zero or a very small value. The background O₃ is now given in inbgair.dat; O₃ will entrain into the plume with increasing time with a plume entrainment rate having the same value as the dilution rate.

In the input file ingeod.dat, the values of the dispersion parameters should be entered in the columns dila and dilcoef. Realistic parameter values of “dila” and “dilcoef” in ingeod.dat have to be provided for Type 1, Type 2 and Type 4.

In the input file dispers.dat, in line 1 the values for hmix_st (initial plume height), dst_st (distance of starting point from source), hsta_st (height of stack above the ground), and ta_st (plume temperature at starting point) need to be entered for all plume dispersion simulations. These values characterize the initial state of the plume and depends on the distance of the starting point location (=station) from the emission source point.

In plume dispersion simulations the box height corresponds to the plume height instead of the boundary layer height (given in ingeod.dat). The height of the box is therefore increased with time and is recalculated every time step. Meteorological data is updated every hour using the values in ingeod.dat.

A test example for plume dispersion Type 1 from a traffic-related aerosol is given in section 5.5 . A test example for plume dispersion Type 3 for the evolution of diesel exhaust particles in a laboratory dilution system is given in section 5.3.

4.5 Nucleation

MAFOR can be used with 12 different nucleation mechanisms to simulate new particle formation. Nucleation will be used if the nucleation switch is set to 1. Then one of the nucleation options 1-13 can be selected. The parameterized nucleation schemes have been described in detail by Karl et al. (2012a).

Table 4.1 shows a brief summary of the nucleation options.

Note that the referenced literature must be cited in all publications that use MAFOR with the corresponding nucleation option.

Table 4.1 Nucleation options in the MAFOR model.

Option no.	Nucleation mechanism	Reference (must be cited)
1	kinetic H ₂ SO ₄	Kulmala et al., 2006
2	homogeneous H ₂ SO ₄ -H ₂ O	Vehkamäki et al., 2002 Vehkamäki et al., 2003
3	homogeneous H ₂ SO ₄ -H ₂ O-NH ₃	Merikanto et al., 2007 Merikanto et al., 2009
4	homogeneous & ion-mediated H ₂ SO ₄ -H ₂ O-NH ₃	Yu et al., 2018 Yu et al., 2020
5	activation H ₂ SO ₄	Kulmala et al., 2006
6	kinetic HNO ₃ -AMINE	Karl et al., 2012b
7	combination H ₂ SO ₄ (activation & ion-mediated)	Karl et al., 2011 Karl et al., 2012a
8	"OS1" activ H ₂ SO ₄ -ORG	Karl et al., 2012a
9	"OS2" kinet H ₂ SO ₄ -ORG	Karl et al., 2012a
10	"OS3" total H ₂ SO ₄ -ORG	Karl et al., 2012a
11	neutral & ion-induced H ₂ SO ₄ -H ₂ O	Määttänen et al., 2018a,b
12	diesel H ₂ SO ₄ -ORG	Pirjola et al., 2015
13	ACDC, H ₂ SO ₄ -H ₂ O-NH ₃	Henschel et al. (2016) Baranizadeh et al. (2016)

The nucleation rate calculated by the following nucleation mechanisms can be scaled by a value provided in column *fnuc* in *ingeod.dat*: activation H₂SO₄, combination and "OS3". If it is not desired to scale the nucleation rate, the values in column *fnuc* should be set to 1.

The organic compound that is involved in the nucleation options 8-10 (“OS1”, “OS2, and “OS3”) and 12 is SOA-2 (see section 2.7; in the above list denoted as “ORG”). The gas phase concentration of SOA-2 is initialized in inchem.dat. Currently it is not possible to fix SOA-2 gas phase concentration at a constant value. SOA-2 is formed by chemical reactions. Examples are: reaction of amines with OH radical, reaction of isoprene peroxy radicals with HO2 and NO, TMB + OH, APIN + O3, reaction of monoterpene peroxy radical with HO2 and NO.

The ion-mediated binary nucleation (option 4) based on the look-up table parameterization of Yu (2010) has been replaced in v2.0 by the more recent look-up table version for ion-mediated ternary nucleation, short TIMN (Yu et al., 2018; Yu et al., 2020). TIMN includes ternary nucleation of H2SO4-NH3-H2O and binary homogeneous nucleation. This option provides the calculation of the nucleation rate due to ion-mediated nucleation based on the look-up table program by Yu et al. (2020) as function of temperature, relative humidity, sulphuric acid concentration, and ammonia concentration, while the ionization rate is set to $2.4 \text{ ion pairs cm}^{-3} \text{ s}^{-1}$ and surface area of aerosol is set to $10 \text{ } \mu\text{m m}^{-2}$. For sulphuric acid concentration $<5 \times 10^5 \text{ molecules cm}^{-3}$, the steady state assumption given by Karl et al. (2011) is used.

4.6 Secondary organic aerosol

Nine SOA compounds are available in the MAFOR model to represent the different categories, volatility and formation routes of secondary organic aerosol. Biogenic secondary oxidized vapors are represented by BSOV (semi-volatile), BLOV (low-volatile) and BELV (extremely low-volatile). Aromatic secondary oxidized vapors are represented by ASOV (semi-volatile), ALOV (low-volatile) and AELV (extremely low-volatile). Primary emitted organic vapors, such as long-chained n-alkanes are represented by PIOV (intermediate volatility), PSOV (semi-volatile) and PELV (extremely low-volatile). All SOA compounds are represented by a gas phase component and a particle phase component.

The initial gas phase concentrations of the SOA gas phase components are entered in inchem.dat. Vapor concentrations of BSOV (“COV”, SOA-1) can be prescribed to the simulation in ingeod.dat when the switch read SOA-1 in sensitiv.dat is set to 1.

By default, the molecular stoichiometric yield of BSOV (SOA-1) is set to 0.40 for its formation in chemical reaction while it is zero for all other SOA compounds. The default molar yield of BLOV (SOA-2) and BELV (SOA-3) are set to 0. The yields of BSOV and BLOV in the photo-oxidation of terpenes can be changed by the user in chamber simulations (in inchem.dat), but not in other types of model simulations.

Table 4.2 gives an overview of the molar yields used in SOA forming reactions of biogenic VOC and aromatic VOC in the MAFOR model.

Table 4.2 SOA formation reactions: molar yields of SOA precursors in the MAFOR model. ELV - extremely low volatile vapor (BELV or ALV), LV - low volatile vapor (BLOV or ALOV), SV - semi-volatile vapor (BSOV or ASOV). Molar yields adopted from: Tsimpidi et al. (2010), Ceulemans et al. (2012) and Couvidat et al. (2012).

Reaction type →	VOC + Ox			RO2 + NO		RO2 + HO2	
	ELV	LV	SV	LV	SV	LV	SV
Isoprene + OH	0	0	0	0.003	0.101	0.024	0.119
Terpene + OH	0	0	0	0.052	0.184	0*	0.40*
Terpene + O3	0.07 **	0.23 **	0	0.052	0.184	0*	0.40*
Toluene + OH	0.04	0	0	0.097	0.748	0.780	0
Xylene + OH	0	0.063	0.424	0	0	0	0
TMB + OH	0	0.04	0	0	0	0	0

* Molar yield can be defined by the model user in chamber simulations (inchem.dat).

** Only in reactions alpha-pinene + O3 and beta-pinene + O3.

Terpene: alpha-pinene (APINENE), beta-pinene (BPINENE), camphene (CAMPHENE), carene (CARENE), sabinene (SABINENE).

Aromatics: toluene (TOLUENE), xylene (LXYL), trimethylbenzene (LTMB).

The yields of SOA-1 and SOA-2 can be changed by the user in the input file inchem.dat (for chamber simulations) in the following reactions (see section 4.2):

- Reactions of amines with the OH radical: MMA + OH, MEA + OH, DMA + OH, CH₂NH₃ + OH, TMA + OH
- For alpha-pinene (APIN), beta-pinene (BPIN), camphene (CAMPHENE), carene (CARENE), and sabinene (SABINENE) in the reaction of monoterpene peroxy radicals with HO₂.

The primary emitted organic vapors (PIOV, PSOV, PELV) are not formed in any chemical reaction. However, they are inter-converted by oxidative aging, oligomerization and fragmentation.

The chemical properties of the condensable organic vapors are defined in the input file organic.dat. They can be changed according to the vapor properties that shall be used in the simulation. The default values of the nine SOA components are listed in Table 4.3.

The particle density of the organic aerosol can be changed in organic.dat. The default value is 1570 kg m⁻³.

Table 4.3 Properties of organic components in the MAFOR model. ΔH_{vap} is the enthalpy of vaporization, C^0 is the saturation concentration over the pure liquid and p_s^0 is the vapor pressure of the pure liquid.

SOA component	Name in inchem.dat	Number carbon atoms (nC) *	Number oxygen atoms (nO) *	ΔH_{vap} * [kJ mol ⁻¹]	C^0 (298 K) * [$\mu\text{g m}^{-3}$]	p_s^0 (298 K) ** [Pa]	Reference ΔH_{vap}
SOA-1	KPP_BSOV	10	2.5	50	2.1	$3.06 \cdot 10^{-5}$	Couvidat et al. (2012)
SOA-2	KPP_BLOV	10	2.5	50	0.03	$4.37 \cdot 10^{-7}$	Couvidat et al. (2012)
SOA-3	KPP_BELV	20	7	50	0.0001	$9.0 \cdot 10^{-10}$	Couvidat et al. (2012)
SOA-4	KPP_ASOV	7	2	50	1.0	$1.8 \cdot 10^{-5}$	Couvidat et al. (2012)
SOA-5	KPP_ALOV	7	2	50	0.01	$2.0 \cdot 10^{-7}$	Couvidat et al. (2012)
SOA-6	KPP_AELV	14	8	50	0.0001	$9.0 \cdot 10^{-10}$	Couvidat et al. (2012)
SOA-7	KPP_PIOV	21	0	108	100	$8.05 \cdot 10^{-4}$	Chickos and Wilson (1997)
SOA-8	KPP_PSOV	26	0	135	0.6	$3.80 \cdot 10^{-6}$	Chickos and Wilson (1997)
SOA-9	KPP_PELV	34	0	177	0.0002	$9.97 \cdot 10^{-10}$	Chickos and Wilson (1997)

* Values can be changed by the model user.

** Vapor pressure of the pure liquid calculated based on the given value of C^0 .

Enthalpy of vaporization:

The temperature dependence of the saturation concentration C^0 is calculated in MAFOR based on the Clausius-Clapeyron equation, using the value of the enthalpy of vaporization provided by the model user in organic.dat. Default values of $\Delta H_{\text{vap}} = 50 \text{ kJ mol}^{-1}$ for the biogenic and aromatic organic vapors can be used (or replaced by a more appropriate value). For the primary emitted (carbon-chain like) vapors, it is recommended to calculate the enthalpy of vaporization by the formula given by Chickos and Wilson (1997): $\Delta H_{\text{vap}} (\text{kJ mol}^{-1}) = 5.43 \cdot nC - 3.3$.

Initial mole fractions in the organic aerosol:

The initial organic aerosol (mass component OC in input file inaero.dat) has to be specified in the input file organic.dat. The mole fraction of the SOA compounds (gamma-oc) in each mode has to be entered in organic.dat. The respective mole fractions should add up to 1 for each mode.

Nucleation involving organic vapors:

BLOV (SOA-2) can be used as nucleating component when setting nucleation options 8, 9, 10, or 12 (see section 2.7).

Plume simulations:

In plume simulations, the SOA gas phase components are diluted with the same rate as the aerosol components.

Three different theoretical approaches are offered to simulate SOA concentrations: **1**) by explicitly calculating the condensation/evaporation driving force, which is the difference between the species concentration in the bulk gas and the concentration just above the particle surface (Jacobson, 1997), **2**) by a hybrid approach of condensation / evaporation and the absorptive partitioning into an organic liquid according to Kerminen et al. (2000), and **3**) by extension of the hybrid approach to also consider the physical adsorption of organics to the surfaces of primary particles (dust and soot) according to Pankow (1994). The first approach is the default, for the second the SOA-partition option in sensitiv.dat has to be set to 1 and for the third the SOA-partition option in sensitiv.dat has to be set to 2. It is noted that the third approach is still under development and should only be used for testing.

4.7 Condensation of sulfuric acid and organosulfur compounds

Relevant property data of sulfuric acid (H_2SO_4) and methane sulfonic acid (MSA) for condensation is compiled in Table 4.4.

Table 4.4 Relevant physicochemical properties of H_2SO_4 and MSA in the MAFOR model.

Comp.	Name in inchem. dat	MW (g mol^{-1})	Density of pure liquid (kg m^{-3})	Surface tension (kg s^{-2})	Acc. coeff.	Sat. Vapour pressure p_s^0 (Pa) at 280 K	Ref. p_s
H_2SO_4	KPP_ H2SO4	98.08	1851	0.052	0.5	6.5×10^{-4} (at $X_a=0.9$)	Bolsaitis and Elliott (1990)
MSA	KPP_ CH3SO3H	96.11	1507	0.053	0.13	1.5×10^{-2}	Kreidenweis and Seinfeld (1988)

The saturation vapor pressure of sulfuric acid over particles, p_s^0 , is calculated as function of temperature and of the mole fraction of H_2SO_4 (X_a). The data by Bolsaitis and Elliott was fit with a multiple regression plot to derive an expression for the dependency, see Figure 4.2.

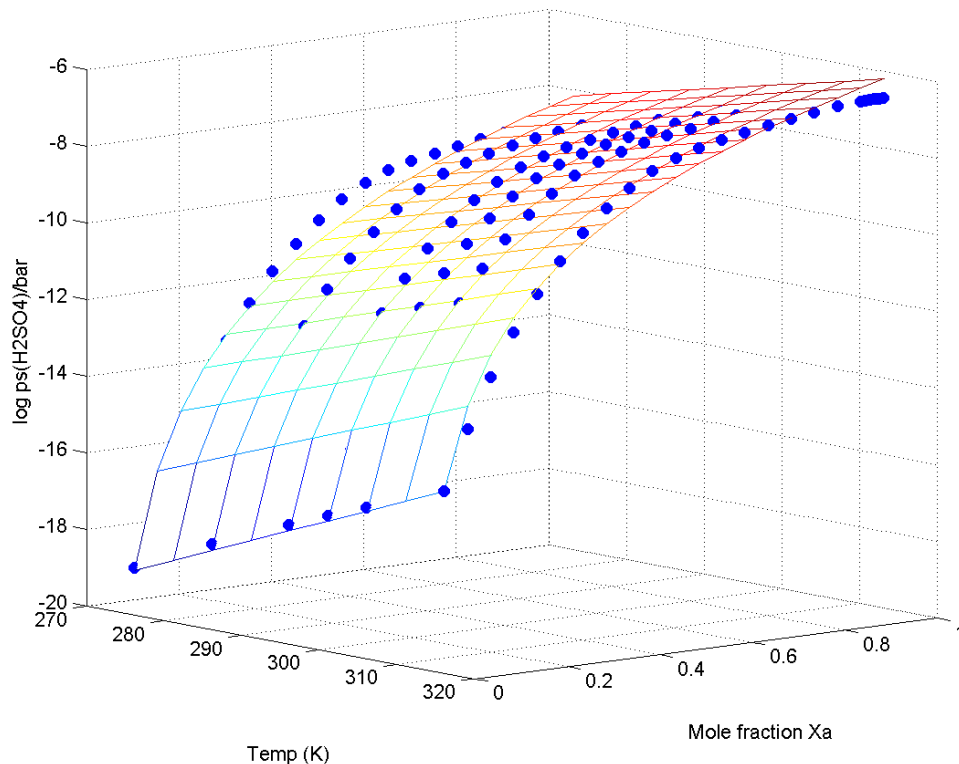


Figure 4.2 Multiple regression plot for sulfuric acid saturation vapor pressure (as $\log(\text{H}_2\text{SO}_4/\text{bar})$).

To correct the condensation flux of H_2SO_4 and MSA by the Kelvin effect, set option “Kelvin effect considered” to 1 in file “sensitiv.dat”.

4.8 Coagulation

Particle coagulation is a process in which smaller particles collide with each other and coalesce completely to form larger particles. A semi-implicit solution is applied to coagulation (Jacobson, 2005a). The semi-implicit solution yields an immediate volume-conserving solution for coagulation with any time step. Brownian coagulation coefficients $K_{i,j}$ between particles in size bin i and j are calculated according to Fuchs (1964) assuming spherical particles. If colliding particles result in a particle that has exactly the same size as particles in size bin i , the particle is attributed to bin i , and the number concentration of bin i increases. In all other cases, particles are redistributed among the nearest size bins according to the resulting particle's volume. When coagulation option 2 is chosen, the effect of the fractal geometry of soot particles on coagulation is taken into account by considering the effect on radius, diffusion coefficient and the Knudsen number in the Brownian collision kernel. It is assumed that the collision radius is equal to the fractal (outer) radius of the aggregate of primary spherules (with radius r_s). The fractal parameters, $r_s = 13.5$ nm and the fractal dimension $D_f = 1.7$, were adopted from Jacobson and Seinfeld (2004). These parameters can be changed by the model user in `organic.dat`.

Van der Waals forces and viscous interactions can affect the coagulation rate of small particles. It has been shown that Van-der-Waals forces can enhance the coagulation rate of particles with diameter < 50 nm by up to a factor of five (Jacobson and Seinfeld, 2004). When coagulation option 3 is used, an empirical enhancement factor, V_E is applied that depends on the value of the particle pair Knudsen number (Karl et al., 2016). When coagulation option 4 is used, an exact solution of the enhancement by van der Waals forces and viscous forces using the interpolation formula for the van der Waals collision kernel between the free-molecular and continuum regimes (Jacobson, 2005a, page 513) is applied. The Hamaker constant of water, $A_H/kT = 20$ is used for all particle types.

When coagulation option 5 is used, both the effect of fractal geometry and the effect of van der Waals/viscous forces (exact solution) are considered. Figure 4.3 illustrates the effect of using the different options on the coagulation rate for the collision with 10-nm particles.

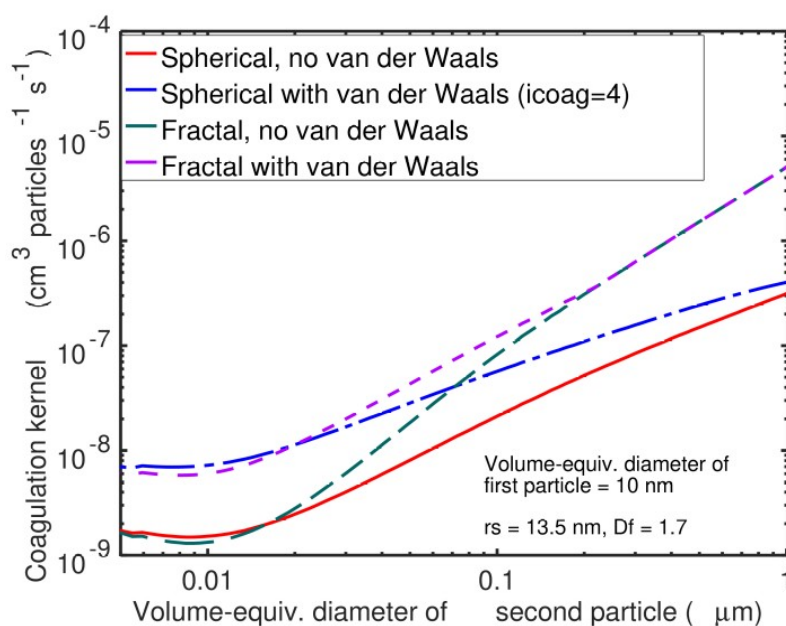


Figure 4.3 Effect of fractal geometry and van der Waals forces when the volume-equivalent diameter is 10 nm and the volume-equivalent diameter of the second particle varies from 5 to 1000 nm. Red line: option 1, blue line: option 4, green line: option 2, purple line: option 5.

4.9 Emission of particles

Continuous emission of a particle size spectrum

Emission of primary particles controlled by input file emitpar.dat. This causes a continuous emission of particles during the simulation. The emitted size spectrum of particles and their chemical composition can be provided per mode (NU, AI, AS, CS) in the input file emitpar.dat. Particle emissions are activated in sensitiv.dat by setting the “emission of particles” option to 1. The source strength of the particles cannot be varied during the simulation. The particle emission rates have to be given in units $\text{ng m}^{-2} \text{s}^{-1}$.

Sea-air flux of sea-salt particles

Emission of sea-salt particles (short: sea-salt emission) is implemented using the parameterization of Spada et al. (2013). This consists of three original parameterizations proposed by Martensson et al. (2003) (MA03), Monahan et al. (1985) and Smith et al. (1993), where MA03 is used for the flux of particles with diameter $< 2.8 \mu\text{m}$. The wind speed dependence is described by the whitecap coverage relating to the 10m wind speed and the fraction of the sea surface covered by whitecaps. Sea-salt emissions depend on wind speed (u_{10} in m/s, ingeod.dat), sea surface temperature (SST in K) and salinity (SAL in g/kg). The latter two can be set to constant values in dispers.dat. Figure 4.4 shows the size-dependent sea-salt particle flux $dF/d\log D_p$ for different wind speed, SST and SAL.

Sea-salt emissions are activated in a run by choosing the option 2 for “emission of particles” in sensitiv.dat.

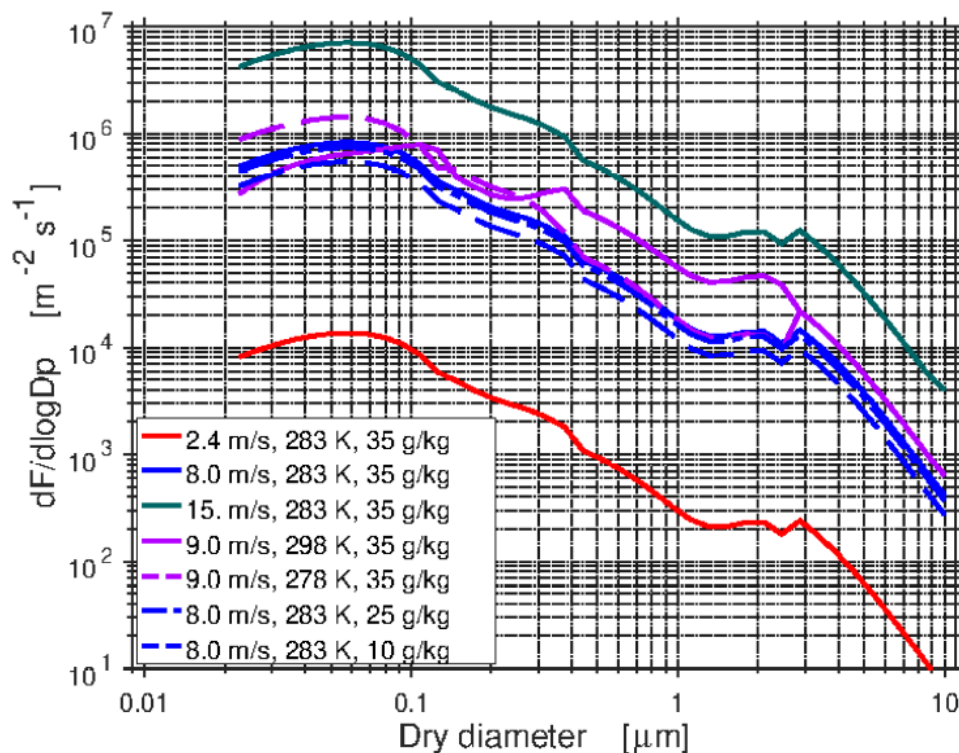


Figure 4.4 Dependence of the sea-salt flux ($dF/d\log D_p$) on wind speed, sea surface temperature and salinity with the implemented parameterization by Spada et al. (2013).

5 Test examples

Four set of test examples including all necessary input files, reference output files and reference plot graphics are available for download and briefly described in this chapter. The reference plots have been generated with Octave v5.2.0. Matlab scripts for plotting graphics are provided in subdirectory “matlab”. The scripts work in Matlab and Octave. When using MATLAB, figure plots have to be saved as *.bmp files instead of *.jpg files. The corresponding line in the plot script has to be changed from:

```
print -djpg '{plot directory}/figureplot.jpg'
```

to:

```
print -dbmp '{plot directory}/figureplot.bmp'
```

MAFOR model output needs to be moved to subdirectory “output” to apply the plot scripts.

5.1 Nucleation event

5.1.1 Description

Simulation of 10 hours at a fixed location in the Arctic Ocean follows an observed new particle formation event with nucleation of new particles and growth by condensation of sulphuric acid, MSA (from oxidation of DMS) and one organic vapor (“COV”, BSOV). Model results for the number size distribution are compared to measured data. Number size distribution of particles is plotted 1) as a series of snapshots and 2) as sequential time series (contour plot). Observation data and model simulation (using MAFOR v1.2) for this nucleation event on DOY 209 (Arctic Ocean Expedition in 1996) have been published by Karl et al. (2012a). The model simulation was modified for the test example.

5.1.2 Input

The input file sensitiv.dat for this example is shown below:

sensitiv.dat ✕								
1	1	1	1	1	1	7	0	
2	1	1	0	0	0	0	1	0
3	1	0	1	1	0	0	1	0
4	1	0	0					

In this example, all aerosol processes are switched on; the nucleation option 7 (combination H₂SO₄) is selected. Condensation of organics and sulphuric compounds is allowed. Chemistry integration switch is on; DMS and SOA-1 concentrations are read from ingeod.dat. Water condensation to particles is on. The debug switch is set to 1 to obtain debugging information in debug.res.

The input file ingeod.dat for this example is shown below:

ingeod.dat ✕																									
1	10	29	7	11	83.46	66.03	272.46	101300.	0.873	60.00	0	2.96	0.00	0.0	1.009	0.0	1.13009	40.E+07	7.39008	0.00	1.50	0.00	7.0	90.0	0.5
2	10	29	7	12	83.46	66.03	272.47	101300.	0.879	60.00	0	2.48	0.00	0.0	1.009	0.0	1.13009	40.E+07	1.22809	0.00	1.50	0.00	7.0	90.0	0.5
3	10	29	7	13	83.46	66.03	272.33	101300.	0.884	60.00	0	2.54	0.00	0.0	1.009	0.0	1.13009	40.E+07	4.89008	0.00	1.50	0.00	7.0	90.0	0.5
4	10	29	7	14	83.46	66.03	272.48	101300.	0.897	60.00	0	2.60	1.00	0.0	1.009	0.0	1.13009	40.E+07	3.26009	0.00	1.50	0.00	7.0	90.0	0.5
5	10	29	7	15	83.46	66.03	272.03	101300.	0.895	60.00	0	2.30	1.00	0.0	1.009	0.0	1.13009	40.E+07	3.89009	0.00	1.50	0.00	7.0	90.0	0.5
6	10	29	7	16	83.46	66.03	271.91	101300.	0.885	60.00	0	2.50	1.00	0.0	1.009	0.0	1.13009	40.E+07	3.65009	0.00	1.50	0.00	7.0	90.0	0.5
7	10	29	7	17	83.46	66.03	271.83	101300.	0.878	60.00	0	2.49	0.70	0.0	1.009	0.0	1.13009	40.E+07	1.29009	0.00	1.50	0.00	7.0	90.0	0.5
8	10	29	7	18	83.46	66.03	271.79	101300.	0.886	60.00	0	2.58	0.60	0.0	1.009	0.0	1.13009	40.E+07	0.70009	0.00	1.50	0.00	7.0	90.0	0.5
9	10	29	7	19	83.46	66.03	271.89	101300.	0.898	60.00	0	2.69	0.50	0.0	1.009	0.0	1.13009	40.E+07	0.50009	0.00	1.50	0.00	7.0	90.0	0.5
10	10	29	7	20	83.46	66.03	275.82	101300.	0.894	60.00	0	2.67	0.40	0.0	1.009	0.0	1.13009	40.E+07	2.34009	0.00	1.50	0.00	7.0	90.0	0.5

In column 13 (rain) of ingeod.dat a rain rate between 0.40 and 1.00 mm/h is entered which will cause wet scavenging of particles. The incloud switch is set to zero during the simulation. NH₃, DMS, and SOA-1 (vapour) concentrations are prescribed to the run. A constant concentration of 40E+07 (molecules cm⁻³) of SOA-1 is used during the simulation. The nucleation rate is scaled by a factor (fnuc) of 1.50. Entries in the last four columns are not relevant to the simulation.

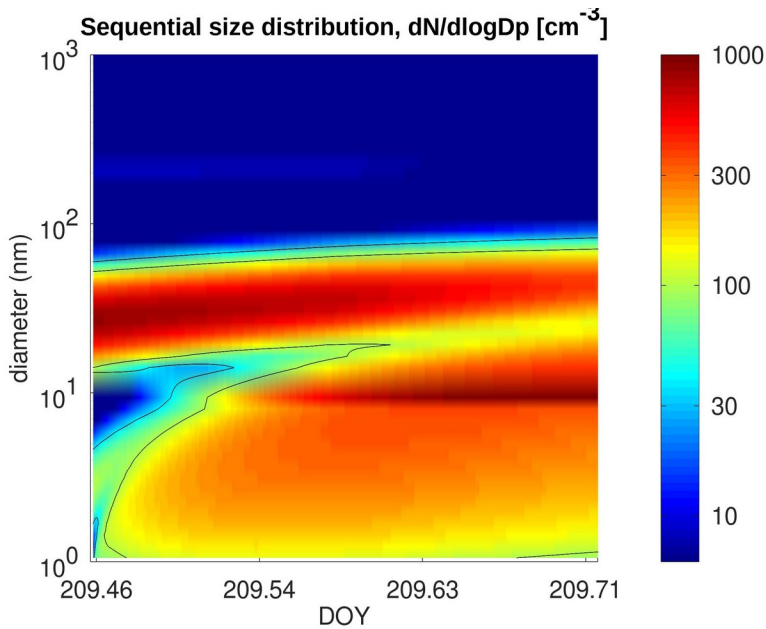
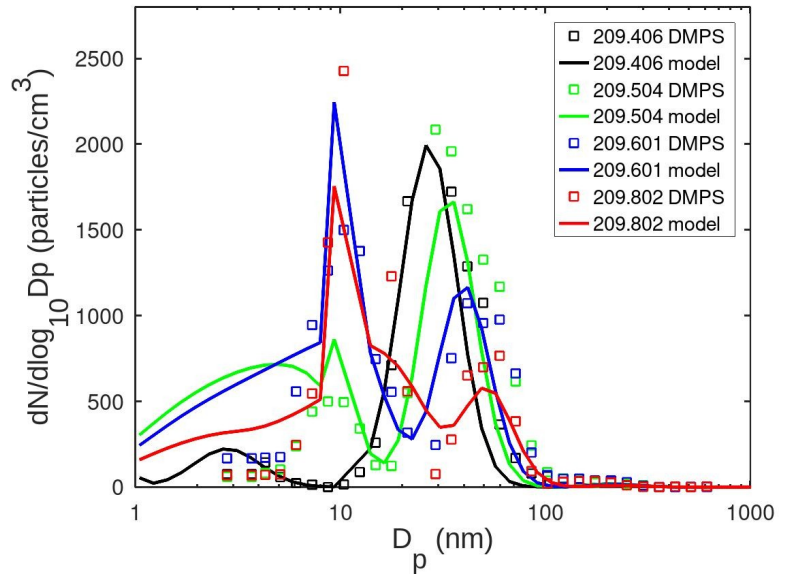
The input file dispers.dat is shown below:

dispers.dat ✕						
1	1.10	12.0	0.25	300.0		
2	0.00	-0.4	5.00	0.00	-0.8	
3	12.0	300.0	0.03	0.12	1.0E16	
4	0.230	0.290	7.00	13.0	22.5	
5	1.17	0.001	1.70	51.8		
6	0.30	0.003	0.20			
7	0.10	275.0	31.0			
8						

Entries in the first four lines are not used in the simulation (input for plume dispersion). The fifth line shows entries for dry deposition of particles over a water surface (section 2.7) which are used when the dry deposition flag in sensitiv.dat is set 1.

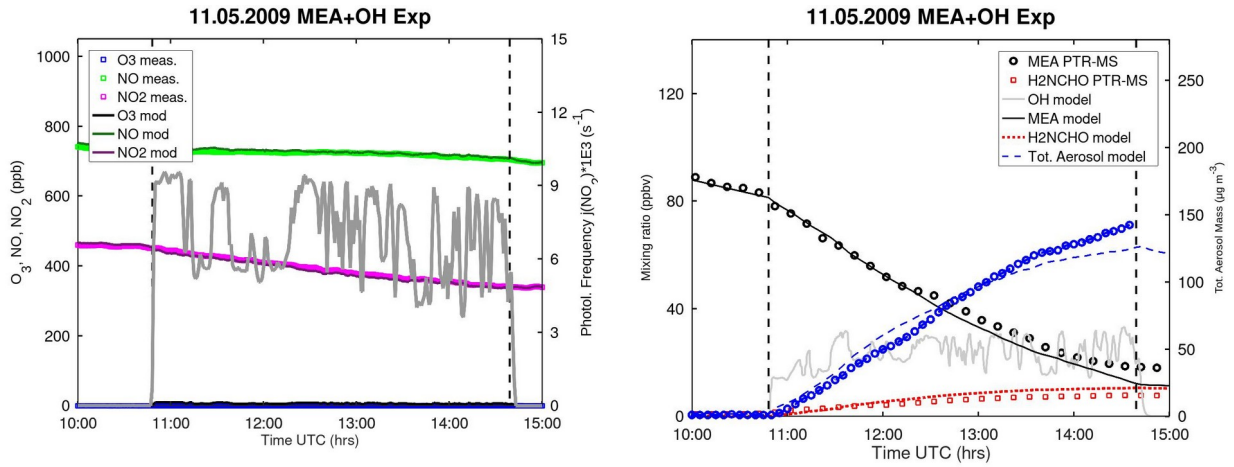
5.1.3 Result plots

The plots created with the MATLAB scripts sizedis_arctic.m and profile_arctic.m are shown below.

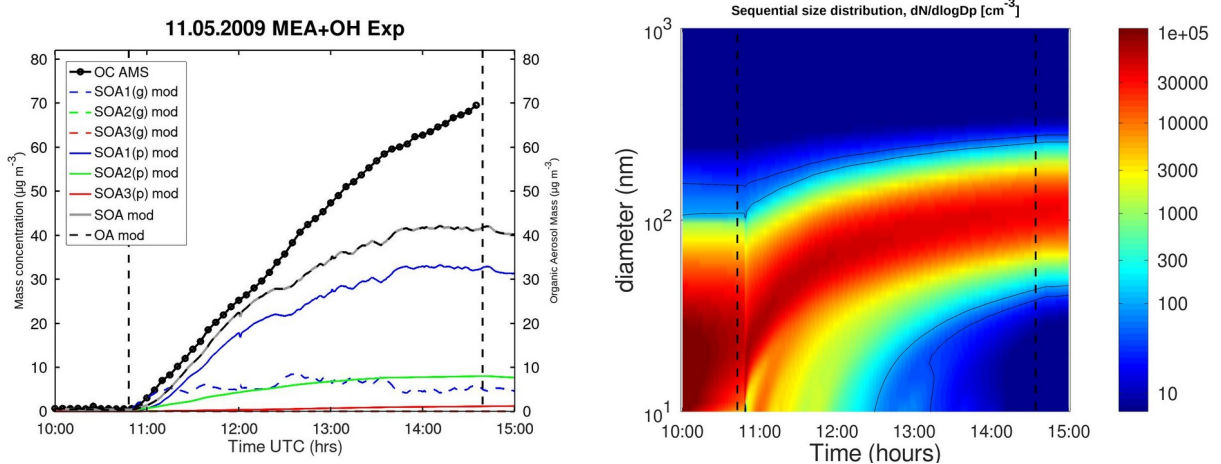


5.2.3 Result plots

The plots created with the MATLAB script monitor_chamber.m are shown below.



The organic aerosol is plotted with the MATLAB script soadis_chamber.m below on the left side, including concentrations of the SOA components (SOA-1, SOA-2, SOA-3) in the gas phase (color dashed lines) and in the particle phase (color solid lines). The modeled total OC (black dashed line) consists fully of modeled SOA (gray line). After the first hour of the experiment, measured OC mass from the Aerosol Mass Spectrometer (AMS) shows a steeper increase than modeled OC. The sequential particle number distribution created with the MATLAB script profile_chamber.m on the right.



5.3 Diesel exhaust dilution and aging

5.3.1 Description

Simulation of an experimental laboratory system of diesel exhaust dilution and aging for a total duration of 60 seconds. The system consists of a primary diluter with relative humidity close to zero and a dilution ratio of 12; followed by an aging chamber to ensure adequate residence time for the condensational growth of the nucleation mode particles in the cooled and diluted aerosol sample. The initial raw exhaust particle distribution at $t = 0.0$ s was assumed to be entirely non-hygroscopic. It is divided into the core mode between 5-15 nm consisting of non-volatile organic matter (OM_{nv}) and the soot mode consisting of elemental carbon. The simulations of the diesel exhaust treatment system (using MAFOR v1.8) are published in Pirjola et al. (2015).

5.3.2 Input

The input file sensitiv.dat for this example is shown below:

sensitiv.dat							
1	0	0	1	1	1	12	0
2	2	1	0	0	0	0	1
3	0	0	0	1	3	0	0
4	1	0	0				

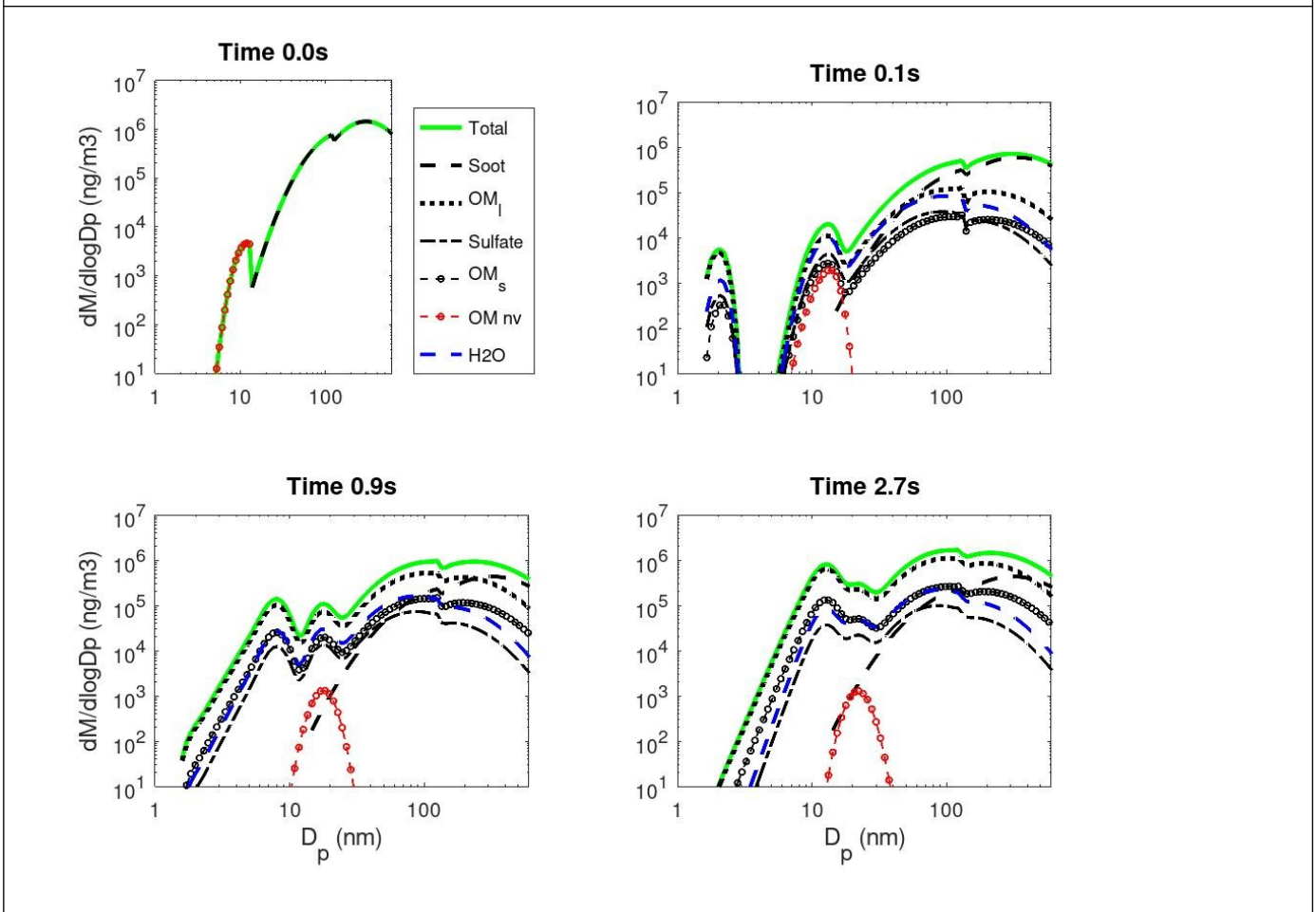
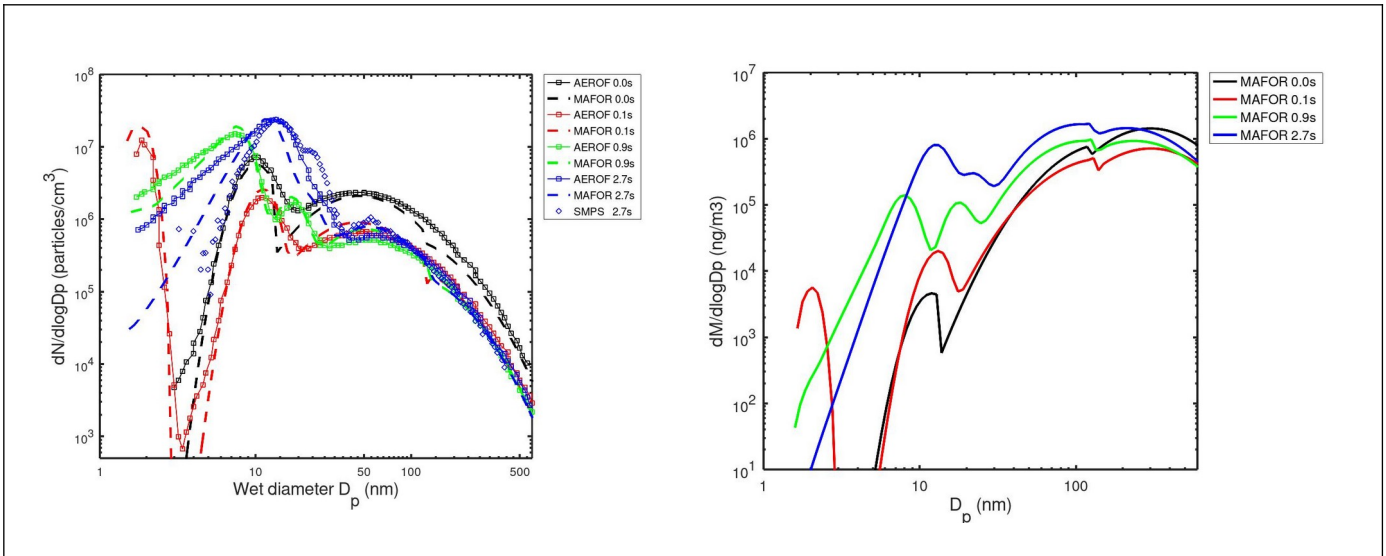
Aerosol processes condensation of H_2SO_4 with unity accommodation, organic vapors (SOA-2 [COV_s] and SOA-9 [COV₁]; Kelvin effect taken into account), coagulation, nucleation (option 12, diesel H₂SO₄-ORG), dilution with particle-free background air and condensation of water are switched on. The wall loss of H_2SO_4 in the aging chamber (chamber option 2) is not activated in this example. Dilution is according to plume type 3. The parameters for this dilution type are in 3rd line of dispers.dat:

dispers.dat					
1	0.025	0.00	0.00	697.0	
2	0.00	-0.4	5.00	0.00	-0.8
3	6.5	300.0	0.03	0.12	1.0E16
4	0.230	0.290	7.00	13.0	22.5
5	1.33	0.0013	4.00	121.0	
6	0.01	0.002	0.20		
7	0.1	280.0	33.0		
8					

The start temperature (ta_{st}) of the raw exhaust is 697.0 K. The final temperature of the diluted exhaust is 300.0 K. The dilution ends at 0.12 s. (τ_d in line 3). Initial concentrations of H_2SO_4 , SOA-2 and SOA-9 are given in inchem.dat. For H_2SO_4 a continuous source from the walls of 1×10^{12} molecules $cm^{-3} s^{-1}$ is prescribed.

5.3.3 Result plots

The plots created with the MATLAB scripts sizedis_diesel_wetdp.m and massdis_diesel.m are shown below. Four time steps are plotted in the figures (0.0 s, 0.1 s, 0.9 s, 2.7 s) showing the evolution of the aerosol distribution in terms of particle numbers, particle mass (top panel) and particle mass composition (bottom panel). The particle number distribution is compared to results from a simulation with AEROFOR (e.g. Pirjola, 1999; Pirjola and Kulmala, 2001) and with measured records from SMPS after 2.7 s.



5.4 Fog cycle chemistry

5.4.1 Description

Scenario represents typical summertime photochemical and meteorological conditions for a refinery area at the west coast of Norway which is best described as moderately polluted marine boundary layer. The scenario is based on monthly average concentrations of pollutants and other atmospheric constituents. Continuous emission of nitrous acid (HONO) is added and the emission rate is adjusted to produce maximum concentrations of 300 pptv HONO. The simulation time is 72 hours (3 days) with a fog cycle. Each fog event starts at 2 a.m. and ends at 10 a.m. (8 hours). Fog forms at approximately 2 a.m. and fog dissipates at approximately 10 a.m. so that three full fog events are simulated. The simulation starts at 5 a.m. of the first day in a fog period. By doing so, the chemical composition of fog droplets is initialized with the aqueous phase concentrations (in inaqchem.dat). The amplitude of the liquid water content during fog ranges from 9 to 106 mg m⁻³. The pH value of fog droplets is prescribed to be fixed at 5.1. Continuous emissions of dimethyl sulphide (DMS), dimethylamine (DMA), and a series of VOC (C₂H₆, C₃H₈, C₂H₄, and toluene) are added (in inchem.dat).

5.4.2 Input

The input file sensitiv.dat for this example is shown below:

sensitiv.dat ✕							
1	0	0	0	0	0	0	0
2	0	0	0	0	0	1	0
3	0	0	0	1	0	0	0
4	1	1	1				

All aerosol processes are switched off. The switch for chemistry integration, aqueous phase partitioning and aqueous phase chemistry is set to 1. The condensation of water to particles is allowed but this does not affect the water content of coarse mode droplets during fog; instead their water content is calculated based on the prescribed droplet distribution by using the switch includ=1 in the input file ingeod.dat.

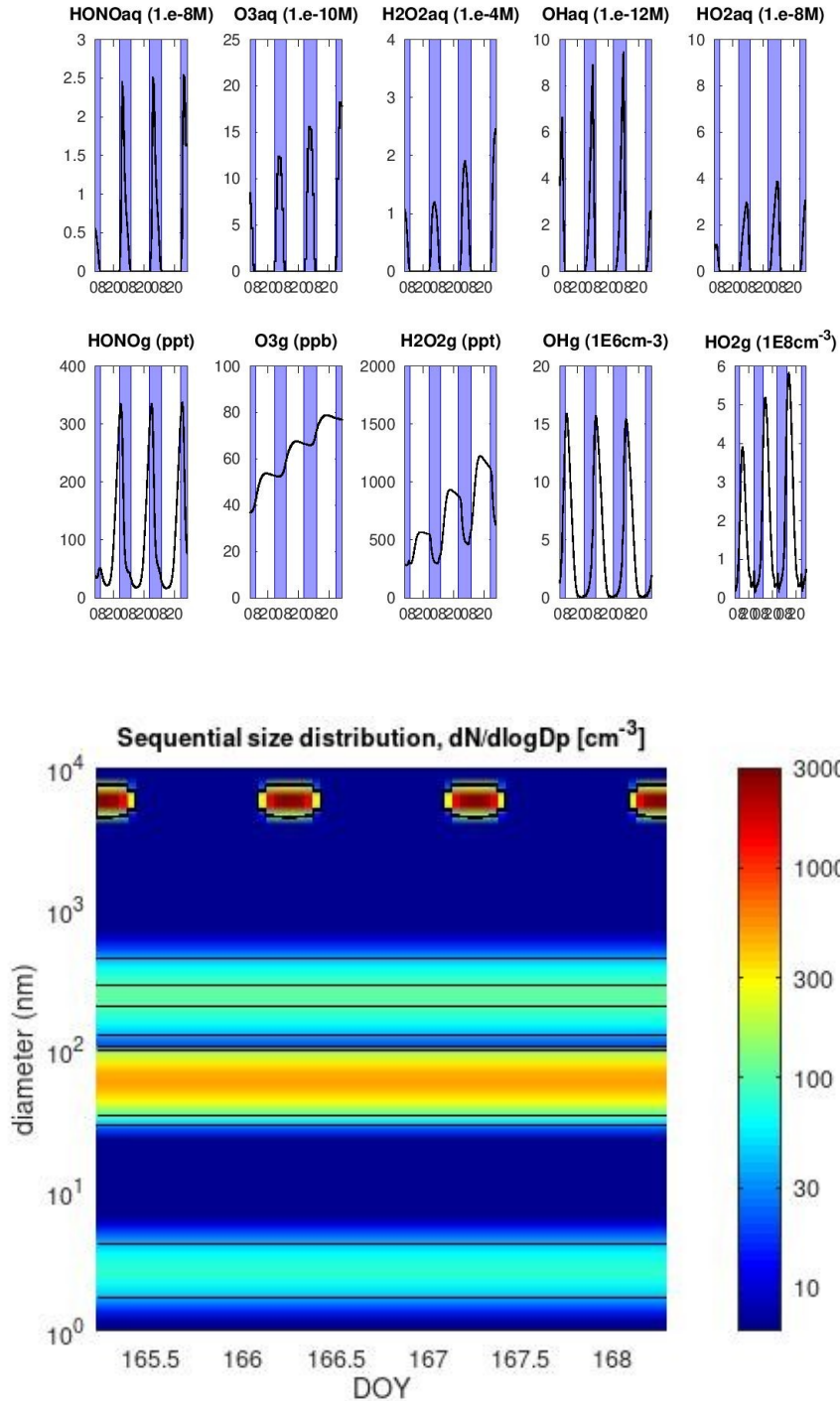
The first lines of the input file ingeod.dat for this example are shown below:

ingeod.dat ✕																									
1	74	15	6	05	60.48	5.02	285.26	101300.	0.950	1000.00	1	5.00	0.00	6.00E+09	0.00	4.00E+09	0.00	0.00	0.00	0.00	1.00	1.00E-07	5.10	86.49	0.92332
2	74	15	6	06	60.48	5.02	285.96	101300.	0.950	1000.00	1	5.00	0.00	6.00E+09	0.00	4.00E+09	0.00	0.00	0.00	0.00	1.00	1.00E-07	5.10	86.49	0.92332
3	74	15	6	07	60.48	5.02	285.81	101300.	0.950	1000.00	1	5.00	0.00	6.00E+09	0.00	4.00E+09	0.00	0.00	0.00	0.00	1.00	8.99E-08	5.10	86.49	0.92332
4	74	15	6	08	60.48	5.02	286.35	101300.	0.950	1000.00	1	5.00	0.00	6.00E+09	0.00	4.00E+09	0.00	0.00	0.00	0.00	1.00	5.75E-08	5.10	86.49	0.92332
5	74	15	6	09	60.48	5.02	286.63	101300.	0.950	1000.00	1	5.00	0.00	6.00E+09	0.00	4.00E+09	0.00	0.00	0.00	0.00	1.00	9.00E-09	5.10	86.49	0.92332
6	74	15	6	10	60.48	5.02	286.62	101300.	0.755	1000.00	0	5.00	0.00	6.00E+09	0.00	4.00E+09	0.00	0.00	0.00	0.00	1.00	1.00E-11	5.10	86.49	0.92332
7	74	15	6	11	60.48	5.02	286.77	101300.	0.748	1000.00	0	5.00	0.00	6.00E+09	0.00	4.00E+09	0.00	0.00	0.00	0.00	1.00	1.00E-11	5.10	86.49	0.92332
8	74	15	6	12	60.48	5.02	286.82	101300.	0.741	1000.00	0	5.00	0.00	6.00E+09	0.00	4.00E+09	0.00	0.00	0.00	0.00	1.00	1.00E-11	5.10	86.49	0.92332
9	74	15	6	13	60.48	5.02	287.03	101300.	0.735	1000.00	0	5.00	0.00	6.00E+09	0.00	4.00E+09	0.00	0.00	0.00	0.00	1.00	1.00E-11	5.10	86.49	0.92332
10	74	15	6	14	60.48	5.02	287.13	101300.	0.726	1000.00	0	5.00	0.00	6.00E+09	0.00	4.00E+09	0.00	0.00	0.00	0.00	1.00	1.00E-11	5.10	86.49	0.92332
11	74	15	6	15	60.48	5.02	287.25	101300.	0.724	1000.00	0	5.00	0.00	6.00E+09	0.00	4.00E+09	0.00	0.00	0.00	0.00	1.00	1.00E-11	5.10	86.49	0.92332
12	74	15	6	16	60.48	5.02	287.19	101300.	0.715	1000.00	0	5.00	0.00	6.00E+09	0.00	4.00E+09	0.00	0.00	0.00	0.00	1.00	1.00E-11	5.10	86.49	0.92332
13	74	15	6	17	60.48	5.02	287.29	101300.	0.723	1000.00	0	5.00	0.00	6.00E+09	0.00	4.00E+09	0.00	0.00	0.00	0.00	1.00	1.00E-11	5.10	86.49	0.92332
14	74	15	6	18	60.48	5.02	287.02	101300.	0.741	1000.00	0	5.00	0.00	6.00E+09	0.00	4.00E+09	0.00	0.00	0.00	0.00	1.00	1.00E-11	5.10	86.49	0.92332
15	74	15	6	19	60.48	5.02	286.65	101300.	0.760	1000.00	0	5.00	0.00	6.00E+09	0.00	4.00E+09	0.00	0.00	0.00	0.00	1.00	1.00E-11	5.10	86.49	0.92332
16	74	15	6	20	60.48	5.02	286.37	101300.	0.771	1000.00	0	5.00	0.00	6.00E+09	0.00	4.00E+09	0.00	0.00	0.00	0.00	1.00	1.00E-11	5.10	86.49	0.92332
17	74	15	6	21	60.48	5.02	285.97	101300.	0.797	1000.00	0	5.00	0.00	6.00E+09	0.00	4.00E+09	0.00	0.00	0.00	0.00	1.00	1.00E-11	5.10	86.49	0.92332
18	74	15	6	22	60.48	5.02	285.9	101300.	0.811	1000.00	0	5.00	0.00	6.00E+09	0.00	4.00E+09	0.00	0.00	0.00	0.00	1.00	1.00E-11	5.10	86.49	0.92332
19	74	15	6	23	60.48	5.02	285.58	101300.	0.807	1000.00	0	5.00	0.00	6.00E+09	0.00	4.00E+09	0.00	0.00	0.00	0.00	1.00	1.00E-11	5.10	86.49	0.92332
20	74	16	6	00	60.48	5.02	285.47	101300.	0.821	1000.00	0	5.00	0.00	6.00E+09	0.00	4.00E+09	0.00	0.00	0.00	0.00	1.00	1.00E-11	5.10	86.49	0.92332

The fog periods during the simulation are triggered by the setting the switch includ (column 11) to 1 in the input file ingeod.dat. For the input lines with includ=1, the lwcm in column 22 and the pH in column 23 will be read by the model and used to calculate the coarse mode droplet distribution. Emissions of DMS (edms, column 14) and emissions of H₂O₂ (eh2o2, column 16) are read by the model. A line with includ=0 following a line with includ=1 has the effect to trigger the immediate evaporation of fog water (no droplets remain) and gases that are dissolved in fog droplets.

5.4.3 Result plots

The plots created with the MATLAB scripts `conc_aqchem.m` and `profile_aqchem.m` are shown below. The upper graphic shows aqueous phase concentrations in the droplet mode in the upper panel and gas phase concentrations in air in the lower panel. In the lower graphic the fog periods are visualized as droplet mode peaks (red spots) in the sequential size distribution.



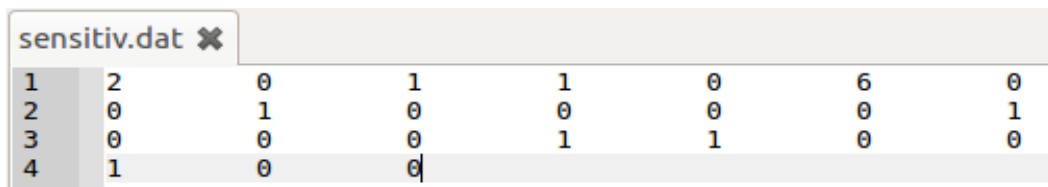
5.5 Traffic plume

5.5.1 Description

In this plume simulation the dispersion of particle downwind of a motorway in the Netherlands are compared to measurements. Aerosol processes considered in the model are condensation/evaporation of n-alkanes, coagulation and dry deposition of particles. Two different n-alkanes, C₂₂H₄₆ (C22) and C₂₈H₅₈ (C28), were used to represent vehicular exhaust gases with different volatility which can condense onto the particles during their transport away from the road. The dilution of the traffic-influenced aerosol by background air was approximated by fitting a power-law function $y = a \cdot x^{-b}$ (where $x = u \cdot t$ with “u” the wind speed and “t” the time) to the measured EC concentrations with distance to road. The mass concentration as function of distance from the road (increasing simulation time) and the particle number size distributions at different distances from the road are plotted in this example. Monitored data and model simulation (using MAFOR v1.2) have been published by Keuken et al. (2012). The model simulation was modified for the test example.

5.5.2 Input

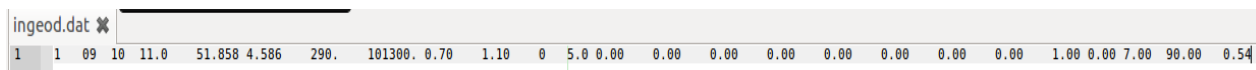
The input file sensitiv.dat for this example is shown below:



Line	Col 1	Col 2	Col 3	Col 4	Col 5	Col 6	Col 7	Col 8
1	2	0	1	1	0	6	0	
2	0	1	0	0	0	0	1	
3	0	0	0	1	1	0	0	
4	1	0	0					

In this example the aerosol processes coagulation, dry deposition and condensation are switched on. The chemistry integration is switched off. Condensation of organics (here: n-alkanes) is switched on, the Kelvin effect during condensation of n-alkanes is considered (last switch in 2nd line). The debug switch is set to 1 to obtain debugging information in debug.res. The dilution switch is set to 1 in order to enable the plume simulation type 1 and reading of the input file inbgair.dat which contains the background aerosol mass composition and distribution. The condensation of water to particles is allowed during the run. Dry deposition option 2 is used.

The input file ingeod.dat for this example is shown below:



Line	Col 1	Col 2	Col 3	Col 4	Col 5	Col 6	Col 7	Col 8	Col 9	Col 10	Col 11	Col 12	Col 13	Col 14	Col 15	Col 16	Col 17	Col 18	Col 19	Col 20	Col 21	Col 22	Col 23	Col 24	Col 25	Col 26				
1	1	09	10	11.0	51.858	4.586	290.	101300.	0.70	1.10	0	5.0	0.00	0.00	0.00	0.00	0.00	0.00	0.00	0.00	0.00	0.00	0.00	0.00	0.00	1.00	0.00	7.00	90.00	0.54

The simulation is for 1 hour and therefore ingeod.dat has only one line. In column 24 and 25, the dilution parameters are provided. Entries in columns 14-23 are ignored.

In the input file organic.dat the carbon number of the n-alkanes is entered and the initial molar fraction (gamma-oc) of SOA-7 and SOA-8 in the organic aerosol (OC) for the modes NU, AI, AS, CS has to be entered. The start concentration of n-alkane 1 and n-alkane 2 vapour (in molecules cm⁻³) is entered in inchem.dat (KPP_PIOV, KPP_PSOV). For both species a concentration of 0.75x10¹⁰ molecules cm⁻³ was used in this example.

The input file organic.dat is shown below:

organic.dat ✕					
1	1570.	1	0.050		
2	1200.	13.5	1.7		
3	10	2.5	50	2.1	
4	10	2.5	50	0.03	
5	20	7	50	0.0001	
6	7	2	50	1.0	
7	7	2	50	0.01	
8	14	8	50	0.0001	
9	22	0	113	34.1	
10	28	0	145	0.074	
11	34	0	177	0.0002	
12	0.00	0.00	0.00	0.00	0.00
13	0.00	0.00	0.00	0.00	0.00
14	0.00	0.00	0.00	0.00	0.00
15	0.00	0.00	0.00	0.00	0.00
16	0.00	0.00	0.00	0.00	0.00
17	0.00	0.00	0.00	0.00	0.00
18	0.00	0.00	0.00	0.00	0.00
19	1.00	1.00	1.00	1.00	1.00
20	0.00	0.00	0.00	0.00	0.00
21	0.90				
22					

The input file inaero.dat is shown below:

inaero.dat ✕													
1	1.00E-06	30											
2	F	6.50E-09	1.55	0.00E+00	0.026	0.168	0.003	0.003	0	0	0	0.000	0.000
3	F	4.50E-08	1.65	0.00E+00	55	443	24	58	0	12	0	146	0.000
4	F	1.20E-07	1.70	0.00E+00	851	1526	370	888	0	185	0	1993	0.000
5	F	2.80E-07	1.5	0.00E+00	920	3120	400	960	0	200	0	2360	0.000

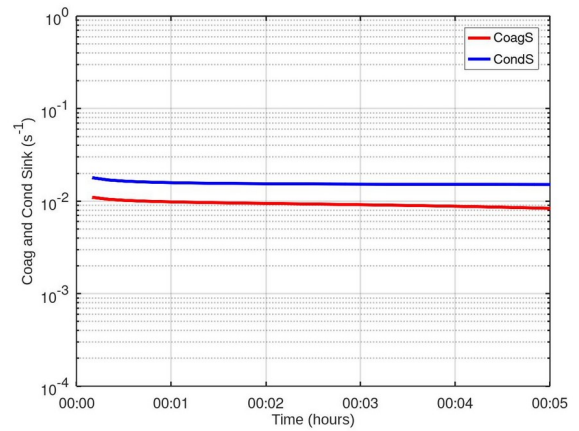
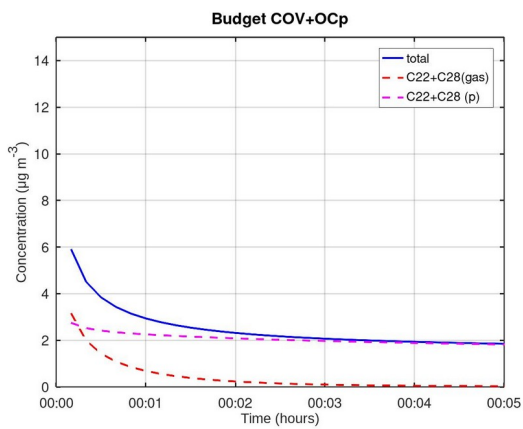
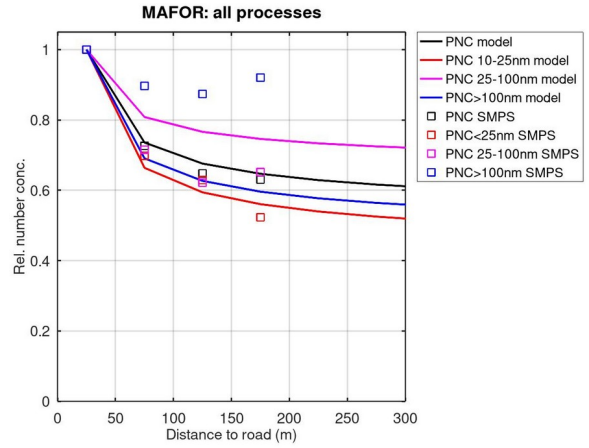
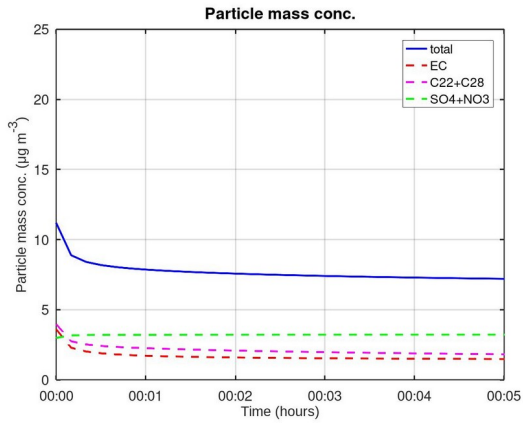
The input file dispers.dat is shown below:

dispers.dat ✕					
1	1.10	12.0	0.25	300.0	
2	0.00	-0.4	5.00	0.00	-0.8
3	12.0	300.0	0.03	0.12	1.0E16
4	0.230	0.290	7.00	13.0	22.5
5	1.33	0.0013	4.00	121.0	
6	0.01	0.002	0.20		
7	0.1	280	33.0		
8					

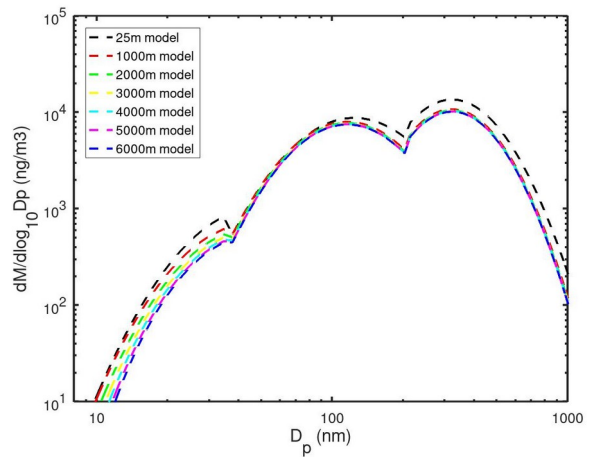
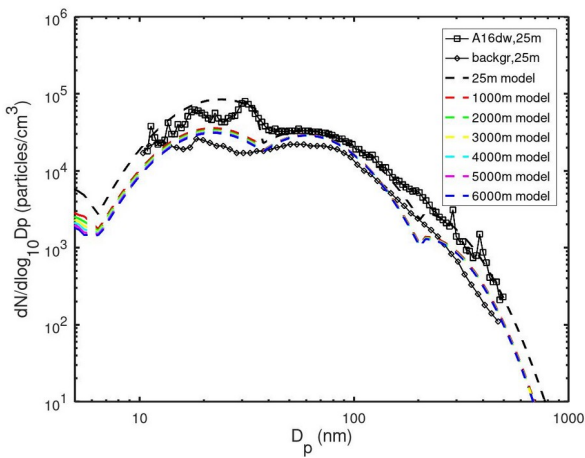
Entries in the first line characterize the initial conditions of the plume, i.e. the initial mixing height, the distance of the start location from the emission source (motorway), the height of the exhaust pipe above ground, and the initial plume air temperature. The second, third and fourth line contain parameters for Type 2, Type 3 and Type 4 dilution which are ignored in this run. The Fourth and fifth line show entries for dry deposition of particles onto the road surface (section 2.7).

5.5.3 Result plots

The plots created with the MATLAB scripts aermass_plume.m are shown on the next page.



The lower left plot displays the budget of OC in gas phase and particle phase and the lower right plot displays the coagulation sink (red line) and condensation sink (blue line) with increasing time (corresponds to distance from road). The number size distribution plot (left) and the mass size distribution plot (right) created with the MATLAB scripts `sizedis_plume.m` is shown below.



5.6 Ammonium nitrate aerosol

5.6.1 Description

In this scenario, the formation of ammonium nitrate particles is simulated for the conditions at the regional background station Cabauw in the Netherlands with emissions of ammonia from agriculture and NO_x from local traffic and long-range transport. Chemical composition of PM_{2.5} in Cabauw, as in the BOP report [“Composition and origin of Particulate Matter in the Netherlands” [Schaap, M., Weijers, E.P., Mooibroek, D., Nguyen, L., Hoogerbrugge, R. (2010)]] was used to derive mass fraction of aerosol components. The average size distribution data for 2011, provided by M.P. Keuken, was fitted using the derived mass fractions. The simulation time is 10 hours on a summer day. Emissions of NH₃ and NO₂ are 5.00x10¹⁰ cm² s⁻¹ and 5.0x10¹⁰ cm² s⁻¹, respectively. Typical values are used as initial concentrations of relevant gases. Two simulations are done: one using dynamic condensation/evaporation (ICONW1) and one using in addition dissolutional growth of nitric acid employing the thermodynamic equilibrium solver MESA (ICONW2).

5.6.2 Input

The input file sensitiv.dat for the ICONW1 run is shown below:

sensitiv.dat							
1	1	1	1	1	0	7	0
2	1	1	0	1	0	1	0
3	0	0	0	1	0	0	0
4	1	0	0				
5							

For ICONW21 run, sensitiv.dat has to be changed as follows:

sensitiv.dat							
1	1	1	1	1	0	7	0
2	1	1	0	1	0	1	0
3	0	0	0	1	0	0	0
4	2	0	0				
5							

Nucleation is turned off in both simulations. Condensation of sulphate, organics and ammonium is on in both runs. The switch for chemistry integration is set to 1. In ICONW1, the water condensation switch is set to 1 and in ICONW2, this switch is 2 to activate the coupling to MESA. The results from the two runs have to be saved to different sub-folders (named iconw1 and iconw2) of the output folder. Temperature is constant at 290 K and RH is constant at 87% in the input file ingeod.dat,

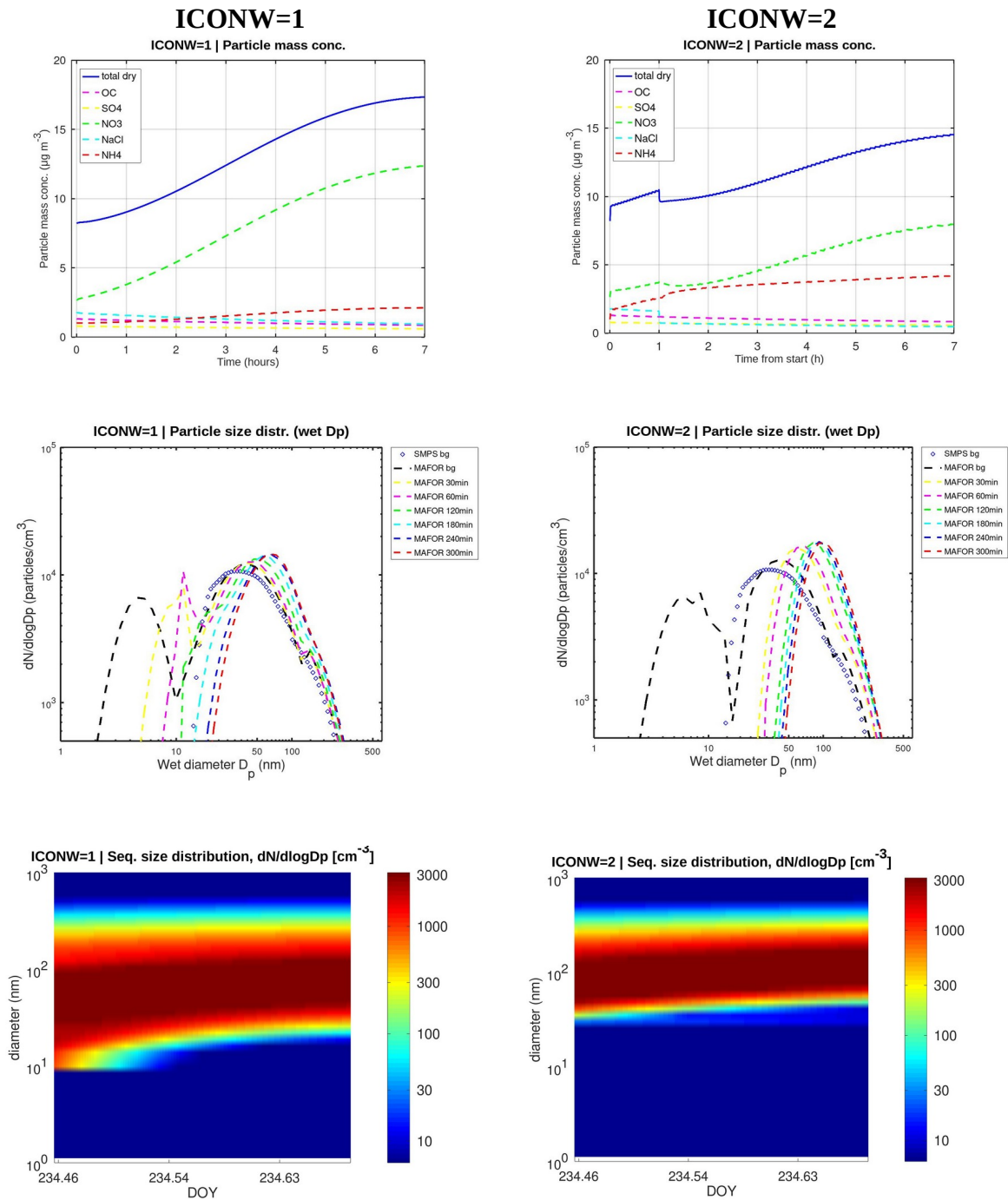
The first lines of the input file ingeod.dat for this example are shown below:

ingeod.dat																									
1	10	24	8	10	51.9703	4.9262	290.00	101300.	0.870	200.00	0	2.96	0.00	0.0	0.009	0.0	9.92D09	00.E+07	7.39D08	0.00	3.50	0.00	7.0	90.0	0.5
2	10	24	8	11	51.9703	4.9262	290.00	101300.	0.870	200.00	0	2.48	0.00	0.0	0.009	0.0	9.92D09	00.E+07	1.28D09	0.00	3.50	0.00	7.0	90.0	0.5
3	10	24	8	12	51.9703	4.9262	290.00	101300.	0.870	200.00	0	2.54	0.00	0.0	0.009	0.0	9.92D09	00.E+07	4.89D08	0.00	3.50	0.00	7.0	90.0	0.5
4	10	24	8	13	51.9703	4.9262	290.00	101300.	0.870	200.00	0	2.60	0.00	0.0	0.009	0.0	9.92D09	00.E+07	3.26D09	0.00	3.50	0.00	7.0	90.0	0.5
5	10	24	8	14	51.9703	4.9262	290.00	101300.	0.870	200.00	0	2.30	0.00	0.0	0.009	0.0	9.92D09	00.E+07	3.89D09	0.00	3.50	0.00	7.0	90.0	0.5
6	10	24	8	15	51.9703	4.9262	290.00	101300.	0.870	200.00	0	2.50	0.00	0.0	0.009	0.0	9.92D09	00.E+07	3.65D09	0.00	3.50	0.00	7.0	90.0	0.5
7	10	24	8	16	51.9703	4.9262	290.00	101300.	0.870	200.00	0	2.49	0.00	0.0	0.009	0.0	9.92D09	00.E+07	1.29D09	0.00	3.50	0.00	7.0	90.0	0.5
8	10	24	8	17	51.9703	4.9262	290.00	101300.	0.870	200.00	0	2.58	0.00	0.0	0.009	0.0	9.92D09	00.E+07	0.70D09	0.00	3.50	0.00	7.0	90.0	0.5
9	10	24	8	18	51.9703	4.9262	290.00	101300.	0.870	200.00	0	2.69	0.00	0.0	0.009	0.0	9.92D09	00.E+07	0.50D09	0.00	3.50	0.00	7.0	90.0	0.5
10	10	24	8	19	51.9703	4.9262	290.00	101300.	0.870	200.00	0	2.67	0.00	0.0	0.009	0.0	9.92D09	00.E+07	2.34D09	0.00	3.50	0.00	7.0	90.0	0.5

The initial concentration and emission rate of NH₃ is provided in the input file inchem.dat. Time-dependent concentrations of ammonia are calculated, which are influenced by condensation and evaporation to/from the particulate phase. The particle size distribution changes dynamically through the simulation

5.6.3 Result plots

The plots created with the MATLAB scripts mesatest_aermass.m, mesatest_sizediswet.m and mesatest_nprofile.m. The concentration time series of the total particle mass and of the various aerosol components are displayed in the upper panel. The step-wise decrease of the total mass for ICONW2 after 1 hour is due to depletion of chloride in the sea-salt particles (degassing of HCl through displacement by HNO₃). MESA solver recalculates $K_p(\text{NH}_4\text{NO}_3)$ and the other solution terms of the mixed inorganic aerosol, after changes of the number concentration and the composition in each size bin. In ICONW2, the quicker equilibration of ammonia leads to higher final NH₄ concentrations. Less nitrate is formed in the case of growth by dissolution. In the middle panel, the number size distributions are shown at certain times up to 300 minutes after starting with the size distribution fitted to measurements with SMPS. The lower panel In the lower graphic the particle growth during the simulation is visualized as sequential size distribution.



6 References

- Abdul-Razzak, H., Ghan, S. J., and C. Rivera-Carpio, A parameterization of aerosol activation, Single aerosol type, *J. Geophys. Res.*, 103, D6, 6123-6131, 1998.
- Abdul-Razzak, H. and S. J. Ghan, A parameterization of aerosol activation, 2. Multiple aerosol types, *J. Geophys. Res.*, 105, D5, 6837-6844, 2000.
- Baranizadeh, E., Murphy, B. N., Julin, J., Falahat, S., Reddington, C. L., Arola, A., Ahlm, L., Mikkonen, S., Fountoukis, C., Patoulias, D., Minikin, A., Hamburger, T., Laaksonen, A., Pandis, S. N., Vehkamäki, H., Lehtinen, K. E. J., Riipinen, I., Implementation of state-of-the-art ternary new particle formation scheme to the regional chemical transport model PMCAMx-UF in Europe, *Geosci. Model Dev.*, 9, 2741–2754, 2016, doi:10.5194/gmd-9-2741-2016, 2016.
- Bolsaitis, P. and J. F. Elliott, Thermodynamic Activities and equilibrium partial pressures for aqueous sulfuric acid solutions, *J. Phys. Chem. Eng. Data.*, 35, 69-85, 1990.
- Ceulemans, K., Compernelle, S. and J.-F. Müller, Parameterising secondary organic aerosol from α -pinene using a detailed oxidation and aerosol formation model, *Atmos. Chem. Phys.*, 12, 5343-5366, doi:10.5194/acp-12-5343-2012, 2012.
- Chickos, J. S. and J. A. Wilson, Vaporization enthalpies at 298.15 K of the n-alkanes from C₂₁ to C₂₈ and C₃₀, *J. Chem. Eng. Data*, 42, 190-197, 1997.
- Chosson, F., Paoli, R., and Cuenot, B., Ship plume dispersion rates in convective boundary layers for chemistry models, *Atmos. Chem. Phys.*, 8, 4841-4853, www.atmos-chem-phys.net/8/4841/2008/, 2008.
- Couvidat, F., Debry, E., Sartelet, K., and C. Seigneur, A hydrophylic/hydrophobic organic (H₂O) aerosol model: Development, evaluation and sensitivity analysis, *J. Geophys. Res.*, 117, D10304, 1-19, doi:10.1029/2011JD017214, 2012
- Donahue, N. M., Epstein, S. A., Pandis, S. N., and A. L. Robinson, A two-dimensional volatility basis set: 1. organic-aerosol mixing thermodynamics, *Atmos. Chem. Phys.*, 11, 3303-3318, doi:10.5194/acp-11-3303-2011, 2011.
- Fuchs, N. A., *The Mechanics of Aerosols*, Pergamon, New York, 1964.
- Henschel, H., Kurtén, T., and Vehkamäki, H.: Computational study on the effect of hydration on new particle formation in the sulfuric acid/ammonia and sulfuric acid/dimethylamine Systems, *J. Phys. Chem. A*, 120, 1886–1896, doi:10.1021/acs.jpca.5b11366, 2016.
- Hussein, T., Smolik, J., Kerminen, V. M., and M. Kulmala, Modeling dry deposition of aerosol particles onto rough surfaces, *Aerosol Sci. Technol.* 46:1, 44-59, 2012.
- Jacobson, M. Z., Numerical techniques to solve condensational and dissolutional growth equations when growth is coupled to reversible aqueous reactions. *Aerosol Sci. Technol.*, 27, 491-498, 1997.
- Jacobson, M. Z., Analysis of aerosol interactions with numerical techniques for solving coagulation, nucleation, condensation, dissolution, and reversible chemistry among multiple size distributions, *J. Geophys. Res.*, 107(D19), 4366, doi: 10.1029/2011JD002044, 2002.
- Jacobson, M. Z., *Fundamentals of Atmospheric Modeling*, Second Edition, Cambridge University Press, 2005a.
- Jacobson, M. Z., A solution to the problem of nonequilibrium acid/base gas-particle transfer at long time step, *Aerosol Sci. Technol.*, 39(2), 92-103, doi:10.1080/027868290904546, 2005b.
- Jacobson, M. Z. and Seinfeld, J. H., Evolution of nanoparticle size and mixing state near the point of emissions, *Atmos. Environ.*, 38, 1839-1850, 2004.
- Karl, M., Gross, A., Pirjola, L., and C. Leck, A new flexible multicomponent model for the study of aerosol dynamics in the marine boundary layer, *Tellus B*, 63(5), 1001-1025, doi: 10.1111/j.1600-0889.2011.00562.x, 2011.

- Karl, M., Leck, C., Gross, A. and L. Pirjola, A study of new particle formation in the marine boundary layer over the central Arctic Ocean using a flexible multicomponent aerosol dynamic model, *Tellus B*, 64, 17158, doi: 10.3402/ tellusb.v64i0.17158, 2012a.
- Karl, M., Dye, C., Schmidbauer, N., Wisthaler, A., Mikoviny, T., D'Anna, B., Müller, M., Clemente, E., Muñoz, A., Porras, R., Ródenas, M., Vázquez, M. and T. Brauers, Study of OH-initiated degradation of 2-aminoethanol, *Atmos. Chem. Phys.*, 12, 1881-1901, 2012b.
- Karl, M., Kukkonen, J., Keuken, M. P., Lutzenkirchen, S., Pirjola, L., and Hussein, T., Modeling and measurements of urban aerosol processes on the neighborhood scale in Rotterdam, Oslo and Helsinki, *Atmos. Chem. Phys.*, 16, 4817-4835, 2016.
- Karl, M., Pirjola, L., Karppinen, A., Jalkanen, J.-P., and Ramacher, M. O. P., Kukkonen, J., Modeling of the concentrations of ultrafine particles in the plumes of ships in the vicinity of major harbors, *J. Environ. Res. Public Health*, 17, 777, 1-24, doi:10.3390/ijerph17030777, 2020.
- Kerminen, V.-M., Virkkula, A., Hillamo, R., Wexler, A. S., and M. Kulmala, Secondary organics and atmospheric cloud condensation nuclei production, *J. Geophys. Res.*, 105(D7), 9255-9264, 2000.
- Keuken, M., Henzing, J. S., Zandveld, P., van den Elshout, S., and M. Karl, Dispersion of particle numbers and elemental carbon from road traffic, a harbor and an airstrip in the Netherlands, *Atmos. Environ.*, 54, 320-327, 2012c.
- Konopka, P., Analytical Gaussian Solutions for Anisotropic Diffusion in a Linear Shear Flow, *J. Non-Equilib. Thermodyn.*, 20, 78-91, 1995.
- Kouznetsov, R. and M. Sovief, A methodology for evaluation of vertical dispersion and dry deposition of atmospheric aerosol, *J. Geophys. Res.*, 117, D01202, 1-17, doi:10.1029/2011JD016366, 2012.
- Kreidenweis, S. M. and J. H. Seinfeld, Nucleation of sulfuric acid-water and methanesulfonic acid-water solution particles: Implications for the atmospheric chemistry of organosulfur species, *Atmos. Environ.* 22(2), 283-296, 1998.
- Kulmala, M., Lehtinen, K. E. J., and A. Laaksonen, Cluster activation theory as an explanation of the linear dependence between formation rate of 3 nm particles and sulphuric acid concentration, *Atmos. Chem. Phys.*, 6, 787-793, 2006.
- Kulmala, M., Kerminen, V.-M., Anttila, T., Laaksonen, A., and C. D. O'Dowd, Organic aerosol formation via sulphate cluster activation, *J. Geophys. Res.*, 109, D04205, doi:10.1029/2003JD003961, 2004.
- Lehtinen, K. E. J. and M. Kulmala, A model for particle formation and growth in the atmosphere with molecular resolution in size, *Atmos. Chem. Phys.*, 3, 251-257, 2003.
- Lemmetty, M., Rönkkö, T., Virtanen, A., Keskinen, J., and L. Pirjola, The effect of sulphur in diesel exhaust aerosol: Models compared with measurements, *Aerosol Sci. Technol.*, 42(11), 916-929, doi:10.1080/02786820802360682, 2008.
- Merikanto, J., Napari, I., Vehkamäki, H., Anttila, T., and M. Kulmala, New parameterization of sulfuric acid-ammonia-water ternary nucleation rates at tropospheric conditions, *J. Geophys. Res.*, 112, D15207, doi:10.1029/2006JD007977, 2007.
- Merikanto, J., Napari, I., Vehkamäki, H., Anttila, T., and M. Kulmala, Correction to "New parameterization of sulfuric acid-ammonia-water ternary nucleation rates at tropospheric conditions", *J. Geophys. Res.*, 114, D09206, doi:10.1029/2009JD012136, 2009.
- Monahan, E. C., Spiel, D. E., and K. L. Davidson, K. L., A Model of Marine Aerosol Generation via Whitecaps and Wave Disruption, 167-174, *Oceanographic Sciences Library*, Springer, Dordrecht, the Netherlands, doi:10.1007/978-94-009-4668-2_16, 1986.
- Määttänen, A., Merikanto, J., Henschel, H., Duplissy, J., Makkonen, R., Ortega, I. K., and H. Vehkamäki, New parameterizations for neutral and ion-induced sulfuric acid-water particle formation in nucleation and kinetic regimes, *J. Geophys. Res.: Atmospheres*, 123, 1269-1296, doi:10.1002/2017JD027429, 2018a.

- Määttänen, A., Merikanto, J., Henschel, H., Duplissy, J., Makkonen, R., Ortega, I. K., and H. Vehkamäki, (2018, April 13). Revised release of a Fortran code including the particle formation parameterizations published in Määttänen et al., JGR D, 2018 (Version v1.0). Journal of Geophysical Research Atmospheres., Zenodo, <http://doi.org/10.5281/zenodo.1217782>, 2018b.
- Nelder, J. A. and Mead, R., *The Computer Journal*, vol. 7, pp. 308-313.
- Nielsen, C. J., D'Anna, B., Dye, C., George, C., Graus, M., Hansel, A., Karl, M., King, S., Musabila, M., Müller, M., Schmidbauer, N., Stenström, Y., and A. Wisthaler, Atmospheric Degradation of Amines. Summary Report: Gas phase oxidation of 2-aminoethanol (MEA). CLIMIT project no. 193438, NILU OR 8/2010, Norwegian Institute for Air Research, Kjeller, Norway, 2010. Available at <http://www.nilu.no>.
- Pandis, S. N., Seinfeld, J. H., and C. Pilinis, Chemical composition differences in fog and cloud droplets of different sizes, *Atmos. Environ.*, 24A(7), 1957-1969, 1990a.
- Pankow, J. F., An absorption model of gas/particle partitioning of organic compounds in the atmosphere, *Atmos. Environ.*, 28(2), 185-188, 1994.
- Pirjola, L., Effects of the increased UV radiation and biogenic VOC emissions on ultrafine aerosol formation, *J. Aerosol. Sci.*, 30, 355–367, 1999.
- Pirjola, L. and Kulmala, M., Development of particle size and composition distribution with a novel aerosol dynamics model, *Tellus*, 53B, 491-509, 2001.
- Pirjola, L., Karl, M., Rönkkö, T., and F. Arnold, Model studies of volatile diesel exhaust particle formation: Organic vapours involved in nucleation and growth?, *Atmos. Chem. Phys. Discuss.*, 2015, 15, 4219-4263, doi:10.5194/acpd-15-4219-2015, 2015.
- Pohjola, M., Pirjola, L., Kukkonen, J., and M. Kulmala, Modelling of the influence of aerosol processes for the dispersion of vehicular exhaust plumes in street environment, *Atmos. Environ.*, 37, 339-351, 2003.
- Pruppacher, H. R. and J. D. Klett *Microphysics of Clouds and Precipitation*, Kluwer Academic Publishers, Dordrecht, The Netherlands, 1997.
- Sander, R., Kerkweg, A., Jöckel, P., and J. Lelieveld, Technical note: The new comprehensive atmospheric chemistry module MECCA, *Atmos. Chem. Phys.*, 5, 445 – 450, 2005.
- Sander, A., Baumgaertner, A., Gromov, S., Harder, H., Jöckel, P., Kerkweg, A., Kubistin D., Regelin, E., Riede, H., Sandu, A., Taraborrelli, D., Tost, H. and Z.-Q. Xie, The atmospheric chemistry box model CAABA/MECCA-3.0. *Geosci. Model Dev.*, 4, 373-380, 2011.
- Sander, A., Baumgaertner, A., Cabrera-Perez, D., Frank, F., Gromov, S., Groß, J.-U., Harder, H., Huijnen, V., Jöckel, P., Karydis, V. A., Niemeyer, K. E., Pozzer, A., Riede, H., Schultz, M. G., Taraborrelli, D., and Tauer, S., The community atmospheric chemistry box model CAABA/MECCA-4.0. *Geosci. Model Dev.*, 12, 1365-1385, <https://doi.org/10.5194/gmd-12-1365-2019>, 2019.
- Sandu, A. and R. Sander, Technical note: Simulating chemical systems in Fortran90 and Matlab with the Kinetic PreProcessor KPP-2.1. *Atmos. Chem. Phys.*, 6, 187 – 195, 2006.
- Sandu, A., Verwer, J. G., Van Loon, M., Carmichael, G. R., Potra, F. A., Dabdub, D. and J. H. Seinfeld, Benchmarking stiff ODE solvers for atmospheric chemistry problems .1. Implicit vs explicit. *Atmospheric Environment*, 31, 3151 – 3166, 1997.
- Schack, C. J., Jr., S. E. Pratsinis, and S. K. Friedlander, A general correlation for deposition of suspended particles from turbulent gases to completely rough surfaces, *Atmospheric Environment*, 19(6), 953-960, doi:10.1016/0004-6981(85)90240-9, 1985.
- Seinfeld, J. H. and S. N. Pandis, *Atmospheric Chemistry and Physics, From Air Pollution to Climate Change*, 2nd Edition, John Wiley & Sons, Inc., Hoboken New Jersey, 2006.

- Smith, M. H., Park, P. M., and I. E. Consterdine, Marine aerosol concentrations and estimated fluxes over the sea, *Q. J. Roy. Meteor. Soc.*, 119, 809-824, doi:10.1002/qj.49711951211, 1993.
- Spada, M., Jorba, O., Perez Garcia-Pando, C., Janjic, Z., and J. M. Baldasano, Modeling and evaluation of the global sea-salt aerosol distribution: sensitivity to emission schemes and resolution effects at coastal/orographic sites, *Atmos. Chem. Phys.*, 13, 11735-11755, doi:10.5194/acp-13-11735-2013, 2013.
- Tsimpidi, A. P., Karydis, V. A., Zavala, M., Lei, W., Molina, L., Ulbrich, L. M., Jimenez, J. L., and S. N. Pandis, Evaluation of the volatility basis-set approach for the simulation of organic aerosol formation in the Mexico City metropolitan area, *Atmos. Chem. Phys.*, 10, 525-546, www.atmos-chem-phys.net/10/525/2010/, 2010.
- Vehkamäki, H., Kulmala, M., Napari, I., Lehtinen, K. E. J., Timmreck, C., Noppel, M., and A. Laaksonen, An improved parameterization for sulphuric acid-water nucleation rates for tropospheric and stratospheric conditions, *J. Geophys. Res.*, 107, D22, 4622, doi:10.1029/2002JD002184, 2002.
- Vehkamäki, H., Kulmala, M., Napari, I., Lehtinen, K. E. J., and M. Noppel, Modelling binary homogeneous nucleation of water – sulfuric acid vapours: Parameterisation for high temperature emissions, *Environ. Sci. Technol.*, 37, 3392-3398, doi:10.1021/es0263442, 2003.
- Vignati, E., Berkowicz, R., Palmgren, F., Lyck, E., and Hummelshøj, P., Transformation of size distributions of emitted particles in streets, *Sci. Tot. Environ.*, 235, 37-49, 1999.
- Virtanen, A., Ristimäki, J., Marjamäki, M., Vaaraslahti, K., Keskinen, J., and Lappi, M., Effective Density of Diesel Exhaust Particles as a Function of Size, *SAE Tech. Pap. Ser. 2002-01-0056*, 2002.
- Vouitsis, E., Ntziachristos, L., and Samaras, Z.: Modelling of diesel exhaust aerosol during laboratory sampling, *Atmos. Environ.*, 39, 1335-1345, 2005.
- Yu, F., Ion-mediated nucleation in the atmosphere: Key controlling parameters, implications, and look-up table. *J. Geophys. Res.*, 115, D03206, doi:10.1029/2009JD012630, 2010.
- Yu, F., Nadykto, A. B., Herb, J., Nazarenko, K. M., and Uvarova, L. A., H₂SO₄-H₂O-NH₃ ternary ion-mediated nucleation (TIMN): Kinetic-based model and comparison with CLOUD measurements, *Atmos. Chem. Phys.*, 18, 17451-17474, doi:10.5194/acp-18-17451-2018, 2018.
- Yu, F., Nadykto, A. B., Luo, G., and Herb, J., H₂SO₄-H₂O binary and H₂SO₄-H₂O-NH₃ ternary homogeneous and ion-mediated nucleation: look-up table version 1.0 for 3-D modeling application, *Geosci. Model Dev.*, 13, 2663-2670, doi:10.5194/gmd-13-2663-2020, 2020.
- Zaveri, R. A., Easter, R. C., and Wexler, A. S., A new method for multicomponent activity coefficients of electrolytes in aqueous atmospheric aerosols, *J. Geophys. Res.*, 110, D02201, doi:10.1029/2004JD004681, 2005a.
- Zaveri, R. A., Easter, R. C., and Peter, L. K., A computationally efficient Multicomponent Equilibrium Solver for Aerosols (MESA), *J. Geophys. Res.*, 110, D24203, doi:10.1029/2004JD005618, 2005b.
- Zaveri, R. A., Easter, R. C., Fast, J. D., and Peters, L. K., Model for Simulating Aerosol Interactions and Chemistry (MOSAIC), *J. Geophys. Res.*, 113, D13204, doi:10.1029/2007JD008782, 2008.
- Zhang, X., Cappa, C. D., Jathar, S. H., McVay, R. C., Ensberg, J. J., Kleeman, M. J., and Seinfeld, J. H.: Influence of vapor wall loss in laboratory chambers on yields of secondary organic aerosol, *P. Natl. Acad. Sci. USA*, 111, 5802-5807, 2014.

7 Appendix A: List of species indices

MAFOR v1.9.9 Species	aq. Mode	matlab no
ind_CH2Cl		2
ind_CH2I2		3
ind_I2O2		4
ind_IPN		5
ind_CH3CHOCH3		6
ind_Nap	a01	7
ind_N2O		8
ind_LNITROGEN		9
ind_LCARBON		10
ind_IPART		11
ind_LSULFUR		12
ind_BELV		13
ind_AELV		14
ind_CH3NO		15
ind_MEANHA		16
ind_HOCH2CH2NO		17
ind_H2NCOCH3		18
ind_TMADF		19
ind_HOCH2CONHCHO		20
ind_CH2CNH2CH3		21
ind_DMCNH		22
ind_H2NCCHOHCH3		23
ind_HNCCH3MOH		24
ind_H2NCCH2MOH		25
ind_HOETNHCH2CHO		26
ind_HOCH2CONETOH		27
ind_AMPOX		28
ind_AMPNA		29
ind_DEANCHO		30
ind_CHEXOL		31
ind_CHEXOOH		32
ind_DEANCOCH2OH		33
ind_CH3SOO2H		34
ind_CH3SO4H		35
ind_DMSOOH		36
ind_DMSO2OOH		37
ind_CH3CHO	a01	38
ind_HO2m	a01	39
ind_IO3m	a01	40
ind_CH3SO3m	a01	41
ind_D1O	a01	42
ind_CH3CO3	a01	43
ind_CH3NHNHCH3	a01	44
ind_NH2C2H4NH2	a01	45
ind_DOCO	a01	46
ind_ROO6R5O2		47
ind_MGLYOAC		48
ind_DMS	a01	49
ind_DMSO	a01	50

ind_ROO6R3O		51
ind_Cl2O2		52
ind_HIO3		53
ind_PIOV		54
ind_PELV		55
ind_PSOV		56
ind_DMOCNH2MOH		57
ind_CHEX		58
ind_CH3SOCH2		59
ind_CH3CO2H	a01	60
ind_DOC	a01	61
ind_BIACET		62
ind_NC4H10		63
ind_CPDKETENE		64
ind_NCPDKETENE		65
ind_MNCPDKETENE		66
ind_CH3CCl3		67
ind_MMNNO2		68
ind_HNCO		69
ind_CH3SCH2		70
ind_CH3COOm	a01	71
ind_C3H8		72
ind_METACETHO		73
ind_CH3COOHCHCHO		74
ind_HCOCCCH3CHOOH		75
ind_IC4H10		76
ind_CO23C4CO3H		77
ind_NMBOBCO		78
ind_PBZQCO		79
ind_PTLQCO		80
ind_NOPINDCO		81
ind_NOPINDOOH		82
ind_OH2MENTHEN6ONE		83
ind_CINO2		84
ind_OCIO		85
ind_C3H7I		86
ind_N2O4		87
ind_NAMP		88
ind_AMPAN		89
ind_CHEXO		90
ind_HSO3		91
ind_DMSO2		92
ind_DMSO2O		93
ind_MSOON		94
ind_MSPN		95
ind_MSADMA		96
ind_MSATMA		97
ind_IO	a01	98
ind_ICl2m	a01	99
ind_CH3NCO	a01	100

a01: Aqueous phase species in the Coarse CS(mode).

Continued.

ind_NCOm	a01	101	ind_LISOPCD		151
ind_C2H4C2O4mm	a01	102	ind_C6125CO		152
ind_C2H5C2O4m	a01	103	ind_IPROPOL		153
ind_CH3NHCHO		104	ind_C109CO		154
ind_NCO		105	ind_Cl2		155
ind_HOC2H4CO2H		106	ind_INO2		156
ind_NC3H7NO3		107	ind_SO3		157
ind_CH3COCOCO2H		108	ind_MEABO		158
ind_BZFUCO		109	ind_TMAO		159
ind_CO14O3CO2H		110	ind_NO3CH2PAN		160
ind_CO2C4DIAL		111	ind_TEA		161
ind_MALNHYOHO		112	ind_NH4p	a01	162
ind_C1ODC2O2C4OOH		113	ind_ClOm	a01	163
ind_ISOPDOH		114	ind_FeOHp	a01	164
ind_C24O3CCO2H		115	ind_HOCH2CO2H	a01	165
ind_C4CO2DCO3H		116	ind_MGLYOX	a01	166
ind_C5DIALCO		117	ind_ETHGLY		167
ind_MMALANHY		118	ind_ADIPAC	a01	168
ind_LHC4ACCO2H		119	ind_CH3NH2CH2p	a01	169
ind_PBZQOOH		120	ind_NH3CH2CHOHp	a01	170
ind_MCPDKETENE		121	ind_DMNHCH2p	a01	171
ind_PTLQOOH		122	ind_DENHp	a01	172
ind_TOLUENE		123	ind_TENHp	a01	173
ind_C8BCCO		124	ind_HOCH2OH		174
ind_C8BCOOH		125	ind_MPROPENOL		175
ind_NORPINIC		126	ind_HCOCH2CO3H		176
ind_NSTYRENOOH		127	ind_EPXDLCO2H		177
ind_PINIC		128	ind_EPXDLCO3H		178
ind_CH3I		129	ind_C512OOH		179
ind_HOETNHCHO		130	ind_C514OOH		180
ind_DMCNH2		131	ind_CHOC3COOOH		181
ind_AMPNNO2		132	ind_JSOPAOH		182
ind_AMPO		133	ind_HOC2H4CO3H		183
ind_DEANCH2O2		134	ind_ACCOME3CO3H		184
ind_CHEXONE		135	ind_MMALNHYOHO		185
ind_DEANCH2CHO		136	ind_NISOPOOH		186
ind_DMSOHOH		137	ind_LMBOABNO3		187
ind_H2SO4	a01	138	ind_C614CO		188
ind_H2NCHO	a01	139	ind_BZEMUCCO2H		189
ind_MALONAC	a01	140	ind_BZEMUCCO3H		190
ind_GLUTARAC	a01	141	ind_CATEC1OOH		191
ind_NH2CH2p	a01	142	ind_NPHEN1OOH		192
ind_H2OH2O		143	ind_C235C6CO3H		193
ind_ALOV		144	ind_C6H5CH2OOH		194
ind_ASOV		145	ind_C6H5CO3H		195
ind_BUT2OLO		146	ind_MCATEC1OOH		196
ind_C513CO		147	ind_OXYL1OOH		197
ind_MBOCOCO		148	ind_TLEMUCCO2H		198
ind_C4MCONO3OH		149	ind_TLEMUCCO3H		199
ind_LISOPAB		150	ind_NCRES1OOH		200

a01: Aqueous phase species in the Coarse CS(mode).

Continued.

ind_C721CO3H		201	ind_TLFUOOH		251
ind_C812OOH		202	ind_C514NO3		252
ind_C89OOH		203	ind_NC4OHCO3H		253
ind_C8BCNO3		204	ind_NTLFUOOH		254
ind_C811CO3H		205	ind_LDISOPACO		255
ind_C85CO3H		206	ind_LHC4ACCO3H		256
ind_C97OOH		207	ind_LIEPOX		257
ind_NORPINENOL		208	ind_CO235C6OOH		258
ind_PROPENOL		209	ind_BZOBIPEROH		259
ind_C96NO3		210	ind_C5CO2DCO3H		260
ind_BUTENOL		211	ind_C6H5OOH		261
ind_MENTHEN6ONE		212	ind_NBZQOOH		262
ind_PERPINONIC		213	ind_IPRHOCO3H		263
ind_PINALOOH		214	ind_C716OOH		264
ind_PINENOL		215	ind_C721OOH		265
ind_HOCl		216	ind_C722OOH		266
ind_ICl		217	ind_MACO3H		267
ind_C312COCO3H		218	ind_TLOBIPEROH		268
ind_N2O3		219	ind_C6H5CH2NO3		269
ind_HNCHCH2OH		220	ind_NPTLQOOH		270
ind_H2NCH2CO3		221	ind_MACROH		271
ind_H2NCOCO3		222	ind_C810OOH		272
ind_MEANNO		223	ind_C813OOH		273
ind_DMNCHOO2		224	ind_C85OOH		274
ind_DMCOONH2		225	ind_C86OOH		275
ind_PROPACID		226	ind_IC4H9NO3		276
ind_MSADMAH2O		227	ind_C89CO2H		277
ind_MSATMAH2O		228	ind_C89CO3H		278
ind_HCl	a01	229	ind_C96OOH		279
ind_FeOH2Fepppp	a01	230	ind_C98OOH		280
ind_HCOCH2CO2H		231	ind_C106OOH		281
ind_CH3NHCH2p	a01	232	ind_RO6R3O2		282
ind_DMNCH2p	a01	233	ind_RO6R1NO3		283
ind_DENIMp	a01	234	ind_ROO6R1NO3		284
ind_NH2OH		235	ind_LAPINABNO3		285
ind_CN		236	ind_LNAPINABOOH		286
ind_ISOPBOH		237	ind_BZFUOOH		287
ind_C2H6		238	ind_CH3SO3H		288
ind_PHCOOH		239	ind_CH2NH		289
ind_C8BC		240	ind_HOCH2CH2O		290
ind_NPROPOL		241	ind_C413COOOH		291
ind_DEA		242	ind_H2NCHO2CHO		292
ind_HOCH2CHNETOH		243	ind_MEANNO2		293
ind_TME		244	ind_CH3CNH2MOH		294
ind_C2H5OH		245	ind_H2		295
ind_FeClp	a01	246	ind_C44OOH		296
ind_H2NCOCH2OH	a01	247	ind_HCOCOHCO3H		297
ind_H		248	ind_TMEO2		298
ind_C511OOH		249	ind_TEAO		299
ind_C59OOH		250	ind_DEANCH2COO2		300

a01: Aqueous phase species in the Coarse CS(mode).

Continued.

ind_DMSOOO		301	ind_C6CO2OHPAN		351
ind_MALANHYOOH		302	ind_DNCRESOOH		352
ind_CH3CO3H		303	ind_MNCATECOOH		353
ind_IC3H7NO3		304	ind_MNNCATCOOH		354
ind_NO4m	a01	305	ind_C1OOHC3O2C4OD		355
ind_GLYOX	a01	306	ind_TLEMUCPAN		356
ind_DMNCHO	a01	307	ind_IBUTOLBNO3		357
ind_MMNp	a01	308	ind_NC3H7OOH		358
ind_PR2O2HNO3		309	ind_STYRENOOH		359
ind_NH3CH2p	a01	310	ind_C810NO3		360
ind_CO2H3CO2H		311	ind_C89NO3		361
ind_NHOH		312	ind_C513OOH		362
ind_MECOACEOOH		313	ind_C2H5NO3		363
ind_LTMB		314	ind_PERIBUACID		364
ind_PINONIC		315	ind_C811PAN		365
ind_DMSOH		316	ind_BPINAOOH		366
ind_NH3	a01	317	ind_C109OOH		367
ind_MENp	a01	318	ind_C106NO3		368
ind_C5DIALOOH		319	ind_C10PAN2		369
ind_IBUTOLBOOH		320	ind_PINALNO3		370
ind_C5PAN9		321	ind_LAPINABOOH		371
ind_CHOC3COPAN		322	ind_LNBPINABOOH		372
ind_DB1NO3		323	ind_HI		373
ind_NC4OHPAN		324	ind_HCOCOHPAN		374
ind_ACCOME PAN		325	ind_DMAO2		375
ind_C4CO2DBPAN		326	ind_C3DIALOOH		376
ind_C5COO2NO2		327	ind_MALDIALPAN		377
ind_LZCPANC23DBCOD		328	ind_BUT2OLNO3		378
ind_IC4H9OOH		329	ind_C3PAN1		379
ind_C614OOH		330	ind_C3PAN2		380
ind_BENZENE		331	ind_PERPROACID		381
ind_BZBIPEROOH		332	ind_C2H5OOH		382
ind_BZEMUCCO		333	ind_FeHO2pp	a01	383
ind_C5COOHCO3H		334	ind_EPXDLPAN		384
ind_C615CO2OOH		335	ind_C2O4mm	a01	385
ind_HOOCH2CO3H		336	ind_DMAp	a01	386
ind_BZEMUCPAN		337	ind_TMAp	a01	387
ind_C5CO2DBPAN		338	ind_DEAp	a01	388
ind_C5CO2OHPAN		339	ind_TEAp	a01	389
ind_DNPHENO OH		340	ind_IPRHOCO2H		390
ind_NCATECOOH		341	ind_NCATECHOL		391
ind_NNCATECOOH		342	ind_ROO6R3O2		392
ind_NPHENO OH		343	ind_C811O2		393
ind_C312COPAN		344	ind_EBENZ		394
ind_C6COOHCO3H		345	ind_LXYL		395
ind_MACO2H		346	ind_LISOPEFO		396
ind_C4PAN5		347	ind_BPINANNO3		397
ind_IC3H7OOH		348	ind_LHAROM		398
ind_TLEMUCCO		349	ind_CRE SOL		399
ind_C7PAN3		350	ind_MMAO2		400

a01: Aqueous phase species in the Coarse CS(mode).

Continued.

ind_MEA		401	ind_OHMENTHEN6ONEO2		451
ind_H2NCH2CHO		402	ind_NBZFUONE		452
ind_DMCNH2CO3		403	ind_LME3FURANO2		453
ind_BIACETOH		404	ind_HOOCH2CO2H		454
ind_CIOHm	a01	405	ind_DMNNO2		455
ind_FeSO4p	a01	406	ind_C44O2		456
ind_CH3COCO3H		407	ind_DEANNO2		457
ind_C2H2		408	ind_DMSOHO		458
ind_LBUT1ENNO3		409	ind_MSAH2O		459
ind_HYPROPO2H		410	ind_MBOACO		460
ind_PHENOOH		411	ind_OXALAC	a01	461
ind_C614NO3		412	ind_HOCH2CHO	a01	462
ind_BZBIPERNO3		413	ind_SUCCAC	a01	463
ind_ISOPBNO3		414	ind_MMAp	a01	464
ind_LC4H9NO3		415	ind_MEAp	a01	465
ind_NDNPHENOOH		416	ind_TMNp	a01	466
ind_CRESOOH		417	ind_HYETHO2H		467
ind_LBUT1ENOOH		418	ind_BUT2OLOOH		468
ind_NDNCRESOOH		419	ind_NCRESOOH		469
ind_PBZN		420	ind_C2H5O2NO2		470
ind_TLEMUCNO3		421	ind_C54CO		471
ind_C721PAN		422	ind_ETHOHNO3		472
ind_C89PAN		423	ind_CH3NH		473
ind_C9PAN2		424	ind_TMAO2		474
ind_TC4H9OOH		425	ind_DB2OOH		475
ind_H2SO4		426	ind_MPAN		476
ind_PROPOLNO3		427	ind_C5CO14OOH		477
ind_MEABO2		428	ind_MALANHY		478
ind_IC4H9O2		429	ind_MALDALCO3H		479
ind_DEAO2		430	ind_FeOH2p	a01	480
ind_DMCNH2CHO		431	ind_PPN		481
ind_CH3CO2H		432	ind_MC3ODBCO2H		482
ind_CHEXO2		433	ind_MALDIALOOH		483
ind_LNISOOH		434	ind_BIACETOOH		484
ind_PIPN		435	ind_CO2H3CO3H		485
ind_TC4H9NO3		436	ind_HOCH2COCH2OOH		486
ind_FeOHHO2p	a01	437	ind_CH3O2NO2		487
ind_C5DICAROOH		438	ind_HOCH2O2NO2		488
ind_HNCO	a01	439	ind_TLEMUCOOH		489
ind_CH3CHCO		440	ind_LC578OOH		490
ind_HOCH2CO3H		441	ind_C511O2		491
ind_NBZFUOOH		442	ind_C813O2		492
ind_HCOCOOm	a01	443	ind_C512O2		493
ind_CH3COCOOm	a01	444	ind_LC4H9OOH		494
ind_MGLYOAC	a01	445	ind_C98O2		495
ind_N2O5		446	ind_TC4H9O2		496
ind_PBZQONE		447	ind_BZEMUCNO3		497
ind_C812O2		448	ind_BZEMUCOOH		498
ind_LISOPACO		449	ind_NCCH2O2		499
ind_C97O2		450	ind_ISOPDNO3		500

a01: Aqueous phase species in the Coarse CS(mode).

Continued.

ind_H2NCOCHO		501	ind_TOL1O		551
ind_NDMA		502	ind_C614O2		552
ind_NDELA		503	ind_C721CHO		553
ind_TEA02		504	ind_CH3ONO		554
ind_CH3COCH2O2NO2		505	ind_C514O2		555
ind_CH3OH	a01	506	ind_NTLFUO2		556
ind_CO2	a01	507	ind_HO12CO3C4		557
ind_FeSO3p	a01	508	ind_PBZQO2		558
ind_PTLQONE		509	ind_BZFUO2		559
ind_C6H5CH2O2		510	ind_CH2CHOH		560
ind_CO235C6O2		511	ind_C32OH13CO		561
ind_HNO4		512	ind_DMSO		562
ind_NH2O		513	ind_HCOCOCH2OOH		563
ind_HMAC		514	ind_NO3CH2CO3		564
ind_MEK		515	ind_C7CO4DB		565
ind_RO6R1O2		516	ind_NBZFUO2		566
ind_HVMK		517	ind_I2_a01		567
ind_HOI		518	ind_C85O2		568
ind_DMSO2OO		519	ind_TLFUO2		569
ind_DEAN	a01	520	ind_CH3COCHCO		570
ind_HC2O4m	a01	521	ind_CH3NHCHO	a01	571
ind_CH2OOA		522	ind_CHOC3COO2		572
ind_MACRO		523	ind_MACRO2		573
ind_C6CO4DB		524	ind_TLBIPEROOH		574
ind_C1OOHC2OOHC4OD		525	ind_PRONO3BO2		575
ind_HOCHCHO		526	ind_CH4		576
ind_LMBOABOOH		527	ind_C106O2		577
ind_PAN		528	ind_CO235C6CHO		578
ind_PHAN		529	ind_MCATEC1O		579
ind_LNMBOABOOH		530	ind_PHENOL		580
ind_NC4DCO2H		531	ind_CATECHOL		581
ind_MEANNO	a01	532	ind_NC3H7O2		582
ind_NC4MDCO2H		533	ind_HOC6H4NO2		583
ind_C513O2		534	ind_C4CODIAL		584
ind_C716O2		535	ind_NCRES1O		585
ind_C1ODC2O2C4OD		536	ind_NPHEN1O		586
ind_NOPINONE		537	ind_TLBIPERNO3		587
ind_NISOPO2		538	ind_C721O2		588
ind_PINALO2		539	ind_C8BCO2		589
ind_LMEKOOH		540	ind_HCOCO3H		590
ind_DB1OOH		541	ind_DNCRESO2		591
ind_HCOCO2CH3CHO		542	ind_INO3		592
ind_HOCOC4DIAL		543	ind_OIO		593
ind_MACRNO3		544	ind_CH3CHOHOOH		594
ind_AMP		545	ind_MNCATECO2		595
ind_AMPN		546	ind_STYRENO2		596
ind_CH3SOO2		547	ind_DNPHENO2		597
ind_CH3SO4		548	ind_MNNCATECO2		598
ind_HCOOm	a01	549	ind_NSTYRENO2		599
ind_FeCl2p	a01	550	ind_IBUTOLBO2		600

a01: Aqueous phase species in the Coarse CS(mode).

Continued.

ind_C59O2		601	ind_HYPERACET		651
ind_HOCH2COCHO		602	ind_SO2	a01	652
ind_C810O2		603	ind_NCATECO2		653
ind_LMEKNO3		604	ind_FeClpp	a01	654
ind_LNAPINABO2		605	ind_MMNNO2	a01	655
ind_CINO3		606	ind_BENZAL		656
ind_C85CO3		607	ind_ME3FURAN		657
ind_CO14O3CHO		608	ind_IPRCO3		658
ind_H2NCHO		609	ind_NNCATECO2		659
ind_IC3H7O2		610	ind_DMNCH2	a01	660
ind_DMSOO		611	ind_ACCOMECHO		661
ind_C1ODC3O2C4OOH		612	ind_CO235C5CHO		662
ind_MBO		613	ind_C4CO2DBC03		663
ind_PTLQO2		614	ind_DENp	a01	664
ind_NH2CH2CHOH	a01	615	ind_CATEC1O2		665
ind_NCRESO2		616	ind_NPHENO2		666
ind_CREZO2		617	ind_NH2		667
ind_C6CO2OHCO3		618	ind_HNO		668
ind_NPTLQO2		619	ind_CH3NO3		669
ind_LHMKVABOOH		620	ind_C312COCO3		670
ind_TENp	a01	621	ind_HCN		671
ind_MEPROPENE		622	ind_LC4H9O2		672
ind_LC5PAN1719		623	ind_ALCOCH2OOH		673
ind_CH3CN		624	ind_C33CO		674
ind_BUT1ENE		625	ind_C109O2		675
ind_CH2CO		626	ind_CO23C4CHO		676
ind_C5CO2DBC03		627	ind_LISOPACNO3O2		677
ind_DMNCHO		628	ind_BPINENE		678
ind_C5DICARBO2		629	ind_LNBPINABO2		679
ind_MVKNO3		630	ind_CH3SOH		680
ind_LNISO3		631	ind_LBUT1ENO2		681
ind_NBZQO2		632	ind_NOA		682
ind_C1OOHC2O2C4OD		633	ind_DENCH2CHOH	a01	683
ind_C5CO14OH		634	ind_CO2C3CHO		684
ind_NO	a01	635	ind_TLEPOXMUC		685
ind_LAPINABO2		636	ind_HSO4m	a01	686
ind_NDNPHENO2		637	ind_CH3COCO3		687
ind_MALDIALO2		638	ind_CH3SO3		688
ind_NDNCRESO2		639	ind_MALDALCO2H		689
ind_HOC2H4CO3		640	ind_CH3O2	a01	690
ind_C722O2		641	ind_BZBIPERO2		691
ind_C5CO2OHCO3		642	ind_CO3m	a01	692
ind_MCATECHOL		643	ind_C615CO2O2		693
ind_MCATEC1O2		644	ind_HOCH2CO2H		694
ind_MMALANHYO2		645	ind_LZCO3C23DBCOD		695
ind_OXYL1O2		646	ind_MEANNO2	a01	696
ind_NC4OHCO3		647	ind_CH3NHCH2	a01	697
ind_CAMPHENE		648	ind_SABINENE		698
ind_HOCH2OOH		649	ind_BPINAO2		699
ind_MACROOH		650	ind_C89O2		700

a01: Aqueous phase species in the Coarse CS(mode).

Continued.

ind_NOPINDO2		701	ind_LMEKO2		751
ind_C5DIALO2		702	ind_CH3NCH3		752
ind_C5134CO2OH		703	ind_BZFUONE		753
ind_CO23C4CO3		704	ind_CH3SOO		754
ind_HCOCC3CO		705	ind_HCO5		755
ind_IO2m	a01	706	ind_lcl	a01	756
ind_CH3COCHO2CHO		707	ind_BIACETO2		757
ind_NCRE1O2		708	ind_CO23C3CHO		758
ind_NPHEN1O2		709	ind_EPXDLCO3		759
ind_C86O2		710	ind_C96CO3		760
ind_ROO6R1O2		711	ind_C2H5CO3		761
ind_LMBOABO2		712	ind_MALANHYO2		762
ind_LNMBOABO2		713	ind_TLEMUCO2		763
ind_IBUTALOH		714	ind_HCOCO		764
ind_LC578O2		715	ind_TOL1OHNO2		765
ind_IPRCHO		716	ind_DNCRE5		766
ind_TLBIPERO2		717	ind_C6H5O		767
ind_APINENE		718	ind_DNPHEN		768
ind_CARENE		719	ind_NH2CH2	a01	769
ind_HYPROPO2		720	ind_EZCHOCCH3CHO2		770
ind_CH2OHSO3m	a01	721	ind_C1ODC2OOHC4OD		771
ind_BZEMUCCO3		722	ind_SO5m	a01	772
ind_HOETNETOH		723	ind_TLFUONE		773
ind_MMA		724	ind_C2H5O2		774
ind_C6H5O2		725	ind_BUT2OLO2		775
ind_C721CO3		726	ind_MACO3		776
ind_TLEMUCCO3		727	ind_DMNp	a01	777
ind_IBUTDIAL		728	ind_NO3CH2CHO		778
ind_BZEMUCO2		729	ind_HOCH2O2		779
ind_EPXC4DIAL		730	ind_C3H7CHO		780
ind_LISOPEFO2		731	ind_C2H5CHO		781
ind_HOCH2COCH2O2		732	ind_C811CO3		782
ind_CATEC1O		733	ind_CH3COCH3		783
ind_HCOCH2CHO		734	ind_DMS		784
ind_ACCOME3CO3		735	ind_NOPINOO		785
ind_C6H5CO3		736	ind_MALDIALCO3		786
ind_MECOACETO2		737	ind_APINAOO		787
ind_HNO3	a01	738	ind_CHOC3COCO3		788
ind_CBUT2ENE		739	ind_CO2H3CO3		789
ind_HOCH2CO		740	ind_O1D		790
ind_STYRENE		741	ind_C5H8		791
ind_BZEPOXMUC		742	ind_HSO5m	a01	792
ind_PHENO2		743	ind_HNO4	a01	793
ind_C3DIALO2		744	ind_HOOCH2CHO		794
ind_HCOCOHCO3		745	ind_MEAN		795
ind_TBUT2ENE		746	ind_H2NCOCH2OH		796
ind_CH3OH		747	ind_CH2NCH3		797
ind_CH3CHOHO2		748	ind_ISOPBDNO3O2		798
ind_MNCATECH		749	ind_C5CO14O2		799
ind_CO235C6CO3		750	ind_HCOCO2H		800

a01: Aqueous phase species in the Coarse CS(mode).

Continued.

ind_CH3SO		801	ind_LHMVKABO2		851
ind_CH3S		802	ind_NDELA	a01	852
ind_HOOCH2CO3		803	ind_DEANNO2	a01	853
ind_CO13C4CHO		804	ind_PINAL		854
ind_CH3OOH		805	ind_ISOPDO2		855
ind_MALDIAL		806	ind_FeOHpp	a01	856
ind_TMA	a01	807	ind_DB1O2		857
ind_HONO		808	ind_HCO3m	a01	858
ind_ISOPBOOH		809	ind_CO2H3CHO		859
ind_MVK		810	ind_HOCH2CO3		860
ind_NC4CHO		811	ind_HCOCH2O2		861
ind_APINBOO		812	ind_LHC4ACCHO		862
ind_DB2O2		813	ind_LISOPACNO3		863
ind_HCOOH	a01	814	ind_CH3		864
ind_EZCH3CO2CHCHO		815	ind_MEA	a01	865
ind_HCOCH2CO3		816	ind_LISOPACOOH		866
ind_IPRHOCO3		817	ind_ISOPBO2		867
ind_CH3CO3		818	ind_LZCODC23DBC00H		868
ind_LDISOPACO2		819	ind_DB1O		869
ind_MBOOO		820	ind_C4MDIAL		870
ind_LHC4ACCO3		821	ind_LZCO3HC23DBCOD		871
ind_MACRO2		822	ind_HCOCO2H	a01	872
ind_C5DICARB		823	ind_CH3CO		873
ind_TEA	a01	824	ind_HOCH2CH2O2		874
ind_HCl		825	ind_MGLYOX		875
ind_NO3	a01	826	ind_DMA	a01	876
ind_MACR		827	ind_CIO		877
ind_CH3COCO2H		828	ind_CH2OO		878
ind_Cl2_a01		829	ind_HNO3		879
ind_CH2O2H2	a01	830	ind_I		880
ind_CH3SOOH		831	ind_CH3CHO		881
ind_CH3SO2		832	ind_GLYOX		882
ind_HCOCO3		833	ind_HCHO	a01	883
ind_NH3		834	ind_FeOpp	a01	884
ind_C2H4		835	ind_CH3OOH	a01	885
ind_CHOCOCH2O2		836	ind_O3P		886
ind_ISOPDOOH		837	ind_MMA	a01	887
ind_LISOPACO2		838	ind_HOCH2CHO		888
ind_BLOV		839	ind_SO4m	a01	889
ind_BSOV		840	ind_DMNNO2	a01	890
ind_NORPINAL		841	ind_NDMA	a01	891
ind_O3	a01	842	ind_CH3O		892
ind_ACETOL		843	ind_N2O4	a01	893
ind_H2O2		844	ind_N2O3		894
ind_C3H6		845	ind_IO	a01	895
ind_DEA	a01	846	ind_Fepppp	a01	896
ind_C89CO3		847	ind_SO3m	a01	897
ind_C96O2		848	ind_Fepp	a01	898
ind_CH3COCH2O2		849	ind_Cl	a01	899
ind_I2		850	ind_H2O		900

a01: Aqueous phase species in the Coarse CS(mode).

Continued.

ind_CO		901
ind_HCOOH		902
ind_NO2	a01	903
ind_HCHO		904
ind_O2	a01	905
ind_NO2m	a01	906
ind_O3		907
ind_H2O2	a01	908
ind_TMA		909
ind_SO3mm	a01	910
ind_O2m	a01	911
ind_OHm	a01	912
ind_HOCl	a01	913
ind_HOI	a01	914
ind_Cl		915
ind_CH3O2		916
ind_SO2		917
ind_SO4mm	a01	918
ind_HONO	a01	919
ind_NO2		920
ind_Cl2m	a01	921
ind_NO3		922
ind_HO2	a01	923
ind_NO3m	a01	924
ind_HO2		925
ind_OH	a01	926
ind_ClM	a01	927
ind_OH		928
ind_HSO3m	a01	929
ind_NO		930
ind_Im	a01	931
ind_Hp	a01	932
ind_DMA		933

a01: Aqueous phase species in the Coarse CS(mode).

8 Appendix B: The Chemical Mechanism of MAFOR v1.9.9

The chemical mechanism in v1.9.9 did not change compared to v1.9.7.

Download as separate PDF document: [meccanism_mafor-v1.9.9.pdf](#).

The Chemical Mechanism of MAFOR v1.9.9

KPP version: 2.2.3_rs3

MECCA version: 4.0

Date: November 2, 2021

Batch file: mafor.bat

Integrator: rosenbrock_posdef

Gas equation file: gas.eqn

Replacement file: maforchem

Selected reactions:

“Tr && (G || Aa) && !Br && !Hg”

Number of aerosol phases: 1

Number of species in selected mechanism:

Gas phase: 781

Aqueous phase: 152

All species: 933

Number of reactions in selected mechanism:

Gas phase (Gnnn): 1869

Aqueous phase (Annn): 232

Henry (Hnnn): 120

Photolysis (Jnnn): 351

Aqueous phase photolysis (PHnnn): 13

Heterogeneous (HETnnn): 0

Equilibria (EQnn): 100

Isotope exchange (IEXnnn): 0

Tagging equations (TAGnnn): 0

Dummy (Dnn): 1

All equations: 2686

9 Appendix C: List of Error Messages

Error Message	Type of Error	Required Action
Fortran runtime error: File {filename} does not exist	Input error	Make sure that the input file {filename} is included in the same directory as the MAFOR executable
(unit = {unit}, file = {filename}) Fortran runtime error: End of file	Input error	Make sure that all required values are entered in input file {filename}
Note: The following floating-point exceptions are signalling: IEEE_INVALID_FLAG IEEE_DENORMAL	Compiler warning	This message occurs after completion of the run and is a known issue with the gfortran compilation. Please ignore.
Note: The following floating-point exceptions are signalling: IEEE_INVALID_FLAG IEEE_DIVIDE_BY_ZERO IEEE_OVERFLOW_FLAG IEEE_UNDERFLOW_FLAG IEEE_DENORMAL	Compiler warning	This message occurs after completion of the run and is a known issue with the gfortran compilation. Please ignore.
File {filename} cannot be opened !	Input error	Make sure that the input file {filename} is included in the same directory as the MAFOR executable
WARNING: RH >=0.99; program may stop	Input, Warning	Input file ingeod.dat: check that RH is not greater or equal 0.99
STOP: RH>1.1 in ingeod.dat	Input error	Input file ingeod.dat: RH cannot be greater than 1.10
STOP: initial SO3 too high (must be <= 5.0e11 cm ⁻³)	Input error	Input file inchem.dat: KPP_SO3 cannot be greater or equal 5.0E11
STOP: allowed range of hvap1 in organic.dat is 10-200 kJ/mol	Input error	Input file organic.dat: values for the enthalpy of vaporization of organic vapors has to be in the range of 10 to 200 kJ/mol
sum of OC molar fractions >1.0 in organic.dat	Input error	Input file organic.dat: mole fractions gamma-oc must not exceed 1.0 per mode
STOP: molar yield > 1.0 in incham.dat	Input error	Input file incham.dat: the sum of ya_soan1 and ya_soan2 must not exceed 1.0
STOP: amine number must be <6 in incham.dat	Input error	Input file incham.dat: select an amine with number 1, ..., 5
STOP: chamber volume must be >0 m3 incham.dat	Input error	Input file incham.dat: the chamber volume must not be zero

Continued.

Error Message	Type of Error	Required Action
STOP: negative input value in monitor.dat	Input error	Input file monitor.dat: Replace negative values by zero
STOP SIGMA too small in inaero.dat. Mode: x	Input error	Input file inaero.dat: increase value of SIGMA for mode x. Typically between 1.1 and 2.2
STOP SIGMA >2.2 not accepted in inaero.dat. Mode: x	Input error	Input file inaero.dat: value of SIGMA for mode x must not exceed 2.2
STOP GMD too small in inaero.dat. Mode: x	Input error	Input file inaero.dat: value of GMD for mode x has to be increased
Type 2: dil2_c has to be between 0 and -2	Input error	Input file dispers.dat: value of dil2_c for Type 2 plume dispersion has to lie between 0 and -2
Type 3: tau_d has to be greater than 0	Input error	Input file dispers.dat: value of tau_d for Type 3 plume dispersion has to be greater than 0
STOP: V_updraft must be < 0.5 m/s in dispers.dat	Input error	Input file dispers.dat: value of vupdra has to be less than 0.5
'before kpp:', c, t, cair 'after kpp:', c, t, cair	Chemistry warning or error	Problem in KPP for concentration c of a species at model time t. Make sure that inchem.dat contains reasonable concentration values. Immediately report problem
WARNING: negative N before Nucl.: m,l,N	Aerosol dynamics warning	Negative number concentration N in mode m, bin i. The model run continues. Most often changing input in inaero.dat for nucleation mode solves this problem, otherwise ignore
EMERGENCY STOP: i=1 vpt(i) >= vpt(i+1)	Severe error	Most likely connected to the condensation of water. Immediately report problem
EMERGENCY STOP: i=imax vpt(i) >= vpt(i+1)	Severe error	Most likely connected to the condensation of water. Immediately report problem
EMERGENCY STOP: 1<i<imax vpt(i) >= vpt(i+1)	Severe error	Most likely connected to the condensation of water. Immediately report problem

Please report any error messages that are not included in this list.